◎ NTNU
Faculty of Engineering Science and Technology
Institute of Civil and Environmental Engineering

MASTER DEGREE THESIS
Spring 2018
For

Marianne Dahl

Investigation of Geotechnical Properties of TBM Spoil from the Follo Line Project

BACKGROUND

Tunnel boring machines(TBMs) were used in the construction of tunnels in connection to several hydropower projects in Norway in the 1970's through 80's, but has since been little used in Norway. In recent years, the use of TBM as tunnel construction method has seen an increase and the method is typically chosen for large projects where the volume of spoil/muck is large. There is considerable potential for saving money through utilization of the TBM spoil. The possibilities of utilizing TBM spoil and other surplus materials otherwise thought of as waste is currently being investigated by NGI in the project "Geomaterials in the circular economy" (GEOreCIRC). The characteristics and behavior of the spoil is in need of investigation. TBM spoil from the Follo line project will be subjected to laboratory testing. The work will be completed with guidance form NGI and Bane NOR.
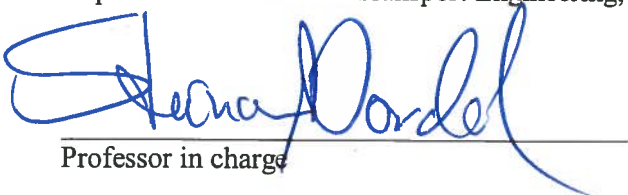
TASK

The project should include a literature study with respect to existing experience in use of TBM spoil and its characteristics. Bane NOR has a database with conducted tests at Åsland deposit site. The results of these tests; Standard Proctor, water content, grain size distributions and plate load tests should be processed and presented. The results should be used to evaluate the material together with large scale oedometer tests performed by the student. The possibility of a field investigation at the deposit site is to be evaluated.

The results of the investigations should be used to evaluate the strength- and deformation properties of the spoil and assess possible utilizations of the material. The work should aim to contribute to recommendations for future testing programmes on TBM spoil and the methods for handling and compacting such material.

Professor in charge:
Steinar Nordal (NTNU)

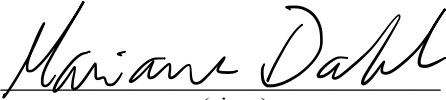Department of Civil and Transport Engineering, NTNU

Professor in charge

NORGES TEKNISK-
NATURVITENSKAPELIGE UNIVERSITET
INSTITUTT FOR BYGG OG MILJØTEKNIKK

Title: **Investigation of Geotechnical Properties of TBM Spoil from the Follo Line Project**	Date: **08.06.2018**
	Number of pages (incl. Appendices): **110**
	Master's thesis	x

Name: Marianne Dahl

Professor in charge/supervisor: Steinar Nordal

External supervisors:
Christian Ofstad (NGI), Gunvor Baardvik (NGI), Jenny Langford (NGI),
Fredrikke Syversen (Bane NOR)

Abstract:
In connection to the Follo line tunnel project this thesis investigate some of the existing experience on use of TBM spoil as a construction aggregate. Compaction control tests provided by Bane NOR for the deposit at Åsland are processed and presented. In order to investigate the deformation properties of the material large scale oedometer tests were conducted at the Norwegian University of Science and Technology (NTNU), Trondheim.

The TBM spoil is found to be a well graded, water sensitive material with a light frost susceptibility. The Troxler density gauge and the dry density from the excavation tests reveal that the achieved compaction is within 95\% of the standard Proctor maximum for field control. While only 22\% of plate load tests pass the requirements set for the specific project it is suspected that this might be caused by not using a layer of plaster to level the surface before conducting the test.

The permeability of the soil is roughly equivalent to that of a fine sand or a coarse silt. This corresponds well with the fines content revealed by the dry sieving of approximately 10\%.

The oedometer tests were conducted on material with 6 - 13\% water content. The water content affected the achieved compaction and strains of each test. The tests resulted in strains of 3.5 to 10\% with a maximum load of 500kPa. The oedometer modulus is between 5 - 20MPa and the achieved dry density at the end of the tests were 1.83 - 2.27 t/m^3 For a possible load of 50kPa on terrain level, the results indicate a maximum settlement of approximately 0.33m for a 30m fill.

Keywords:

1. TBM spoil
2. Large scale oedometer
3. Deformation properties
4. Compaction

(sign.)

Preface

This thesis is the final project of my master's degree in civil engineering at the Norwegian University of Science and Technology (NTNU) in Trondheim, Norway. The project was proposed by the Norwegian Geotechnical Institute (NGI) and Bane NOR, and approved by Professor Steinar Nordal at NTNU. This master's thesis constitutes a workload of 30 SP credits.

The aim of the project is to supply knowledge of the material properties of the tunnel spoil produced by the Follo line railway tunnel construction. The material is being used as a fill at the previous rock quarry at Åsland, Oslo. Field excavation tests and plate load tests were conducted at the deposit site. Compaction control data from Bane NOR has been processed and samples of spoil were collected and transported in sealed barrels to Trondheim for oedometer testing.

I would like to thank my supervisors from NGI and Bane NOR for invaluable discussions and advise. I wish to thank Bane NOR and Acciona Ghella (AGJV) for allowing me to be a part of the field investigations at the deposit at Åsland and for getting to see the tunnel boring machines in action, it has been a great learning experience. I would also like to thank the laboratory staff at NTNU for setting up the equipment and my friend Kjersti for helping me with heavy lifting in the laboratory, I don't think it would have been possible alone.

Trondheim, 04.06.2018
Marianne Dahl

Abstract

The Follo Line tunnel project is under construction using four tunnel boring machines (TBMs) starting from adits near Åsland, Oslo. Bane NOR is using the excavated TBM spoil to create a building platform for a new residential area for Oslo municipality. TBMs were used in the construction of tunnels in connection to several hydropower projects in Norway in the 1970's through 1980's, but has since seen little use in Norway. In recent years, the use of TBM as tunnel construction method has seen an increase and the method is typically chosen for large projects where the volume of excavated tunnel spoil is large. There is considerable potential for saving money and decreasing environmental impact through utilization of the TBM spoil. Possible usages of TBM spoil and other surplus materials otherwise thought of as waste is currently being investigated by the Norwegian Geotechnical Institute (NGI) as part of the project "Geomaterials in the Circular Economy" (GEOreCIRC).

This thesis investigate some of the existing experience on use of TBM spoil as a construction aggregate. Compaction control tests provided by Bane NOR for the deposit at Åsland are processed and presented. In order to investigate the deformation properties of the material large scale oedometer tests were conducted at the Norwegian University of Science and Technology (NTNU), Trondheim. In addition, a plate load test and field excavation test were conducted at the deposit at Åsland.

The investigation of the TBM spoil from the Follo line tunnel project covered in this report consists of the following field and laboratory investigations:

- standard Proctor compaction tests
- *in situ* Troxler moisture/density readings
- washing and dry sieving
- plate load tests
- wet sieving and falling drop for grain size distribution
- field excavation tests
- field permeability tests
- large scale oedometer tests

The standard Proctor, washing and dry sieving, Troxler and plate load tests are conducted by KSR Maskin AS for each layer of the deposit. The results are systematized and presented in this report. In addition, large scale oedometer tests have been conducted at the NTNU geotechnical laboratory in Trondheim, Norway. Four field excavation tests were conducted in April, the first of which contained a layer of frozen ground. The excavations investigated the achieved dry density of larger volumes and the permeability of the soil. During the last excavation test, soil samples were collected after compaction for sieving and investigation of fines content to evaluate the water sensitivity and frost susceptibility of the material. The results are compared to the data collected on TBM spoil from hydropower projects in the 1970's and 1980's.

The TBM spoil is found to be a well graded, water sensitive material with a light frost susceptibility. The Troxler density gauge and the dry density from the excavation tests reveal that the achieved compaction is within 95% of the standard Proctor maximum for field control. While only 22% of plate load tests pass the requirements set for the specific project it is suspected that

this might be caused by not applying a layer of plaster to level the surface before conducting the test.

The permeability of the soil is in the magnitude of 10^{-5} - 10^{-6} m/s, roughly equivalent to that of a fine sand or a coarse silt. This corresponds well with the fines content revealed by the dry sieving of approximately 10%.

The oedometer tests were conducted on material with 6 - 13% water content. The water content affected the achieved compaction and strains of each test. The tests resulted in strains of 3.5 to 10% with a maximum load of 500kPa. The oedometer modulus is between 5 - 20MPa and the achieved dry density at the end of the tests were 1.83 - 2.27t/m^3. For a possible load of 50kPa on terrain level, the results indicate a maximum settlement of $\approx$ 0.33m for a 30m fill.

Abstrakt

Tunnelprojektet *Follobanen* utføres ved bruk av fire tunnelboremaskiner(TBM) som starter fra tverrslag ved Åsland (tidligere pukkverk) i utkanten av Oslo. Bane NOR, sammen med Oslo kommune benytter tunnelboremassene som fyllmasse til etablering av ny bydel i Oslo. TBM ble mye brukt i Norge i forbindelse med vannkraftutbygging på 70 og 80 tallet, men har siden falt bort til fordel for tradisjonelle sprengningsmetoder. De siste årene har likevel tunnelboremaskinen sett en oppgang og metoden benyttes først og fremst for store prosjekter hvor mengden TBM masser blir stor. Potensialet for å spare både penger og miljø ved å utnytte disse massene lokalt er derfor enormt. Norges Geotekniske Institutt (NGI) holder på med et forskningsprosjekt om utnyttelse av tunnelboremasser og annet overskuddsmateriale som ellers blir sett avskrevet som avfall, "Geomaterials in the Circular Economy" (GEOreCIRC).

Denne rapporten redgjør for tidligere erfaringer om TBM materiale og undersøker og evaluerer materialegenskapene til tunnelboremassen fra Follobaneprosjektet. For undersøkelse av deformasjonsegenskapene er det benyttet et kjempeødometer på NTNU, Geoteknisk avdeling i Trondheim.

Resultater fra felt- og laboratorieundersøkelsene som er behandlet i denne rapporten består av:

- standard Proctor
- *in situ* Troxler densitet- og vanninnhold måler
- vasking og tørrsikting
- platebelastningsforsøk
- våtsikting og "falling drop" for finstoffanalyse
- graving av testgrop
- permeabilitetsmålinger i felt
- kjempeødometer

Standard Proctor, vasking og tørrsikting, Troxler og platebelastningsforsøkene blir utført av KSR Maskin AS for hvert lag i deponiet. Resultatene er systematisert og presentert i denne rapporten. Metode og resultater fra kjempeødometer og feltforsøk er presentert og dirkutert.

Resultatene viser at massen er velgradert, vannsensitiv og er lettere telefarlig. *In situ* målingene av oppnådd tørrdensitet etter komprimering viser at komprimeringsarbeidet er innenfor 95% av proctor optimal komprimering. Kun 22% av platebelastningsforsøkene møter kravene satt til komprimeringskontroll. Forsøkene mangler gipsavretting av overflaten under platen som er beskrevet i forsøksmetoden og det er sannsynlig at dette påvirker resultatene fra platebelastningen slik at de fremstår dårligere.

Permeabiliteten målt ved feltforsøk er i størrelsesorden 10^{-5} - 10^{-6} m/s, tilnærmet lik fin sand eller grov silt. Dette stemmer bra med finstoffinnholdet som er målt til $\approx 10\%$.

Ødometerforsøkene ble utført på materiale med vanninnhold mellom 6 - 13%. Forsøkene ble stegvis kjørt til et trykk på 500kPa og forsøkene målte tøyninger mellom 3.5 - 10%. Forsøkene ga ødometermoduler mellom 5 - 20MPa og oppnådd tørrdensitet ved slutten av forsøket varierte fra 1.83 - 2.27t/m^3. Resultatene fra ødometerforsøkene tilsier en maksimal forventet setning ved 50kPa pålagt last på terrengnivå på ≈ 0.33m for en 30m høy fylling.

Contents

List of Figures

List of Tables

Symbols

a stress path exponential

B diameter or side dimension [m]

c cohesion [kPa]

$\mathbf{C}_u$ coefficient of uniformity

D diameter [m]

e void ratio

E Young's modulus [MPa]

$\mathbf{E}_{def}$ deformation modulus [MPa]

$\mathbf{E}_{oed}$ oedometer modulus [MPa]

H Height [m]

$\mathbf{I}_L$ Pantelidis coefficient

k permeability [m/s]

K compression modulus

$\mathbf{k}_s$ coefficient of subgrade reaction

m modulus number

M oedometer modulus [MPa]

n porosity [%]

p load [kPa]

S settlement [m]

$\mathbf{S}_c$ primary consolidation [m]

$\mathbf{S}_e$ initial compression [m]

$\mathbf{S}_s$ secondary consolidation [m]

Sr saturation [%]

T frost susceptibility classification

u pore pressure / percent mass $< 22.4mm$ [kPa / %]

V volume [m^3]

w water content [%]

γ unit weight of material [kN/m^3]

γ_s unit weight of grains [kN/m^3]

γ_w unit weight of water [kN/m^3]

δ deformation [m]

ε strain [%]

ν Poisson's ratio

ρ density [t/m^3]

ρ_d grain density [t/m^3]

ρ_s dry density [t/m^3]

σ stress [kPa]

φ Angle of friction [°]

1   Introduction

1.1   Background

The Follo Line tunnel project is under construction using four tunnel boring machines (TBMs) starting from adits near Åsland, Oslo. Bane NOR is using the excavated TBM spoil to create a building platform for a new township for Oslo municipality. TBMs were used during the construction of tunnels in connection to several hydropower projects in Norway in the 1970's and the 1980's, but since then this method has seen little use in Norway. In recent years, the use of TBM as tunnel construction method has been on the rise, and the method is typically chosen for large projects where the volume of excavated tunnel spoil is large. There is considerable potential for saving money through utilization of the TBM spoil. The possibilities of utilizing TBM spoil and other surplus materials otherwise thought of as waste is currently being investigated by NGI in the project "Geomaterials in the Circular Economy" (GEOreCIRC).

This thesis summarizes some of the existing experiences on the use of TBM spoil as a construction aggregate and processes the results of compaction control tests provided by Bane NOR for the deposit at Åsland. In order to investigate the deformation properties of the material, large scale oedometer tests were conducted at the Norwegian University of Science and Technology (NTNU), Trondheim.

1.2   The deposit

Figure 1.1 – *Deposit area. taken:05.05.2018, aerial photo - provided by Bane NOR*

The deposit at Åsland is built in layers and compacted using vibratory rollers. The spoil accumulates quickly in the spoil shed and is continuously transported out in fills and is then evenly distributed in a 0.7m thick layer above the last compacted layer. The material is water sensitive and spoil is not transported to the deposit or compacted when rain or snow causes unfavorable conditions. The deposit area is shown in figure 1.1. The picture is an aerial photo taken 05.05.2018. An extended deposit area is marked in red.

The ground conditions beneath the deposit is of varying quality. The former quarry to the southwest is backfilled with rock fill and some surplus masses from the quarry. The centre and perimeter consist of either bare rock or a shallow soil cover. The northern part of the area consists of soft, marine sediments. Vertical drains are placed in the marine sediments in order to accelerate the consolidation process of this layer. The concept is illustrated in figure 1.2.
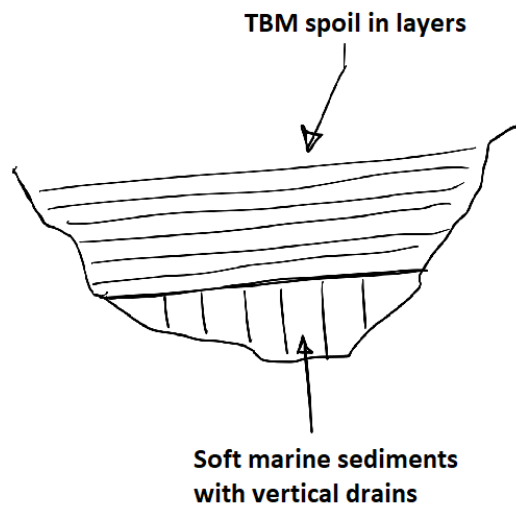
Figure 1.2 – *Deposit principle sketch*

Uneven settlements in the original soil will reflected in the deposit until the consolidation is finished.

1.3 Scope

The scope is limited to investigating the deformation properties of the TBM spoil layers and evaluating the achieved compaction. The challenges and monitoring of the original ground conditions are not part of this thesis. Creep settlements over time is not a part of this study.

1.4 Methodology and challenges

The standard Proctor, washing and dry sieving, Troxler and plate load tests are conducted by KSR Maskin AS for each layer of the deposit as part of the procedure to document the quality of the fill. The results are systematized and presented in this report. In addition, large

scale oedometer tests have been conducted at the NTNU geotechnical laboratory in Trondheim. Finally, field excavation- and plate load tests were conducted at the Åsland deposit site.

The oedometer tests were conducted on TBM spoil collected from the spoil shed at Åsland. The material was transported in sealed containers to NTNU, Trondheim. The oedometer test were performed by building in samples of spoil compacted in layers using a vibrating compaction plate. The tests were then incrementally loaded up to a total of 500kPa. After the tests were completed approximately 30kg of material was collected from each sample for drying and sieving.

The large scale oedometer tests were more time consuming than originally thought. The oedometer cell has inner diameter = 49.9cm and inner height = 57.7cm. Between 150 - 215kg of material was used for each oedometer test. The material was moved from barrels to the oedometer and back using shovels and buckets. The complete process of building in a sample, incrementally loading to 500kPa and removing the material from the cell took approximately 13 hours per test for two people.

The field excavation tests were conducted by excavating a trench of approximately 6-7m^3 after measuring the moisture content over the area with a Troxler moisture gauge. The volume of the pit was measured with water and laser mapping, and later only with laser. The excavated material was weighed and the wet- and dry density were established. The pit was then filled with water and the hydraulic conductivity was calculated by measuring the fall in water head over time. During the last excavation test, soil samples were collected for sieving and investigation of fines content to investigate the frost susceptibility and water sensitivity of the material.

The results are compared to data from other studies presented in the literature survey.

1.5   Content

The report consists of a literature study on TBM spoil and its usages as construction aggregate. A brief explanation of the theory of settlements and how the plate load- and oedometer tests might be used in assessing the deformation properties of a material is presented in Chapter 2. Chapter 3 contains an overview of the deposit and results of the compaction control- and field excavation tests. The results of the oedometer tests are presented in Chapter 4 and an evaluation of the material properties is discussed in Chapter 5. All data from the oedometer- and excavation tests are attached in in Appendix A and B. Concluding remarks and a recommendation for further work are presented in Chapters 6 and 7.

2 Literature survey and theory

2.1 TBM spoil: Experience and documentation

Tunnel spoil is a term which describes the loose material consisting of rock or ore that has been crushed and fragmented by blasting or boring during tunnel construction. The Tunnel Boring Machine (TBM) is a full scale bore which allows for easier and faster tunnel construction. Avoiding blasting also makes for less pollution of the produced tunnel spoil. The cutting head of the TBM consists of many cutter discs, the spacing of the discs is the main factor in deciding the produced grain sizes. The largest grains will seldom exceed the cutter spacing in diameter (Norwegian Soil and Rock Engineering Association 1998). TBM spoil is generally a well graded material with a relatively high fines content, material $<63\mu$m. The fines content is not large enough to cause the larger particles to float in a matrix of fine grains. The material is normally considered water sensitive and frost susceptible because of it's high fines content (NGI 2015). Figure 2.1 shows the TBM cutter head and the conveyor belt transporting spoil out behind the head.
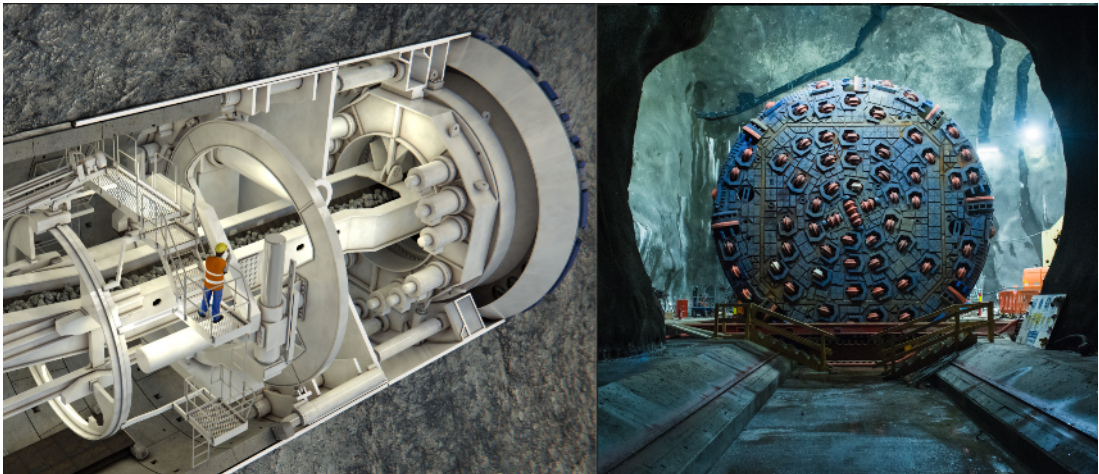
Figure 2.1 – *Tunnel boring machine. Right: Cutter head with disc cutters. Left: Behind cutter head, spoil being transported out on a conveyor belt. The photos are press photos from the Follo line project (Bane NOR 2018)*

The excavated material is simultaneously transported from the four TBMs to the spoil shed at Åsland by conveyor belts. The resulting spoil is therefor a mix of the different geological conditions at the current locations of the four cutter heads. The four TBMs may produce material of different fines- and water content depending on the geological conditions around the cutter head. Figure 2.2 shows the TBM spoil from the four machines stored in the spoil shed at Åsland.

Figure 2.2 – *TBM spoil in spoil shed at Åsland - 13.02.2018*

The tunnel boring machine works by thrusting disc cutters against the rock surface while simultaneously rotating the cutter head. This results in fissures spreading radially from each cutter disc track, effectively crushing and breaking of the rock surface as shown in figure 2.3.
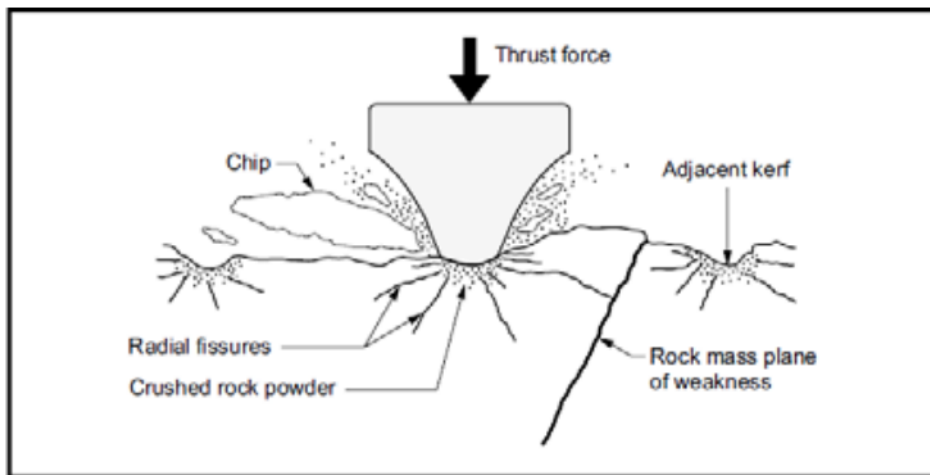
Figure 2.3 – *Cutter head principle from Bruland (1998)*

Figure 2.4 shows typical grading of TBM spoil from Bruland (1998). According to Bruland the grading of TBM spoil is dependent upon the geological conditions, but the spoil is generally well graded and containing 15 - 20% fines.
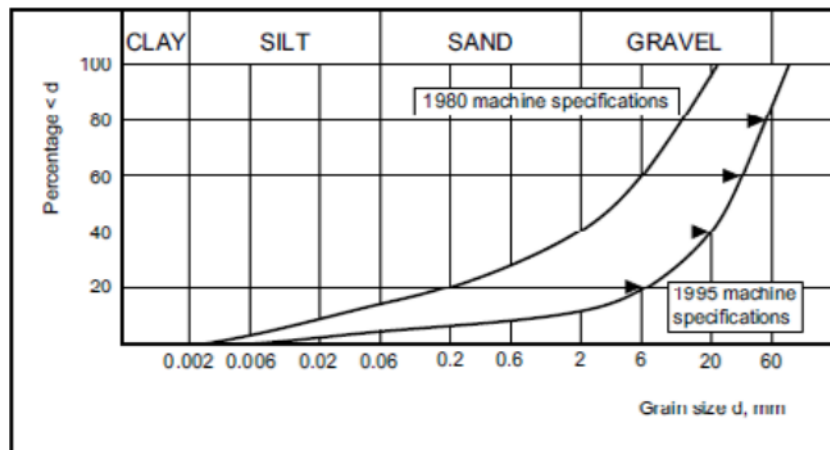
Figure 2.4 – *Typical grading of TBM material from Bruland (1998)*

The geological report conducted for the Follo line project reveal that the rock largely consists of Precambrian gneiss with significant intrusions from the Perm period and occurrences of amphibolite dykes (Jernbaneverket 2014).

2.1.1   TBM spoil as a construction material

The amount of generated spoil from a tunnel construction is large and the potential for environmental and economical benefits from utilizing tunnel spoil for construction purposes is great. Gertsch et al. (2000) Analyzed TBM cuttings created by a laboratory tunnel boring machine with the intention of investigating the materials suitability for different applications. The study includes descriptions of several tunneling projects were the TBM spoil has been analyzed or used further as a construction material. A short summary of the projects he described is presented here.

Among the projects that have found a use for the TBM spoil is a project in Milwaukee (U.S.) completed in 1992. The mother-stone in this project was limestone, and the spoil was used to construct an island and in erosion control of beaches. The rest of the material was processed and sold as gravel. In Massachusetts (U.S.) TBM muck of kaolinite was evaluated for use as an aggregate in concrete, it was however deemed unsuitable because of its potential for alkali-silica reactivity. The kaolinite spoil was instead deemed usable as fill material in a road sub-base, landfill or cofferdam fill.

In Norway, hydropower projects have been the reason for several tunnel constructions. This has lead to many kilometers of TBM excavated tunnels producing massive amounts of spoil which has been used as fill material in and around the hydropower construction projects. Gertsch et al. (2000) mentions, among others: the *Kobbelv hydropower project* and the *Jostedal hydropower project*. In the Kobbelv project TBM spoil of brittle, granitic gneiss without further processing was used as fill and subbase in highway construction. The material did not work well as a subbase material due to problems with frost heave, uneven settlement leading to cracking of the asphalt layer. It was concluded that because the rock was brittle, traffic caused a great deal of crushing which increased the fines content of the subbase and thus increasing frost susceptibility and causing heave damage. The same brittle TBM material was also used in construction of a

temporary road to a construction site with better results. Despite the heavy truck traffic the road resisted track formation, had good drainage and produced smooth surfaces, however the crushed fines on the surface caused the road to become slippery during rainfall. Another granitic gneiss spoil was used in the *Fløyfjellet road tunnel* project in Bergen, Norway in 1985. In this project the material was screened and sorted and the particles <35mm was bound in cement creating a base material which performed well as base fill in a road construction.

The TBM spoil from the *Jostedal hydropower project* was used as an aggregate in concrete. The spoil was mixed with 30% natural gravel and crushed stone, and material coarser than 10mm was crushed. This was not entirely successful as there was large variations in the quality of the concrete. It was concluded that variations in grading, grain shape and mechanical strength of the untreated spoil caused the uneven quality and strength of the concrete. TBM spoil with a majority of phyllite was used as fill in a housing area in Stavanger, Norway. In this project, the TBM materials were mixed with blasted tunnel material of unknown type. The fill did experience problems with water sensitivity, making the material slippery and muddy during rain. After compaction however, the fill was stable and did not settle. In Klippen, Sweden, most of the TBM spoil was used for landscaping near the tunnel construction area because long transport distances made it economically unfavorable to use it in other projects.

Based on the laboratory study and the previous projects Gertsch et al. arrived at the following conclusions:

- TBM spoil has successfully been applied in many construction projects

- The suitability is dependent upon the mineralogy and geologic structure of the parent rock and the parameters of the TBM

- Unprocessed TBM spoil of **hard rock** is generally well graded with large, flat, elongated chips and relatively few fines.

- The properties of the spoil may be altered by processing such as crushing, sieving and sorting and mixing with other materials

- Hard and not too brittle parent rock results in the best spoil for use in constructions

Tokgöz (2013) investigated whether TBM spoil from tunnel excavations in Istanbul was suitable as fill material in abandoned quarry pits to be used for water storage. He state that in order to prevent absorption of water into the fill and particles being washed out and accumulating on the bottom of the reservoir it is important to wash out any clay minerals in the TBM spoil. The study showed that the TBM material was suitable for use in the abandoned quarry pits after washing out the finer particles.

Berdal (2017) investigated the possibility of using chips from TBM spoil as concrete aggregate. He concludes that TBM spoil of hard rock is a high quality construction aggregate with an unfavorable shape and excessive filler amount (grains <0.125mm). He further states that crystalline rock may contain sulphur, mica or alkali reactive minerals which is unfavourable for use in concrete, however the technology to process the material in order to remove these impurities, while expensive, does exist.

In summary, TBM spoil/muck has successfully been utilized in various constructions with many showing good results. The mechanical properties and behavior of the material depends upon the properties of the parent rock and the cutter disc spacing of the TBM. The spoil has been used as fill material in dam constructions, road constructions and landfills with success, but it is important to properly investigate the material at hand. Use of spoil as a concrete aggregate is

being researched and processing of the spoil, sieving, sorting and removal of impurities is believed to be a good substitute for conventional fillers. The strength and resistance to crushing of the aggregate is of great importance for use in concrete and asphalt. The utilization of TBM spoil can be challenging if it is necessary to alter the material as the amounts of material being produced is generally very high in tunnel construction projects and it accumulates fast. In addition, it is not possible to obtain detailed information about the material before it is produced and stored. Expedient handling and utilizing of the material is therefore a big and complicated task, but the environmental and economical gain is considerable compared to transporting and depositing it as waste.

2.1.2 TBM material behavior

In 1985 the Norwegian Geotechnical Institute (NGI) investigated 19 different TBM spoil samples from 16 tunnel projects in order to gain a better understanding of TBM spoil as a material. The samples represents a wide variety of rock; Schist, Granite, Greenschist, Granodiorite, Limestone and Shale, Gneiss and Phyllite. The samples were cut with TBMs from different manufacturers with different diameters. All used disc cutters at high cutter load.

Grain size distribution:
The grain size distribution revealed a higher fines content for the Phyllite and Schist, but otherwise little variations in the samples. The spoil is well graded with an average fines content ($<63\mu$m) between 7 - 15% and content <22.4mm between 53-90%. In accordance with the Norwegian Public Roads Administration (Statens vegvesen 2014) the spoil is defined as water sensitive. The consequence of which is that the material is not free draining because the relatively high amount of fine particles will retain water. Permeability tests were conducted at medium relative density, with a porosity just under 30%. The permeability of the material is equal to that of a silty sand, in the order of 10^{-3}-10^{-4}cm/s. Further testing of the fines with hydrometer analysis revealed that the amount of particles < 0.02mm varies between 4-10%. The material is classified as somewhat frost susceptible (Statens vegvesen 2014). The TBM spoil has a low crushing resistance as revealed by a dropping mortar test.

Triaxial tests:
Drained triaxial tests were conducted on the presumed weakest and strongest materials, Phyllite containing 15.1% fines (weak) and Granodiorite containing 8.5% fines (strong). The results are shown in figure 2.5 together with data points on crushed rock and blasted rock from tunnel construction.
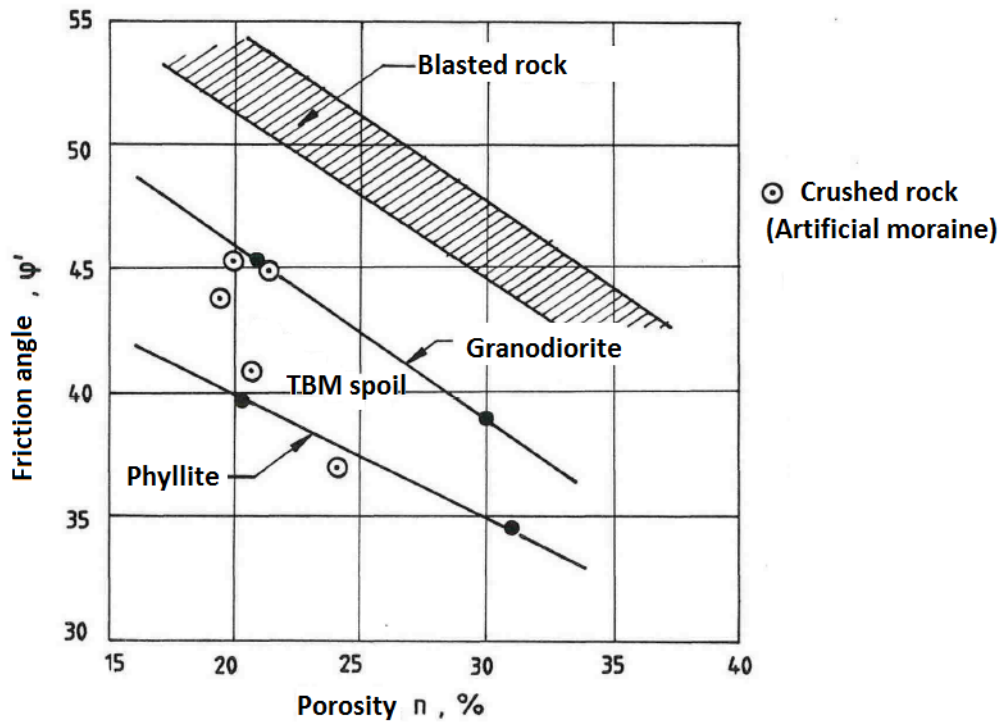
Figure 2.5 – *Friction angle versus porosity from triaxial tests on TBM spoil samples tested by NGI. (NGI 1986)*

The angle of friction, φ', in coarse materials is dependent upon the porosity of the material and the shape and size of the particles. The friction between grains of the soil skeleton is higher in well graded samples than in uniformly graded samples. The friction is also larger for materials where the individual grains are sharp edged rather than round. Densely packed materials will also have a higher resistance to shear stress because of the increase in friction between particles as they are pressed together (Kjærnsli et al. 2003).

The TBM spoil yields friction angles roughly 10° lower than blasted rock of the same porosity. NGI (1986) further state that because the TBM spoil has a higher potential for compaction, the material will have a lower porosity and therefore a friction angle closer to the blasted rock material for the same amount of compaction work.

The triaxial tests revealed that the TBM spoil achieves relatively high cohesion (c) - values with results between 75 - 145kN/m^2. The report states that the high c - values most likely are caused by the extra friction created by the surface of the lief shaped grains in the TMB spoil and that this "cohesion effect" is expected to be anisotropic $\rightarrow$ The shear strength is expected to vary with the direction of the shear stress.

9

2.1.3 Strength and deformation properties of crushed rock

Shear strength:

In 1970, T. M. Leps assembled a large number of triaxial shear strength data from various rockfills. Figure 2.6 is a collection of the results made by Leps showing peak friction angle of the rockfills versus the estimated normal effective stress on the failure plane.

Leps results show a clear decrease in angle of friction with increased effective stress in granular materials. They further support Kjærnsli with results showing higher resistance to shear stress for well compacted, well graded, high strength particles. Samples of loosely compacted, uniformly graded, weak particles yielded friction angles roughly 10° lower.
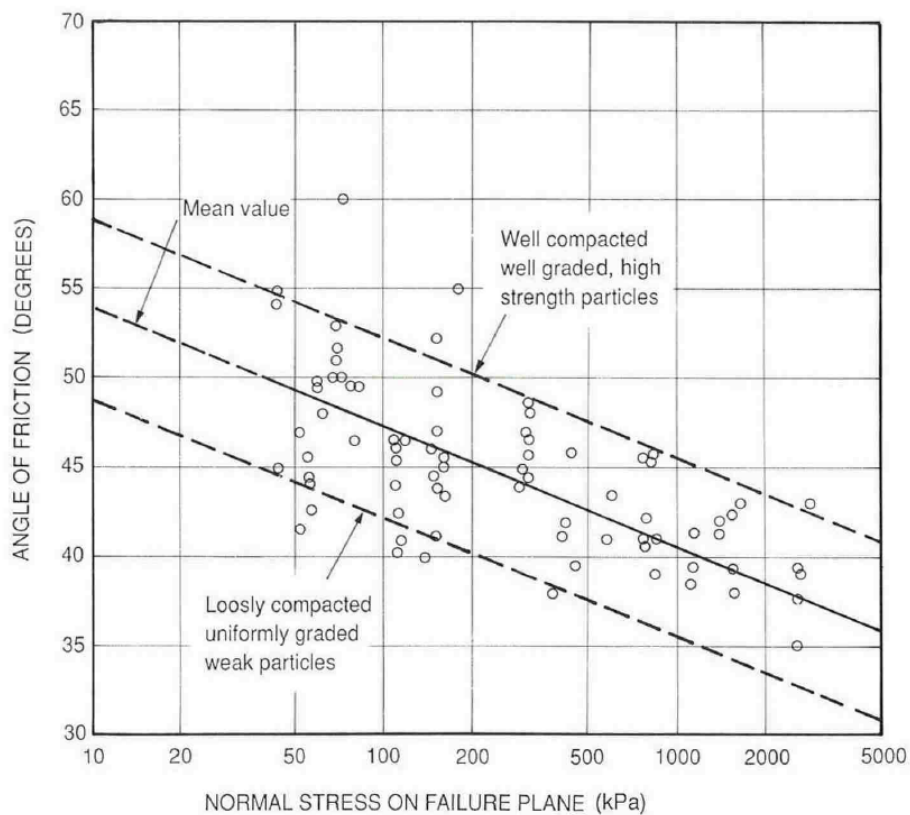
Figure 2.6 – *Rockfills of different grading and porosity plotted with friction angle versus effective stress on the failure plane (Leps 1970)*

Deformation properties:

Kjærnsli et al. (2003) investigated the strength and deformation parameters on crushed syenite at different porosity and with different grain size distributions. The materials resistance to deformation was tested using a 600mm diameter oedometer cell. The results indicate that the compression of a coarse material is a direct consequence of structural change and crushing because of interparticle contact. Kjærnsli concludes that the structure of compacted fills depends on the size and shape of the particles and on how the material is placed and compacted. The samples became more stable with vibratory compaction methods shaking the particles into place than with static pressure alone. Figure 2.7 show results from the 600mm diameter oedometer tests of crushed syenite.
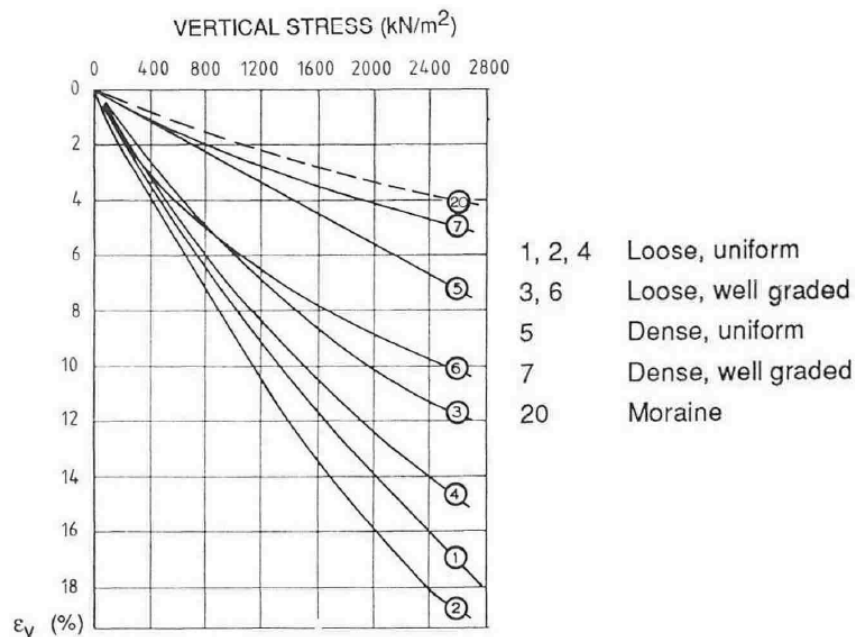
Figure 2.7 – *Oedometer tests on crushed syenite with varying grading and degree of compaction (Kjærnsli et al. 2003, p.45)*

The resistance to deformation in the oedometer is higher for well graded, compacted material, curves 20(Moraine) and 7(Dense, well graded). The materials with least resistance to deformation are uniformly graded, loose material, curves 1, 2 and 4. The tests indicate an increase in resistance to deformation (modulus) with increasing stress level. The increase is greatest for well graded, loose rockfill; curves 3 and 6.

The conclusion is that well graded material with rounded particles will be less compressible than sharp edged and flaky, uniformly graded material. Because mineral strength and particle shape affect the extent of crushing at interparticle contact points, rounded grains of hard, sound rock are the most resistant to compression Kjærnsli et al. (2003).

In the master's thesis *Creep deformation of rockfill* from 2014 Veronica Gustafsson gathered some recommended values for oedometer modulus and Young's modulus for crushed rock based on reports provided for the project by COWI. The values are presented in figure 2.8 (Gustafsson 2014).

Oedometer modulus, E_{ocd}	Source
20-30 MPa for uncompacted rockfill	Lindblom (1972)
Up to 60 MPa for compacted rockfill	
45 MPa Above water level for probably compacted crushed rock	COWI (2011)
35 MPa Below water level for probably compacted crushed rock	
50-60 MPa from tests on Danish rockfill	

Table 2 Young's modulus – recommended values from the literature

Young's modulus, E	Source
14 MPa for a rockfill with grain sizes between 70 and 100 mm	COWI (2011)
45-50 MPa above water level	COWI (2011)
35-40 MPa below water level	
45 MPa long term for compacted crushed rockfill	COWI (2012)
90 MPa short term for compacted crushed rockfill	
15 MPa long term for uncompacted crushed rockfill	
30 MPa short term for uncompacted crushed rockfill	

Figure 2.8 – *Oedometer modulus and Young's modulus on crushed rock as presented by (Gustafsson 2014, p.4) The vertical stress range is not provided in the text*

The rockfill material in the study is presumed to consist of sandy gravel mixed with larger cobbles and boulders. The grain size distribution is unknown.

By back calculation of a full scale creep monitoring on uncompacted rockfill Gustafsson got significantly lower modulus results than suggested by the literature. For a mean vertical stress level of 74kPa the calculation results were M = 4.6 MPa and M = 6.0 MPa. Mean vertical stress of 57kPa yielded M = 2.9 and 4.7 MPa. The stress range in which the recommended values are valid is not provided in the report. Higher vertical stress range in the tests from the literature may be the cause of the large difference in modulus.

In a publication by NGI (*Publication 073*), Kjærnsli presents a figure that shows the deformation of various coarse materials typically used in fills. They are presented in a load versus deformation diagram and the results are from oedometer testing. Figure 2.9 is a translated copy of the one presented in *publication 073* (Kjærnsli, B. 1968).
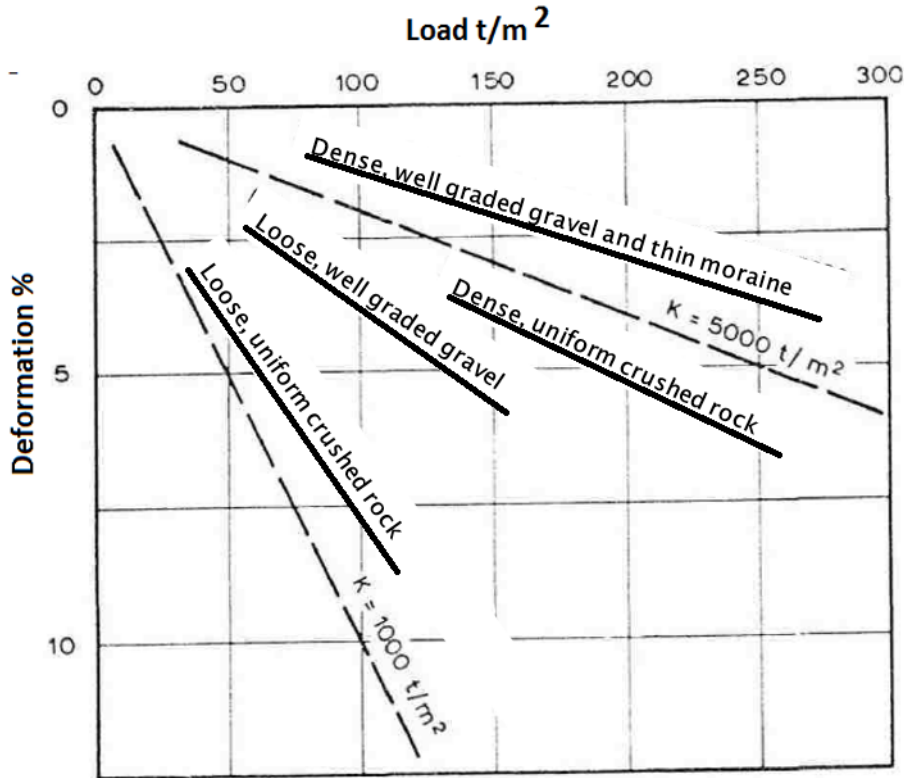
Figure 2.9 – *Compression of different materials found using oedometer, translated from (Kjærnsli, B. 1968, p.2). K denotes the compression modulus and is a measurement of the materials compressibility*

In the report the compression modulus, denoted K (usually referred to as the oedometer modulus, M), is used as the modulus of deformation and is a measurement of the materials compressibility. The modulus relates to the load - settlement curve with the equation:

$$\varepsilon = \frac{\delta}{H} = \frac{p}{K} \tag{2.1}$$

Where δ is the deformation of the specimen with a height = H, p is the vertical load and K is the compression modulus. ε is the measured vertical deformation in % (strain). The load reaches a maximum of 300t/m² ≈ 3000kPa. These results are in line with previously discussed parameters of coarse materials. Dense, well graded materials shows the highest restraint against deformation while loose, uniformly graded materials are the easiest to deform.

2.2   Coarse fills and compaction control

As Kjærnsli concluded from his investigation of compaction and deformation properties of different coarse materials, the compression of a compacted sample is a consequence of structural changes and local crushing of particles (Kjærnsli et al. 2003). The structure of a compacted fill will depend on the size and shape of the particles in the material and how it is placed and compacted.

A central issue in geotechnical engineering is settlements after construction, which can result in damages and shorter structural life. All material will experience settlements as a consequence of construction and compaction when exposed to a new load higher than the stress history of the material. It is important to predict, design for and if necessary add preventive measures against unwanted settlements of the fill. In general, damage to buildings and structures are most commonly caused by uneven deformation. Therefore it is important that the degree of compaction and stiffness of the material is relatively uniform throughout the area. An extreme example of uneven settlements beneath a construction is the leaning tower of Pisa. Figure 2.10 from the soil compaction handbook by Multiquip (2011) illustrates the possible foundation problems that may occur as a result of improper or poor soil compaction.

Basement & Pool
Cracks & Leaks

Slab Cracks

Pipe Leakage
& Breaks

Foundation Erosion

Erosion Gullies
Under Abutments

Utility Trench
Settling
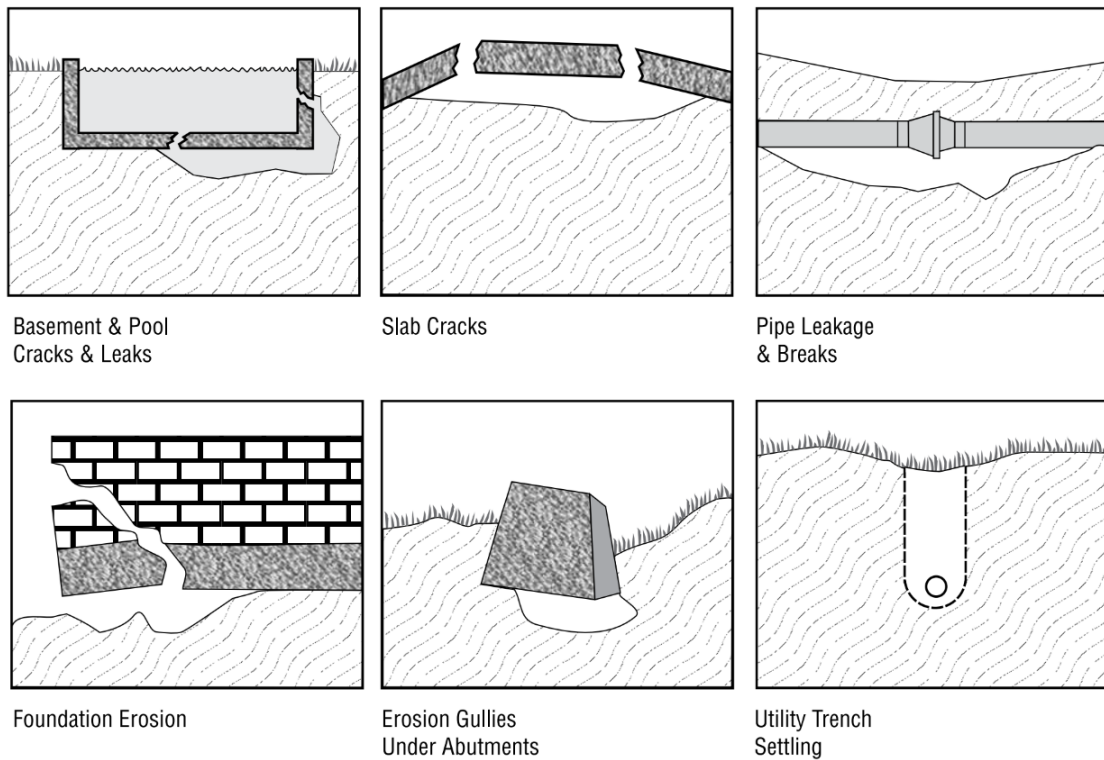
Figure 2.10 – *Results of improper compaction (Multiquip 2011)*

2.2.1   Layer thickness

The vibratory roller has a limited ability to compact at depth. Because the vibrations are applied to the surface of the layer, the effect of the compaction will decrease with depth. Bertram (1987) conducted a comprehensive field study on compaction of crushed rock for use in dam construction. Bertram developed a test quarry with materials as equal as possible to the actual dam construction. The aim was to use this material in test fills in order to establish acceptable layer thickness before compaction. While thicker layers will reduce both time and costs for the project the need for maximum compaction throughout the dam construction is essential for the structural integrity of the construction. His results show that the settlements in the rock fill was independent of layer thickness for layers thicker than 45cm. This supports the conclusion that vibratory rollers are not effective on crushed rock materials at greater depths.

Increasing the weight of the roller will not necessarily produce deeper and better compaction, according to Bertram the increased weight increases the pounding on the surface in such a way that unwanted fines may be created by crushing and beaten upwards, collecting on the surface of each layer.

While Bertram's findings from 1987 is highly relevant for compaction work and control tests, the vibratory rollers have seen some upgrades since then. Kim et al. (2014) conducted a field test inquiring whether new and improved equipment could satisfactory compact thicker layers of coarse grained fills than what is commonly used based on older specifications. The coarse grained material used in this study was silty sand and uniform sand. By testing different compacting equipment on a lift thickness of commonly used 0.2m for a coarse grained road construction and a lift thickness of 0.3m they concluded that today's equipment could be used for compaction of 0.3m thick sand layers without compromising the quality of the compaction work. Most importantly the study confirmed that equipment used for compaction today does indeed distribute compaction energy further down in the material than what older standards are based on.

The Norwegian standard *NS 3458:2004. Compaction Requirements and execution* (Standard Norge 2004) provides an up to date maximum layer thickness for crushed rock fills (Crushed rock from crushing facility). Table 2 states that the maximum layer thickness (before compaction) of a crushed rock fill using a vibratory roller is 0.8m, while the maximum layer thickness for gravel is set to 0.7m with the same equipment.

2.2.2   Compaction control

The standard Proctor test is used to find the compaction properties of the specific soil. The Norwegian Public Roads Association states that the compacted soil after construction should be within 95% of standard Proctor maximum compaction values (Statens vegvesen 2015). Based on allowable deformations of different fills/area of the fill the required degree of compaction and stiffness is set. A green area will not have the same requirements as a road construction or the area beneath a footing. The compaction control is important to document and check that the compacted fill does indeed meet the requirements set by the reference procedures.

In soils where obtaining undisturbed samples is difficult or impractical, isotope sounding may be used to determine density and water content. A commonly used device for shallow isotope sounding near the surface is the Troxler device. It uses a radioactive source of isotopes to measure the density and water content of the material. Figure 2.11 is a principle sketch of the Troxler nuclear density gauge.
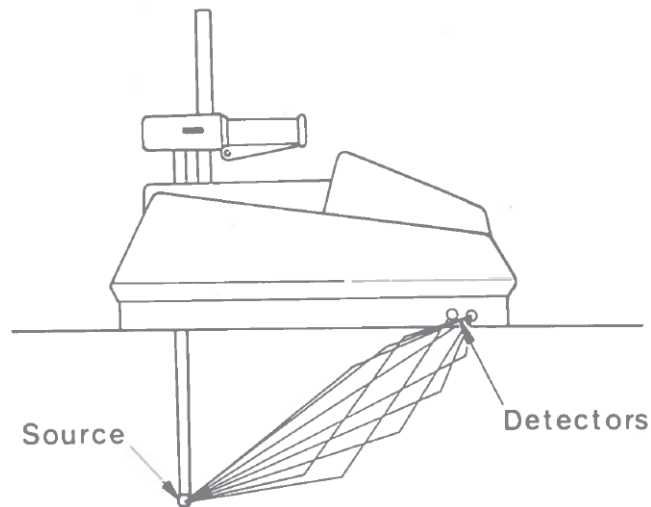
Figure 2.11 – *Principle sketch of the Troxler isotope sounding (NTNU 2015, p.293)*

The isotope moisture sounding works by emitting neutrons which collides with hydrogen atoms decreasing their energy effectively, the detectors then count the low energy neutrons and calculate the amount of hydrogen atoms in the material. It is assumed that nearly all the hydrogen is bound to water molecules. The density is investigated by emitting gamma rays and detecting how much of the energy is absorbed by the material. The detectors counts the gamma rays which are not absorbed and calculates the subsequent density of the soil (NTNU 2015).

The plate load test (PLT) is frequently used as a tool in compaction control in road constructions. The principle of the test is explained in section 2.3.1 of this report. The plate load test is used to investigate the stiffness of the material and estimate settlements of footings based on the obtained results. As a tool in compaction control however, the allowable settlements for the fill are decided and requirements for the plate load test is set for control.

2.3   Settlements

It is most common to view settlements in soil as a three stage process; immediate/initial compression(S_e), primary consolidation(S_c) and secondary compression/consolidation commonly referred to as creep(S_s). The total settlement is then equal to the sum of the three, $S_{tot} = S_e + S_c + S_s$.
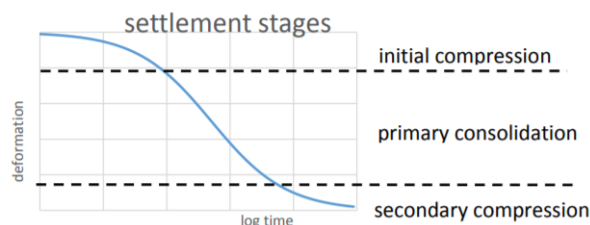
Figure 2.12 – *Typical view of the settlement process. Illustration by Gustafsson (2014), based on settlement theory from Olson (1989), Janbu (1970)*

For this model of settlement calculation it is assumed that the three stages of settlements are separated in time, as shown in figure 2.12. It is however generally acknowledged that there exists no clear line between the stages and that primary and secondary consolidation happen simultaneously (Olson 1989, Janbu 1970).

Initial compression describes the immediate settlements that occur when load is applied. This is an elastic deformation of the soil before water begins to dissipate. The deformation is caused by a reduction in volume of air, not a reduction in volume of water (NTNU 2015). The initial compression predominates in cohesionless soils and unsaturated clays. According to *aboutcivil.org* analysis of the initial compression is used for fine grained soils with a degree of saturation $< 90\%$ and for coarse grained soils with a large coefficient of permeability.

Primary consolidation is defined as the time dependant process caused by an *increase in effective vertical stress* which is a result of dissipation of excess pore water pressure with time. This process transfers the loads from the water to the soil skeleton. The deformations caused by the drainage of water is plastic, and will not fully regress after unloading. The primary consolidation is most important in materials with low permeability where dissipation of water takes some time and the settlement is delayed. In coarse grained materials with high permeability the compression caused by water dissipation will happen almost instantly, overlapping with the initial elastic compression (Olson 1989).

Secondary consolidation/Creep is defined as the time dependant increase in strain under a *constant vertical effective stress*. The strain is caused by a constant rearrangement of the particles under stress into a more stable form. This may be caused by shifting or crushing of particles into place.

The traditional view of settlement as a three stage process places the secondary consolidation after the primary consolidation separated in time so that creep does not begin until all pore water is drained. In reality however, it is believed that the primary and secondary consolidation are occurring simultaneously and overlapping. Olson explains that because different size pores and voids in the material will drain at different speed the crushing and rearrangement after dissipation will overlap with the primary consolidation process.

2.3.1   Calculating settlements

In order to investigate settlements of soil based on the field- and laboratory investigations conducted in this project the understanding of the soil's resistance to deformation is crucial. The oedometer (one-dimensional) and plate load (three-dimensional) tests are incomparable due to the different conditions of the soil samples. $\mathbf{M} = \mathbf{E}_{oed}$ is the oedometer stiffness. This is used to describe the resistance to deformation of a soil element constrained to the sides but free to move in the vertical direction when exposed to a vertical stress σ'_1. The Young's modulus, $\mathbf{E}$ describes the resistance to deformation with applied vertical stress, σ'_1 but for a soil element which is restrained only at the bottom and free to deform to the sides.

The general expression for calculations of settlements is written: (Tan et al. 2003)

$$\delta = strain \cdot stressed\ length = \varepsilon H = \frac{\Delta\sigma'}{E}H \tag{2.2}$$

Where:
δ = Deformation/settlement
ε = Strain
H = Height of sample
E = Young's modulus/Other modulus based on conditions
$\Delta\sigma'$ = change in effective stress

The modulus is chosen based on the boundary conditions of the soil:

Unconfined $\rightarrow$ E = Young's modulus

Confined modulus = $\frac{E(1-\nu)}{(1+\nu)(1-2\nu)} = E_{oed}$

It is important to assess the conditions (boundary conditions and restrictions) of the situation when calculating settlements. It is common to use the Young's modulus in calculations of settlements for narrow footings and the oedometer modulus for widespread loads. Plate load results are commonly used to estimate settlements of footings.

Calculations based on oedometer tests

In geotechnical engineering the soil stiffness is most frequently determined by the oedometer test in the laboratory. The purpose of which is to determine the deformation parameters of the soil and establish the stress - strain relationship. Settlements are then predicted by calculating strains (ε) due to increased effective stress ($\Delta\sigma$'), and find the vertical deformation (δ).

During the construction period the ground will experience increased stress which creates an excess pore pressure (u_{excess}). As water dissipates, the excess pore pressure decreases, which results in settlements of the soil due to the increase in effective stress, $\sigma' = \sigma - u$. Consolidation settlements will continue as long as there is an excess pore pressure.

The stress state is three dimensional, but in the calculations it is assumed that the deformation only occur in the direction of the load. In the oedometer test, these assumptions are represented by the boundary conditions. In cases where the foundation is highly loaded, oedometer tests are known to present a stiffness which is too high due to the high shear mobilization beneath the foundation (NTNU 2015).

From the oedometer, which is a one-dimensional compression test, the one dimensional constraint modulus M $= 1/m = \frac{\Delta\sigma_v}{\Delta\varepsilon}$. As M varies with both the current stress level, σ' and the stress history of the sample Nilmar Janbu developed a method for calculating settlements based on the parameters he called Janbu's modulus number, m and the stress path exponential, a.(Tan et al. 2003)

The modulus number is a parameter which describes the increase in M with stress while a is an exponential which is used to regulate the curve of the modulus with increasing stress level. Figure 2.13 shows how the exponential a typically varies with the compaction/pore volume of different materials.
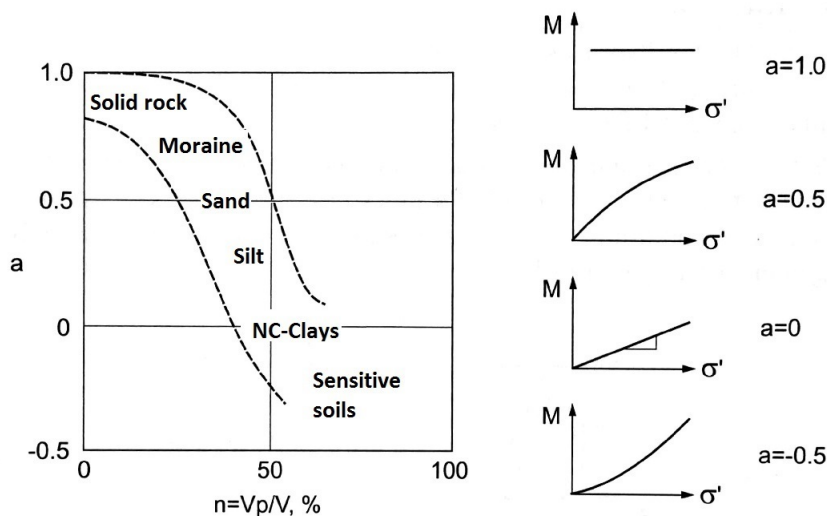
Figure 2.13 – *Typical stress curve exponential of the oedometer modulus according to Janbu (1970)*

Granular materials (i.e. Sand or gravel) will typically follow the curve where the exponential a = 0.5. These materials experience a parabolic increase in stiffness with increased load, and thus varies between 0 and 1.0.

a = 1 corresponds to elastic behavior, this yields a constant M and is considered true for materials which have completed consolidation as long as the load does not exceed the preconsolidation stress, p'_c. For normally consolidated clays and silt a is typically equal to zero and the stiffness increases linearly with stress after p'_c. In some cases the modulus will increase rapidly with increased stress and a < 0, this may occur in sensitive materials where the stiffness suddenly increases as the structure collapses under loading and becomes more stable (Emdal 2014).

The general expression for the oedometer modulus from Janbu (1970) is expressed as:

$$M = m \cdot \sigma_a \Big(\frac{\sigma'}{\sigma_a}\Big)^{1-a} \tag{2.3}$$

Where:
σ' = Effective stress
σ_a = Reference pressure of 1 atmosphere or 100kPa
a = The stress curve exponential

Emdal further states that when a soil element is exposed to a change in stress level $\Delta\sigma'$ from σ'_0 to σ' the resulting strain may be expressed as:

$$M = \frac{d\sigma'}{d\varepsilon} = m \cdot \sigma_a \Big(\frac{\sigma'}{\sigma_a}\Big)^{1-a} \tag{2.4}$$

$$\rightarrow \varepsilon = \frac{1}{am}\left[\Big(\frac{\sigma'}{\sigma_a}\Big)^a - \Big(\frac{\sigma'_0}{\sigma_a}\Big)^a\right] \tag{2.5}$$

The parameters a and m are decided by interpreting the stress-strain relation from the oedometer test and so an estimate for the deformation may be found:

$$\delta = \varepsilon H \tag{2.6}$$

For fully consolidated materials a will typically be equal to 1, as described in figure 2.13. This results in $M = m\sigma'$ and the material is considered to have a constant stiffness with increasing stress level. In compacted fills it is therefore common to estimate the settlements for added loads using the oedometer modulus M = E_{oed} from the appropriate stress state with the general equation for calculating deformations:

$$\delta = \varepsilon H = \frac{\Delta\sigma'}{M} H \tag{2.7}$$

This is generally accepted as a good estimation method for well compacted fills and should return results of reasonable quality. If loads exceed preconsolidation stress or the compaction has not resulted in complete consolidation, estimations of settlement should be done by establishing m and a from the acquired modulus - stress curve. m is the slope of the curve after preconsolidation, a may then be found by fitting Janbu's modulus equation to the modulus - stress curve with Eq.2.3:

Calculations based on plate load tests

The plate load test is commonly used as an *in situ* test in foundation design and in the construction of roads. The method provides an indication of the compaction of the soil and provides data for the load - settlement curve of the material. The test thereby yields information on the strength- and deformation properties of the soil without the risk of sample disturbance which may occur during sampling and transportation of samples for laboratory testing. The test is performed by incrementally loading a round plate which is placed on the surface of the soil. The resulting vertical deformation of the plate is measured. It is common to apply two loading cycles, and the resistance to deformation E is found (Statens vegvesen 2018). The equipment, method and calculation of results are explained in section 3.1.4 of this report.

Because most soils show an elastoplastic behavior the *resistance to deformation modulus*, $E_{1,2}$ is the modulus of deformation, E_{def} and not the modulus of elasticity, E. $E_{1,2}$ is obtained from the load - settlement curve of the plate bearing test as the resistance to deformation of the first and second loading cycle.

Pantelidis (2005) investigated the connection between the deformation modulus, E_{def} from the plate bearing test and Young's modulus of elasticity, E using the Finite Element Method. Dr.Pantelidis established a correlation between E and E_{def} and introduced a coefficient, $I_L \geq 1$. Thus, the E-modulus of the soil is larger than the E_{def} determined using the plate loading test. The coefficient I_L is a function of the shear strength parameters of the soil, ϕ and c, the radius of the bearing plate, α and the load, p.

$$E = E_{def} \cdot I_L \tag{2.8}$$

Calculation of the coefficient, I_L for a loading plate with diameter = 300mm as found by Pantelidis, is shown in figure 2.15.

Figure 2.14 explains the definitions of the modulus of elasticity and the modulus of deformation. The elasticity modulus is defined as the slope of the tangent line in a stress-strain diagram, in the area where the material has a completely elastic behavior. Within the elastic zone any displacements are resilient and not permanent. The modulus of deformation is similarly defined as the slope of the straight line crossing through (p, ε) and (p_0, ε_0).
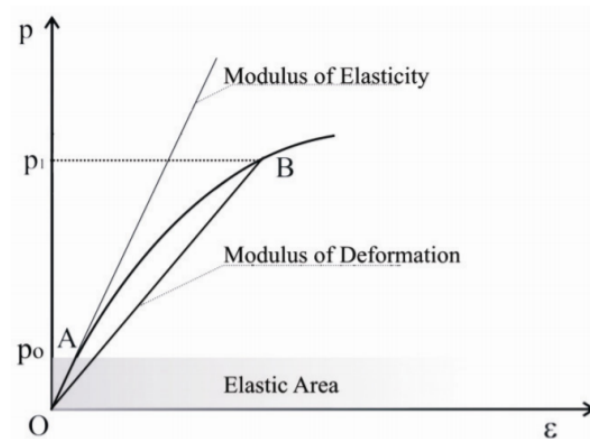
Figure 2.14 – *Modulus of elasticity and modulus of deformation definition (Pantelidis 2005)*

p (kPa)	10<φ≤23 $$I_L = \frac{k}{(\sin\phi)^l \cdot \left(\frac{c-c_o}{c_o}\right)^m}$$			23<φ≤45 $$I_L = \frac{k}{(\sin\phi)^l \cdot \left(\frac{c}{c_o}\right)^m}$$		
	k	l	m	k	l	m
200	0.296	1.954	2.037-4.034·sinφ	0.535	2.242	2.464-3.176·sinφ
250	0.224	2.234	2.406-4.938·sinφ	0.488	2.417	2.723-3.475·sinφ
300	0.195	2.357	2.619-5.616·sinφ	0.488	2.451	2.575-3.236·sinφ
350	0.216	2.257	2.507-5.381·sinφ	0.480	2.496	2.647-3.285·sinφ
400	0.327	1.898	1.979-3.686·sinφ	0.510	2.376	2.319-2.786·sinφ
450	0.186	2.399	2.594-5.502·sinφ	0.505	2.391	2.416-2.888·sinφ
500	0.146	2.622	2.773-6.045·sinφ	0.483	2.477	2.443-2.859·sinφ
$c_o = 0.03 \cdot p$ and $c_{min}=1kPa$						

Figure 2.15 – *Calculation of I_L for a d=300mm bearing plate (Pantelidis 2005)*

The plate load test is ideal for compaction control on road or foundation construction. The load - settlement curve is obtained without delay and the deformation modulus for for the two loading cycles will yield information of the compaction of the material and how much of the compaction potential of the material is achieved.

In addition to compaction control, the plate load test is commonly used to calculate settlements of footings, rather than for a widespread area. This is achieved by establishing a ratio between load and settlement called the coefficient of subgrade reaction, k_s. Figure 2.16 shows relation between subgrade deformation characteristics and contact pressure on the surface with a perfectly rigid footing.
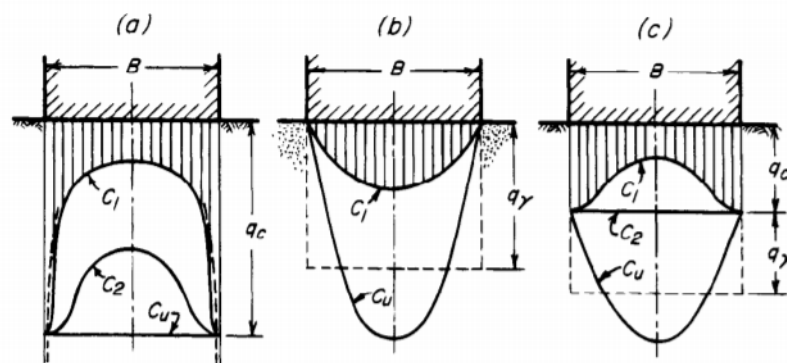
Figure 2.16 – *Distribution of contact pressure on the base of a smooth rigid footing. (a) - elastic material, (b) - cohesionless sand and (c) - Soil with intermediate characteristics. C_u refers to contact pressure when footing is loaded to ultimate value (Terzaghi et al. 1996, p.299)*

Because the relationship between the subgrade reaction and the surface load is so complicated, even under the assumption of smooth, perfectly rigid footing, it is necessary to simplify the assumptions and then compensate for the error by an adequate factor of safety. (Terzaghi et al. 1996).

Wrinkler's hypothesis assumes that the soil is a system of identical, closely spaced, linearly elastic springs. Thereby viewing the subgrade reaction k_s as the spring stiffness so that: $k_s = \frac{load}{settlements}$. The simplification is based on the assumption that the ratio between load and deformation is constant. By investigating small areas with the plate load test it is possible to establish the modulus for subgrade reaction by reading the load-settlement curves after one loading cycle.

Teodoru & Toma (2009) explains that because the coefficient of subgrade reaction is not an intrinsic property of the soil but rather a value dependent on not only the soil stiffness but also on the geometry and stiffness of the structural soil element, it is wise to be skeptical to this simplified view of the subgrade behavior. They further explain another approach to assess the settlement properties when designing a footing based on the plate load test, *the elastic continuum idealization*. This method is based on the assumption that the soil is a linear elastic half space and isotropic. Figure 2.17 shows a typical presentation of results from a plate load test with one loading cycle. Here, p_l and w_l denotes the limits of applied load and settlement in which the soil reaction is still within the elastic zone.
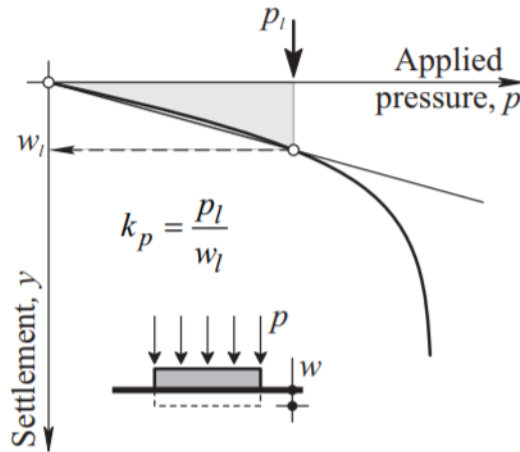
Figure 2.17 – *Typical presentation of load-settlement curve from a plate load test (Teodoru & Toma 2009, p.2)*

For *the elastic continuum idealization* method the Young's modulus(E), coefficient of subgrade reaction(k_s) and Poisson's ratio(ν) are derived using the following equations (Teodoru & Toma 2009):

$$w_l = \frac{\pi}{4}\frac{p_l D(1 - \nu^2)}{E} \tag{2.9}$$

$$E = \frac{\pi}{4}\frac{p_l}{w_l}D(1 - \nu^2) \tag{2.10}$$

$$k_s = \frac{4E}{\pi D(1 - \nu^2)} \tag{2.11}$$

23

Where:

D is the diameter of the bearing plate and ν is the Poisson's ratio.

Because the subgrade coefficient is dependent upon the area of the footing used to apply the load, one should not use the plate load test result directly to calculate settlements of a full size footing. Terzaghi et al. (1996) suggest that the adjusted coefficient of subgrade reaction beneath a footing may be calculated through the following equations:

$$For \ \ clayey \ \ soils \rightarrow k_s = k_p \frac{B_p}{B} \tag{2.12}$$

$$For \ \ sandy \ \ soils \rightarrow k_s = k_p \left(\frac{B + B_p}{2B} \right)^2 \tag{2.13}$$

Where:

B_p is the plate diameter or side of a square plate used in the plate load test

B is the diameter or side dimension of the full sized footing

k_p is the coefficient of subgrade reaction found by the plate load test

k_s is the coefficient of subgrade reaction for the full sized footing

Terzaghi further recommends the following equations for directly estimating settlements beneath a footing:

For cohesive soils:

$$S_f = S_p \frac{B_f}{B_p} \tag{2.14}$$

For non-cohesive soils:

$$S_f = S_p \left[\frac{(B_f(B_p + 0.3))}{(B_p(B_f + 0.3))} \right]^2 \tag{2.15}$$

Where S_p and S_f are the settlements-, and B_p and B_f are the widths of the plate and the foundation, respectively.

Typical load - settlement curves of different materials loaded until shear failure obtained from PLT are presented in figure 2.18.
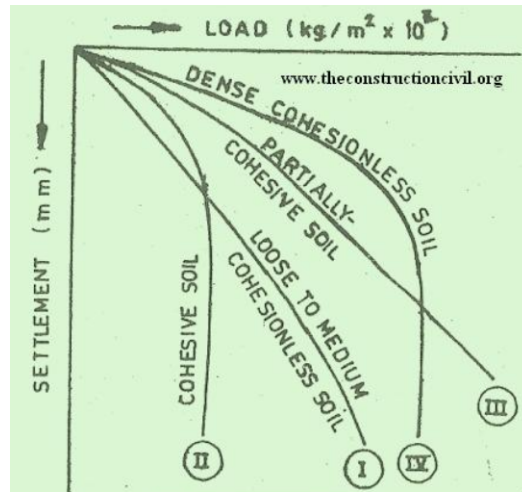
Figure 2.18 – *PLT characteristic load - settlement curves of different materials (Construction civil 2018)*

The load - settlement curve will present information on the soil properties by comparing the shape and size with experience based values and curves. The criteria set by the Norwegian Public Roads Administration for compaction control with PLT on road constructions are: E_2 (Modulus of the second loading cycle) $\geq$ 120MPa, and E_2/E_1 <3.5 for the frost protection layer of sand, gravel or crushed rock (Statens vegvesen 2014, p.255). In the German standard for PLT a maximum settlement of 5mm on the first loading cycle with 500kPa load for road constructions is proposed. The allowable settlements are typically stricter for a road construction than for a fill.

3   The deposit and Field investigations

Figure 3.1 is an aerial photo of the deposit area. An extended deposit area is located to the south. The deposit is divided into 14 sections labeled A1 - A14 and *extended area*. The sections are shown in figure 3.2.

<p align="center">Figure 3.1 – Deposit overview, provided by Bane NOR</p>

The deposit at Åsland is built in layers and compacted using vibratory rollers. The spoil accumulates quickly in the spoil shed and is continuously transported out in fills before it is evenly distributed in a 0.7m thick layer above the last compacted layer. Compaction control is performed on each layer and consists of the following tests:

- standard Proctor compaction test
- washing and sieving for grain size distribution
- *in situ* Troxler moisture and density measurement
- plate load test

Requirements set for compaction control state that measured dry density must be within 95% of the Proctor compaction test results. The plate load test results are required to achieve $E_1 > 20$MPa, and $E_2/E_1 \leq 3$ (NGI 2015).

KSR Maskin AS has conducted and documented results of field tests on each layer of the deposit. In this chapter the results are presented and evaluated. For each layer the water content and dry

density after compaction is measured with a nuclear moisture/density gauge (Troxler), samples of spoil are collected and sent to washing and dry sieving and standard Proctor compaction tests. In addition, 2-4 plate load tests are conducted for each layer after compaction.
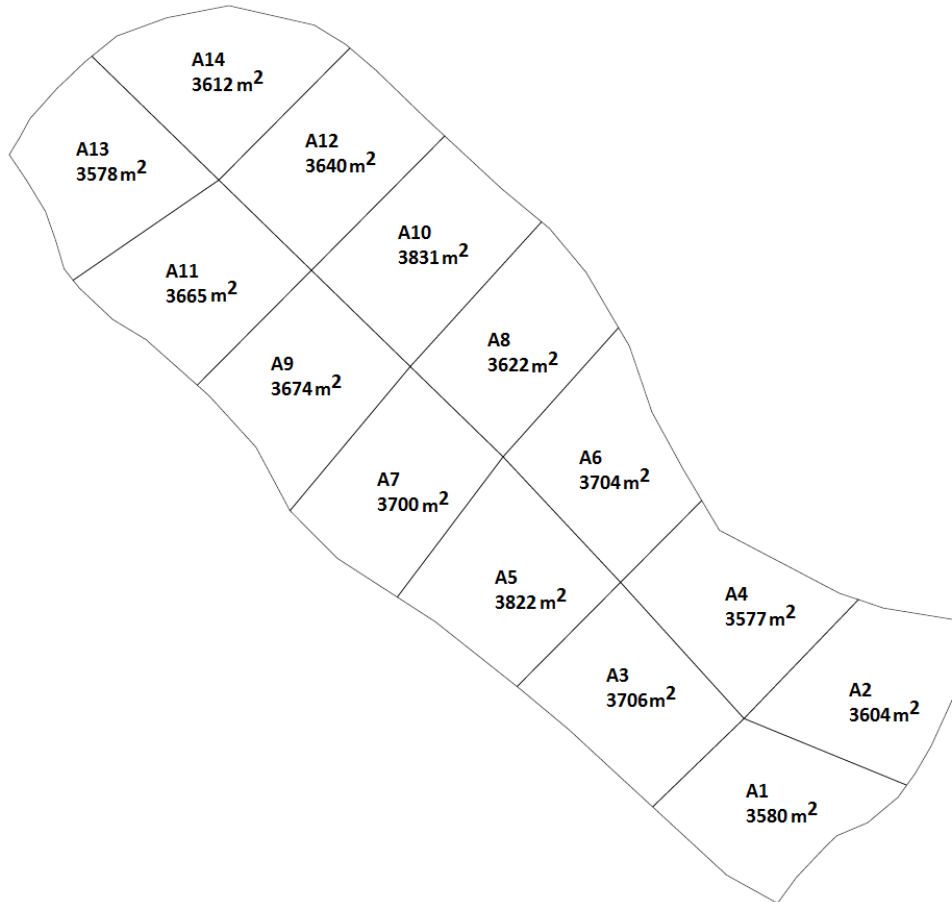
Figure 3.2 – *Sections of the deposit, provided by Bane NOR*

The deposit spans a total area of 51315m^2, with sections ranging from 3517 - 3831m^2 in size. The deposit area is large and the different tests are not conducted in close proximity to each other. This is a normal way to cover large areas with quality control. It is important to have in mind that the data from each layer must not be compared directly. For instance the dry density measured by the Troxler is not necessarily representative for the location of the plate load tests in the same layer and section. A direct correlation between dry density and stiffness of the material is not possible to extract from these data. The field- and laboratory investigations which are part of compaction control provide valuable data on the general behavior and characteristics of the TBM spoil.

In this chapter the data provided from Bane NOR is processed, presented and explained. In addition, a plate load test conducted by the author is presented in greater detail. Finally, field excavation tests (shaft tests) for determining density and permeability are presented.

3.1   Deposit overview

3.1.1   Grain size distribution

Investigating the grain size distribution of the material is important in order to predict the behavior, mechanical properties and possible usages of the spoil. The distribution affects the materials compressibility, sensitivity to water, frost susceptibility and strength. Two samples from each layer have been taken for washing and dry sieving, in all 52 samples. The tests are performed by KSR Maskin AS and in accordance with NS-EN 933-1/NS-EN 13242 (Standard Norge 2009). Figure 3.3 shows all grain size distributions from the deposit layers.
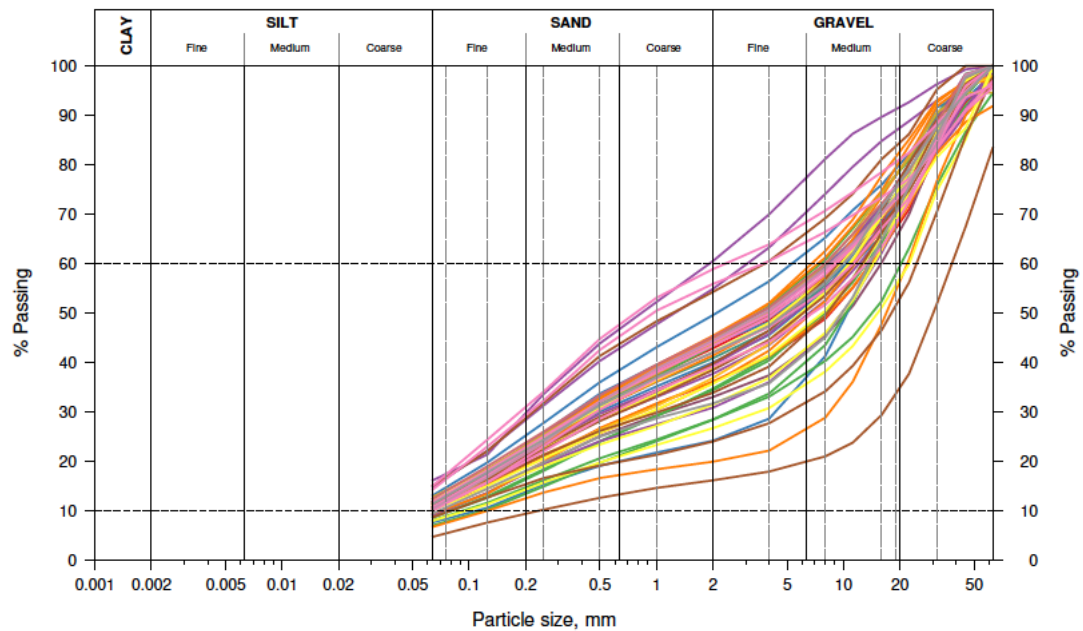
Figure 3.3 – *All grain size distributions from deposit tests*

The results show a fines content ranging from 4.6 - 16.0% with an average fines content of **10.7%. Of the material <22.4mm in diameter, the fines content ranges between 9.4 - 18.4% with an average of 14.1%**. The average coefficient of uniformity, $C_u = d_{60}/d_{10} \approx 11.2/0.063 = 178$, which classifies as a **well graded material** in accordance with the Norwegian standard *Handbook R210: Laboratory investigations* (Statens vegvesen 2016). d_{60} is the sieve size which 60% of the material pass through and d_{10} where 10% pass through.

Water sensitivity and frost susceptibility
It was decided to investigate the water sensitivity and frost susceptibility of the material by conducting grain size distributions, complete with falling drop analysis of the fines distribution. Moum (1965) explain the falling drop test for determining particle size distributions of fine materials. The method is based on Stoke's law and measures the sedimentation process over time in order to estimate the particle sizes of the sample.

The samples were taken from the bottom of field excavation test number four, which is described

in section 3.2. Frost susceptibility and water sensitivity are determined and classified based on the grain size distribution of the particles with a diameter $< 22.4mm$, in accordance with the Norwegian Public Roads Administration (Statens vegvesen 2014).

A material is classified as water sensitive when % - mass of material $< 22.4mm$ smaller than 0.063mm exceeds 7% Statens vegvesen (2014). The water sensitivity is higher for a well graded material due to the high degree of compaction and low pore volume preventing excess water from draining. The material is classified as **water sensitive** with an average fines content of 14.1% - of the material <22.4mm.

Figure 3.4 shows examples of the grain size distributions one might expect for the different frost-susceptibility classes. Table 3.1 shows frost susceptibility classifications as described in the Norwegian standard *Handbook N200: Road construction* (Statens vegvesen 2014).

Table 3.1 – *Frost susceptibility classification, translated from (Statens vegvesen 2014, p.211)*

Frost susceptibility classification				
Classification		Of materials $< 22.4mm$		
		% mass		
		$< 2\mu m$	$< 20\mu m$	$< 200\mu m$
Not frost susceptible	T_1		< 3	
Light frost susceptibility	T_2		3 - 12	
Moderate frost susceptibility	T_3	(1)	> 12	< 50
Highly frost susceptible	T_4	< 40	> 12	> 50

(1) Materials containing more than 40% $< 2\mu m$ is also classified as moderately frost susceptible, T_3
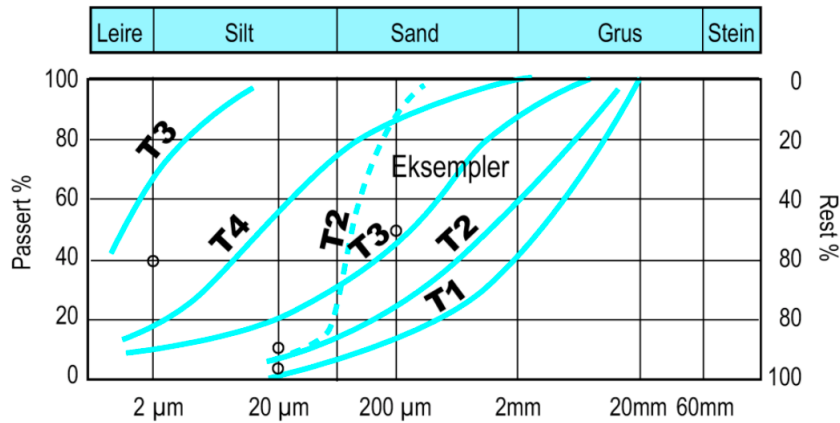
Figure 3.4 – *Examples of grain size distributions for frost susceptibility classification, (Statens vegvesen 2014, p.212)*

Figure 3.5 shows the complete grain size distribution of the samples collected in field excavation test 4 together with the examples of frost susceptible materials shown in figure 3.4. Part of the samples were washed and dry sieved, other parts of the same samples were simply sieved down

to 2mm and the retain was analyzed with wet sieving and falling drop. The distributions were then connected by adjusting the percent passed from the wet sieve and falling drop tests for the percent fines in the dry sieve samples. The numbers are presented in Appendix A, pages A-5 and A-6.
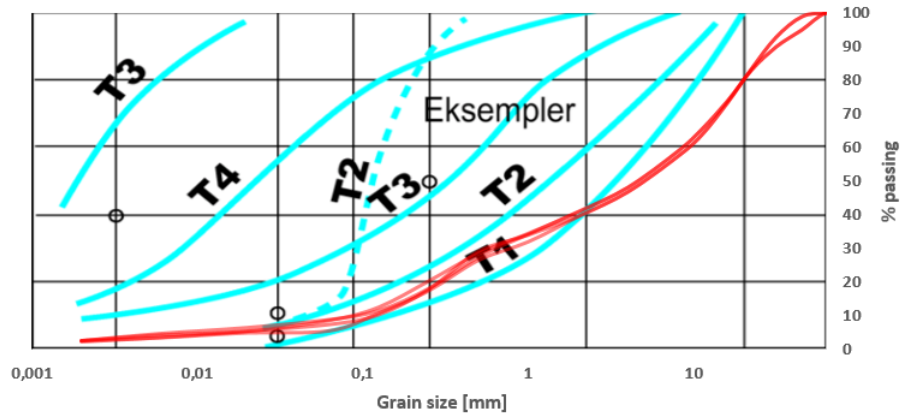
Figure 3.5 – *Frost susceptibility of Follobanen TBM spoil*

The results show that the TBM spoil is in the category T_2, light frost susceptibility, with % mass $< 20\mu m$ between 4.3 - 5.4% of material < 22.4mm.

3.1.2   Standard Proctor compaction tests

In a soil containing fine material a maximum dry density is obtained at a certain water content, labeled the optimum water content. The standard Proctor compaction test is used to establish the maximum compaction that can be achieved with the material. A standardized compaction procedure is followed and the material is tested at different levels of saturation starting $\approx 4\%$ beneath the assumed optimum water content. Typical dry density - water content curves from Proctor tests are shown in figure 3.6.
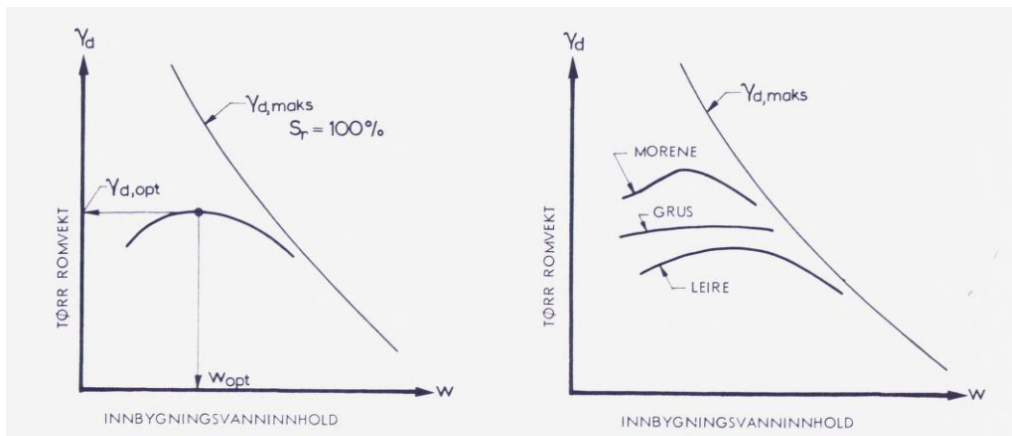
Figure 3.6 – *Standard Proctor curves of different materials by (Janbu 1970, p.80). Typical curves for moraine (morene), gravel (grus) and clay (leire). w = water content and γ_d is the dry density*

(Kjærnsli et al. 2003) explain that the compressibility of a soil or rock is dependent on the amount of water present in the material. When dry, separate cohesive lumps or large grains may be firm enough to prevent the material from breaking and filling the voids in the material, resulting in a lower dry density. By increasing the water content the soil will become more plastic as fine grains begins to flow and fill the voids of the material. Brittle rocks breaks more easily into place when they are covered in water and larger particles are lubricated by the water and slips in place with less effort. Increase in water will therefore result in a higher dry density. When the water level becomes too high the pore volume will become saturated. Because water is incompressible and the material is saturated, no decrease in pore volume will be achieved by compaction. Increasing the water level too much will therefore result in decreased dry density. The grain size distribution of the material is another important factor in compaction work. Well graded material where the different size grains may fill the pores created by larger particles will result in a more compact soil.

For each layer of the deposit, two standard Proctor compaction tests have been performed by KSR Maskin AS. Figure 3.7 shows the optimum water content versus the maximum dry density of all 52 tests.
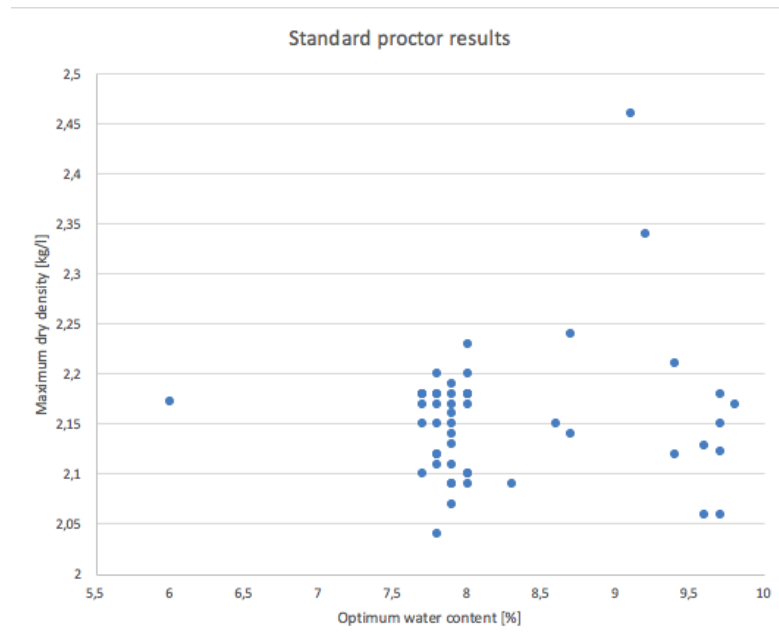
Figure 3.7 – *Maximum achieved dry density versus optimum water content for all 52 standard Proctor tests. The results are not corrected with respect to maximum grain size*

The average maximum dry density achieved for this material is **2.15t/m^3** with an average optimum water content of **8.24%** before correction for field compaction control.

Correction of maximum dry density with respect to grain size:
Statens vegvesen (2016) states that in order to apply the standard Proctor test results as a reference in compaction control in field the results need to be corrected. This is because large particles ($> 22.4mm$) are removed for the laboratory investigation. With KSR Maskin AS following the Norwegian standard presented in Handbook R210 (Statens vegvesen 2016, p.151), particles >22.4mm are removed from the test sample. The corrected maximum dry density is then calculated using the following equation:

$$\rho_{d,field} = \rho_{d,lab}(1 - \frac{u}{100}) + 0.9\rho_s\frac{u}{100} \tag{3.1}$$

Where:
$\rho_{d,field}$ = dry density in field
$\rho_{d,lab}$ = dry density in laboratory on material <22.4mm
ρ_s = grain density of the material
u = percent mass of material >22.4mm removed for the laboratory test

The amount removed material is not provided as a part of the standard Proctor results. Instead, a correction is done based on the average mass <22.4mm from 52 grain size distributions on the average maximum dry density from the Proctor tests. The grain density ρ_s is provided by a pycnometer test performed by NGI, $\rho_s = 2.69$kg/m^3. The average percent material passing 22.4mm is 75.46%, making the average retained material 24.54% = u. Inserting the numbers into Eq.3.1:

$$\rho_{d,field} = 2.15 \cdot (1 - \frac{24.54}{100}) + 0.9 \cdot 2.69 \cdot \frac{24.54}{100} = 2.22t/m^3$$

For compaction control the result of maximum compaction for this material should yield dry densities of approximately **2.22t/m^3**.

In summary the results of the standard Proctor compaction tests are:

Optimum water content	Maximum dry density without correction	Maximum dry density with correction
8.24%	2.15t/m^3	2.22t/m^3

3.1.3   Troxler tests

The Troxler testing device is a nuclear moisture/density gauge used to measure the water content and density of materials *in situ.* The device transmits a radioactive gamma ray into the material from a source which is lowered down to desired depth for the investigation.

Approximately 10 tests are conducted for each layer spread across the different areas A1-A14. One test includes two measurements for the same location. The device is placed on the layer surface, taking care to level the surface so that the Troxler is in full contact. Two holes are made with a hammer and large nail down to the desired depth and the measurements are done by lowering the gamma ray source into one hole at a time. Figure 3.8 shows the equipment used at Åsland deposit site.

Figure 3.8 – *Troxler device: The plate, hammer and nail in the background is used to make two holes for the nuclear transmitter to be lowered down to desired depth*

The moisture content found in laboratory investigations are oven dried and reveals the moisture content of the material by removing all water from the sample. The moisture gauge of the Troxler measures the water content by detecting and "counting" the hydrogen present in the soil. The Troxler is therefore prone to measure a falsely high moisture content in materials with naturally occurring hydrogen, some common materials that may contain hydrogen is listed by *Troxlerlabs*: Mica, lime, fly ash, cement, organic materials, gypsum, coal, phosphates, etc. In some rare cases the Troxler may give a falsely low reading. This may occur if the material has a high salt or iron oxide content, or contain boron, lithium or cadmium.

The Troxler results from the deposit site are shown in figure 3.9. The average dry density and water content for each layer is mapped in blue and red dots, respectively. The overall average values for the whole deposit are marked with a blue and a red line.
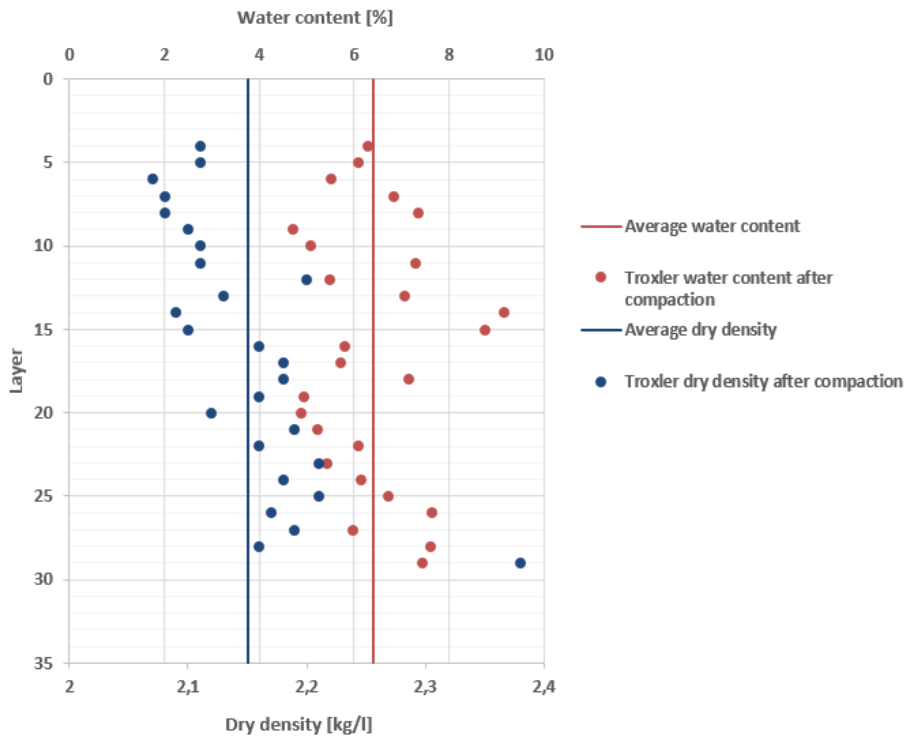
Figure 3.9 – *Average values for Troxler tests on each layer. Layer 0 is the bottom of the fill. Water content in red and dry density in blue*

All readings are performed after compaction of the layer and before a new layer is placed on top. The average dry density of each layer shows a positive development with an increase in achieved compaction with time (layers). The average results of all Troxler tests conducted on the deposit is a dry density of **2.15t/m^3** and water content of **6.4%**.

The first excavation tests described in section 3.2 of this report a frozen layer approximately 25cm down and 40cm thick was observed. In frozen conditions the manufacturer, *Troxlerlabs* informs on their website that the moisture readings will be elevated and the dry density will be lower as a result of the material being frozen (Troxlerlabs 2018). Water expands when frozen and will take up a larger volume in the material where the gauge is placed. Water has a lower density than the soil and the dry density of the material will be registered falsely low while the moisture content will be read as higher than it really is.

3.1.4   Plate load tests

Plate load tests are conducted by KSR Maskin AS for every layer of the deposit after compaction is complete. In order to achieve a good foundation with little to no settlements after construction the following criteria was set by NGI: $E_1 > 20MPa$, and $E_2/E_1 \leq 3$. The criteria was to be adjusted during the earthworks due to the inexperience with the material.

The plate load test is one of the most frequently used field tests for shallow foundations and pavement design. From the test a deformation modulus is established and this may be further used in calculations of settlements of footings and tolerable bearing pressure based on acceptable deformations. The equipment is shown in figure 3.11 and 3.12.

The strain modulus E_v is found from the load - settlement curves from the field measurements, where E_1 denotes the strain modulus for the first loading cycle and E_2 from the second loading cycle. In accordance with the German standard *DIN 18134 Soil-Testing procedures and testing equipment - Plate load test* (Deutscnes Institut fur Norrnung 2012), E_1 is calculated by using the settlements over 0.3 to 0.7 of the maximum load, while E_2 is calculated over 0.3 to maximum load, σ_{max}. Figure 3.10 shows the principle of evaluating the load - settlement curve.
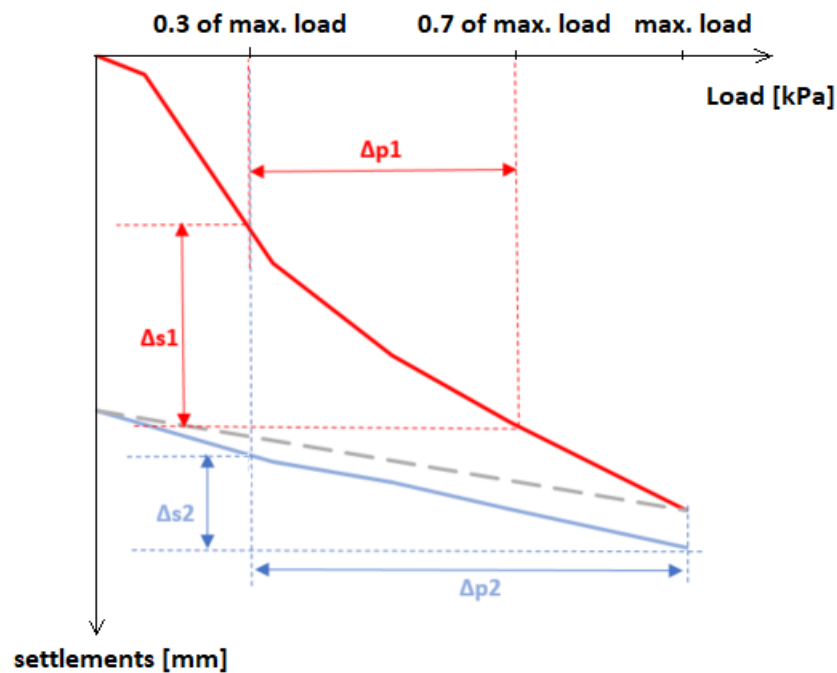
Figure 3.10 – *Plate load test - load versus settlement curve. Red indicates the first load cycle and blue indicates the second load cycle*

The following equations are used to calculate E_1 and E_2:

$$E_1 = 0.75 \frac{\Delta p}{\Delta s} D \qquad\qquad (3.2)$$

where

$$\Delta p = 0.7\sigma_{max} - 0.3\sigma_{max}$$

and

$$E_2 = 0.75 \frac{\Delta p}{\Delta s} D \qquad\qquad (3.3)$$

where

$$\Delta p = \sigma_{max} - 0.3\sigma_{max}$$

and Δs is the difference in settlements over the defined stress level.

The modulus of subgrade reaction, k_s is a simplification of the relationship between pressure and settlements, and is given by the relation between stress and settlements: (Terzaghi et al. 1996)

$$k_s = \frac{\sigma_0}{s^*} \qquad\qquad (3.4)$$

Equipment
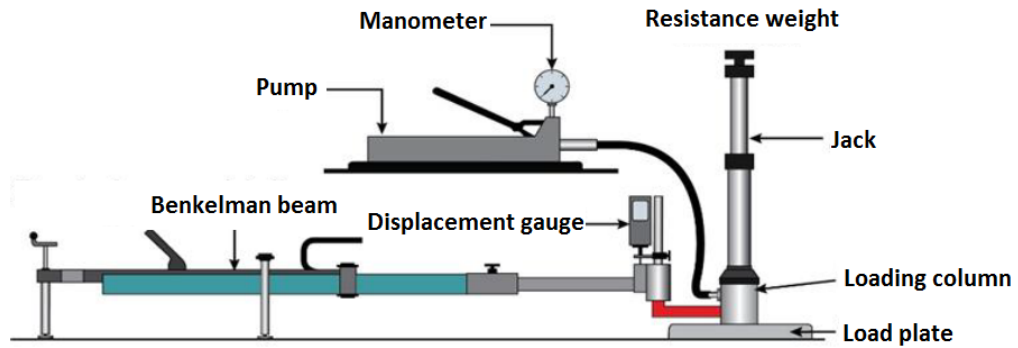
Figure 3.11 – *Plate loading equipment. Figure translated from (Statens vegvesen 2018) confirmed as the same equipment used by KSR Maskin AS*

Figure 3.12 – *Plate load test equipment rigged for testing at Åsland deposit site*

The equipment consists of a benkelman beam which is anchored 1.5m from the loading plate. A displacement gauge is fastened to the beam which is again connected to the loading column. Three adjustable feet ensures that the beam is level. A manual pump connected to a hydraulic

jack and equipped with a manometer is used to apply the load in steps. The equipment is placed beneath a resistance weight which is used to generate the load onto the ground. It is important that the benkelman beam is anchored at least 1.5m away from the load plate to prevent the settlements readings to be affected by the peripheral of the deformation. Figure 3.11 and 3.12 shows the equipment in its entirety.

Test procedure

The equipment is assembled beneath a resistance load, typically a heavy truck. Care is taken that the load plate is placed on a flat surface with full contact before beginning. According to Deutscnes Institut fur Norrnung (2012) and Statens vegvesen (2018) a thin layer of plaster or sand is to be placed beneath the loading plate to level the surface before starting the test. This is not done as a part of the procedure at Åsland. The effect of not using plaster is evaluated in Chapter 5. When the equipment is in place the manual pump is used to make contact with the resistance weight and then to apply a contact pressure of 20kPa before resetting the deformation to zero. Load is then applied in the following steps: 50 - 180 - 300 - 420 - 600 (kPa). Each step is held until the settlements has stabilized. After the final step has stabilized, the load is relieved down to zero and a second loading cycle is performed in the same manner as the first.

Results
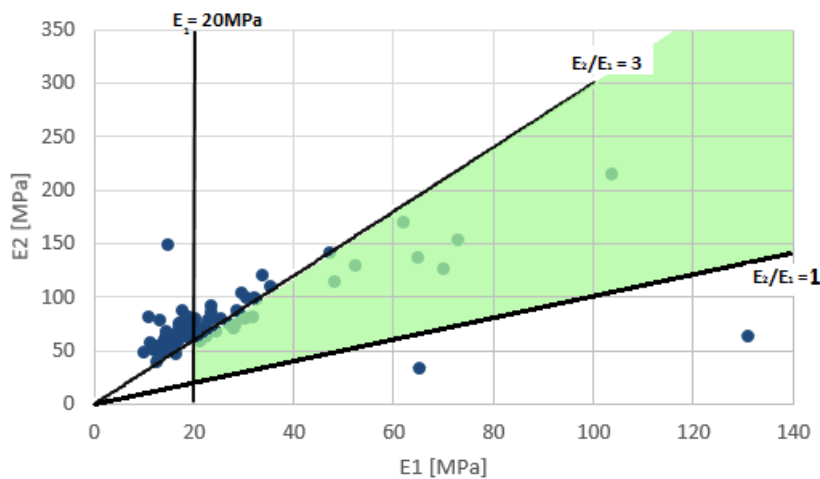
Figure 3.13 – E_1 and E_2 values of all plate load tests at the deposit. The acceptable values are within the green area

23 out of 80 tests have an E_2/E_1 value ≤ 3 while 38 out of 80 tests have an $E_1 > 20$MPa. Of the 80 tests presented in figure 3.13 only 22 (28%) passes both criteria set by NGI. The overall average E_1 value is **26.5MPa** and the average value of E_2/E_1 is **3.5.** Figure 3.14 and 3.15 shows the E_1 and E_2/E_1 values of the plate load tests on each layer for the deposit and the extended area of the deposit, respectively.
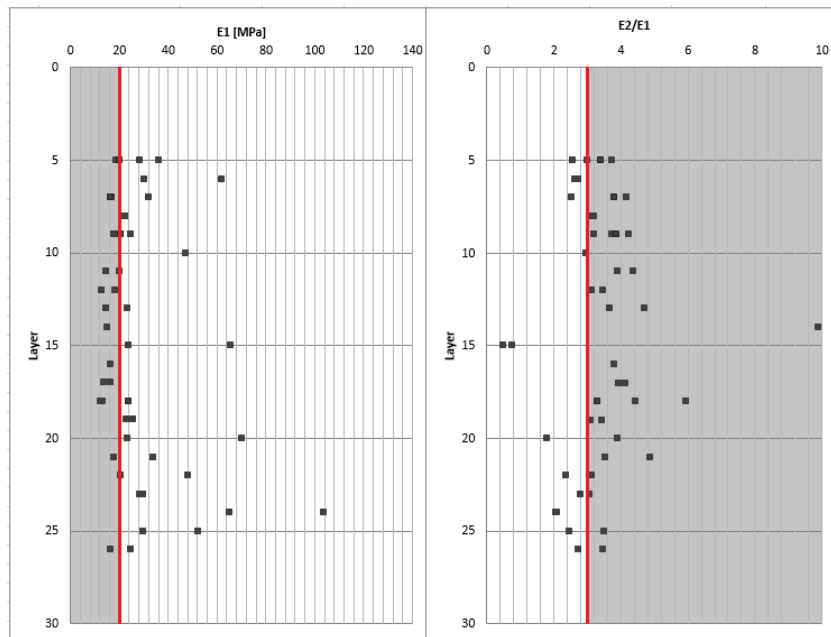
Figure 3.14 – *Results of plate load tests for the layers of the deposit. The red line marks the criteria set by NGI. Results falling in the grey zone are not within the criteria*
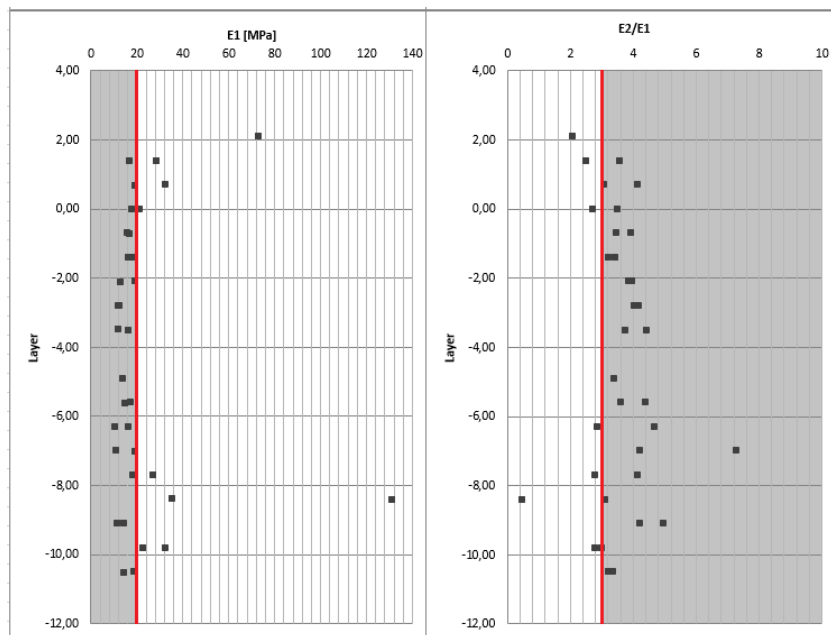
Figure 3.15 – *Results of plate load tests on extended deposit area. The red line marks the criteria set by NGI. Results falling in the grey zone are not within the criteria*

Because the TBM spoil is water sensitive and the water content varies in the spoil shed the compacted layer exhibit variations in consistency. Some areas are muddy and in some places water is visible on the surface. These areas are too soft for the plate load test, and a dryer area is chosen within the same section. If the test is performed on a frozen layer this might affect the results of the plate load tests. E_2 will present a higher value because the frozen layer is stiffer than usual, while E_1 will be lower as the topmost layer is soft, contain water that is prevented from dissipating through the frozen ground beneath.

The results of the plate load tests are highly scattered and many do not fulfill the specified criteria. In order to better understand the results and procedure a plate load test was arranged for the author to document the procedure.

The test was carried out on a newly compacted layer with the same equipment and procedure used for all plate load tests on the deposit. The equipment (shown in figure 3.12) and procedure are in accordance with the German standard for plate load tests: DIN 18134, with the exception that no plaster or sand was used in order to level the surface area beneath the bearing plate. The loading plate was placed in a flat spot with no large or loose particles on the surface. The measurements, calculations and load - settlement curve is presented:

Load [kPa]	Measurement 1 Settlements [mm]	Measurement 2 Settlements [mm]	
0	0	7,48	
50	1,01	7,6	
180	4,33	8,29	
300	6,16	8,7	
420	7,51	9,12	
600	9,17	9,84	
Δp	240	420	
Δs	3,18	1,55	

$$E_1 = 0,75 \frac{\Delta p}{\Delta s} D = 0,75 \frac{240}{3,18 \cdot 10^{-3}} 0,3 = 17,0 \ [MPa]$$

$$E_2/E_1 = 3,6$$

$$E_2 = 0,75 \frac{\Delta p}{\Delta s} D = 0,75 \frac{420}{1,55 \cdot 10^{-3}} 0,3 = 61,0 \ [MPa]$$
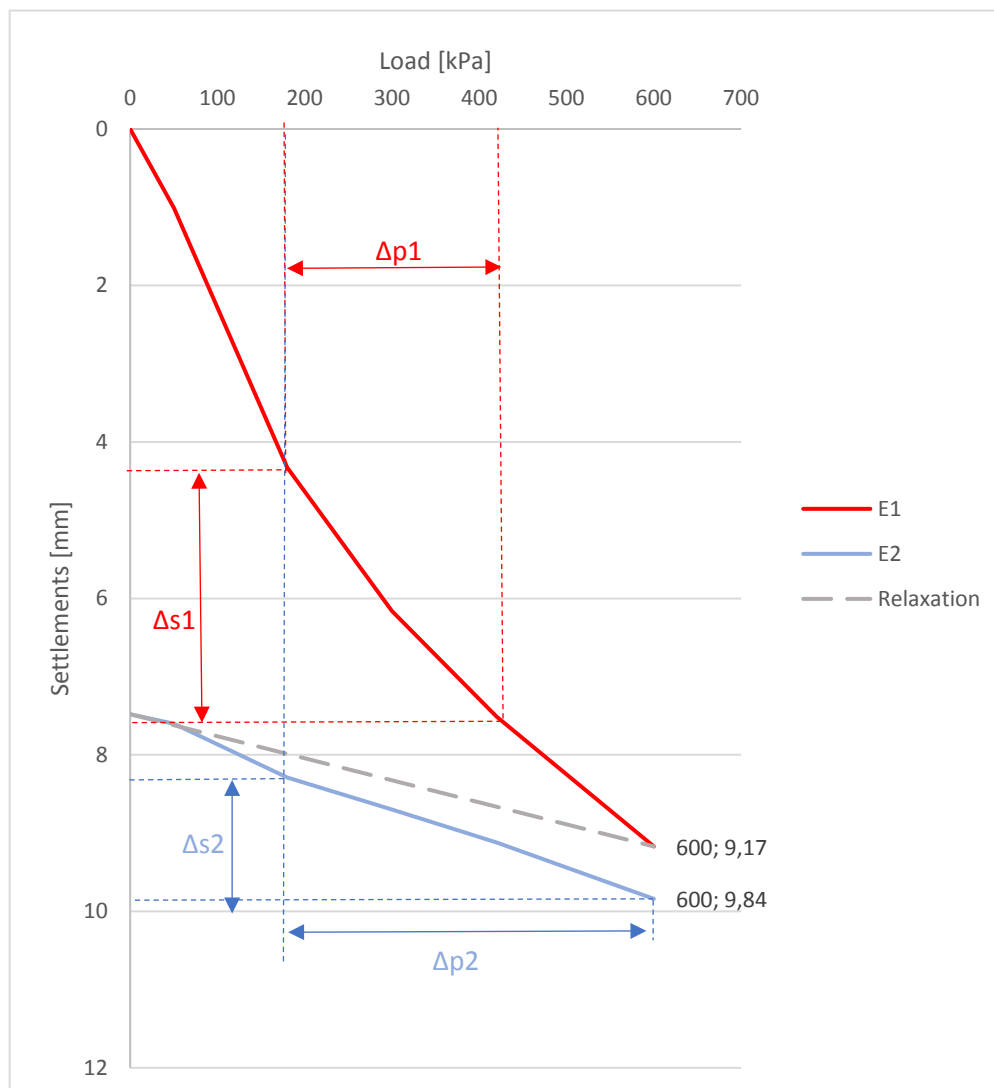
3.2   Field investigation: Determination of dry density and permeability

Figure 3.16 – *Excavation of test pit*

Because few plate load tests are passing the criteria in the specifications, a larger field investigation was arranged in order to further investigate the achieved dry density of larger volumes. The field investigation is based on a method described by (Bertram 1987, p.14) who performed similar tests in connection to investigations on rockfills for use in dam constructions. Four tests were performed in April using the exact same method for all tests.
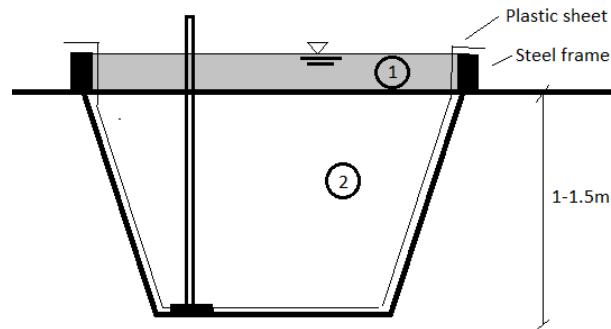
Figure 3.17 – *Principle sketch of field density test*

The procedure of the investigation is explained with the following steps:

1. Measure the dry density and moisture content with the Troxler in two - three places before starting

2. Install the frame

3. Cover the soil with a plastic sheet secured to the frame. Fill it with water and measure volume (1). Remove plastic sheet

4. Excavate, approximately 1 - 1.5m deep and with a total volume of 5 - 10m^3. Measure the weight of the excavated material

5. Cover the area with a plastic sheet secured to the frame. Fill with water and measure volume (1) + (2)

6. Calculate density

7. Remove plastic sheet and fill the excavated pit with water again

8. Measure falling head of water with time

9. Calculate the permeability of the soil

A laser was used to map the excavated hole as a control to the volume. Because the result of the laser mapping was of very high quality and contains less possibilities of error, the volume measured by water was disregarded. Figure 3.17 is a principle sketch for the test.

A roughly 40cm thick layer of frost was discovered during the first test (shown in figure 3.19).

It was arranged to collect samples from the bottom of test 4 to perform dry sieving and falling drop tests. The purpose is to assess the full grain size distribution of the material. The grading of the material influences the compaction work. The distribution is therefor measured in order to see correlations between the different tests. The results of these complete grain size distributions from test 4 are presented in section 3.1.1 and in Appendix A.

Figure 3.18 – *Right: Filling frame with water, volume measured through flowmeter. Left: Pit filled with water measured as sum of several flowmeters*

Figure 3.19 – *Frozen layer discovered during field test 1, early April*

3.2.1   Results of shaft tests
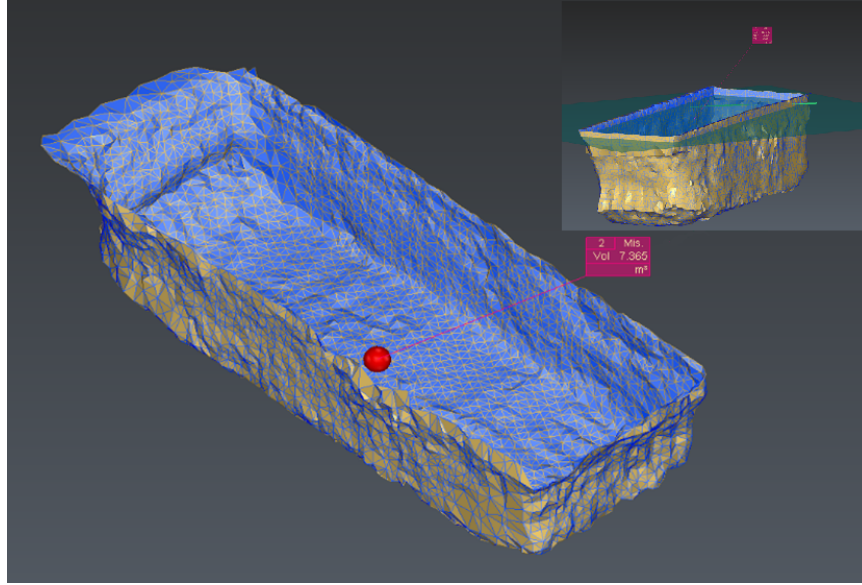
Figure 3.20 – *Volume of test-pit 1 mapped with laser*

The results; density and hydraulic conductivity are presented in table 3.2 and 3.3 together with porosity, saturation and void ratio of the investigated area. Results from each test is presented in greater detail in Appendix A.

The hydraulic conductivity is calculated by measuring the decrease in water level over time and accounting for the surface area of the pit (bottom area + sides), the results are in the magnitude of $\mathbf{10^{-5}}$ **-** $\mathbf{10^{-6}m/s.}$ The degree of saturation, porosity and the void ratio are calculated using the following equations (NTNU 2015):

$$Saturation = Sr = \frac{V_w}{V_p} = \frac{w \cdot \gamma}{\gamma_w(1 + w - \frac{\gamma}{\gamma_s})} \tag{3.5}$$

$$Porosity = n = \frac{V_p}{V} = 1 - \frac{\gamma}{\gamma_s(1 + w)} \cdot 100\% \tag{3.6}$$

$$Voidratio = e = \frac{V_p}{V_s} = \frac{\gamma_s(1 + w)}{\gamma} - 1 \tag{3.7}$$

Where V_p is the volume of pores/voids, V_s is the volume of solids and V_w is the volume of water. w is the water content, γ is the unit weight of the material, γ_s is the unit weight of the grains and γ_w is the unit weight of water.

Table 3.2 – *Results of field density and permeability tests*

Test	Water content %	Volume $\mathbf{m^3}$	Weight(kg) wet	dry	Density(t/$\mathbf{m^3}$) wet	dry
1*	8.3	6.50	17450	16008	2.68	2.22
2	10.3	6.34	14450	12964	2.28	2.34
3	7.5	6.67	16800	15546	2.52	2.33
4	5.3	6.18	14550	13779	2.35	2.22
Average	7.9				2.46	2.28

Test 1 contains frozen layer

Table 3.3 – *Results of field density and permeability tests*

Test	Porosity, n %	Void ratio, e -	Saturation, Sr %	Hydraulic conductivity m/s
1*	7.9	0.085	26.2	1.38E-06
2	23.3	0.303	9.1	7.74E-05
3	12.9	0.148	13.6	6.32E-05
4	16.9	0.204	7.0	1.39E-06

Test 1 contains frozen layer

The results reveal a dry density consistently higher than the maximum dry density found from the standard Proctor tests in section 3.1.2 and higher than the dry density measured with the Troxler tests shown in section 3.1.3 and the Troxler measurements taken at the beginning of the field tests. The average dry density from the field tests is **2.28t/$\mathbf{m^3}$**. These can be found in Appendix A.

Grain size distribution

Figure 3.21 shows the grain size distribution from the bottom of test pit 4. Two samples were washed and dry sieved and combined with results of wet sieve and falling drop from the same sample. The The red lines show the area limits of the grain size distributions found on TBM spoil samples by NGI (1986). The results fit well with the earlier findings.
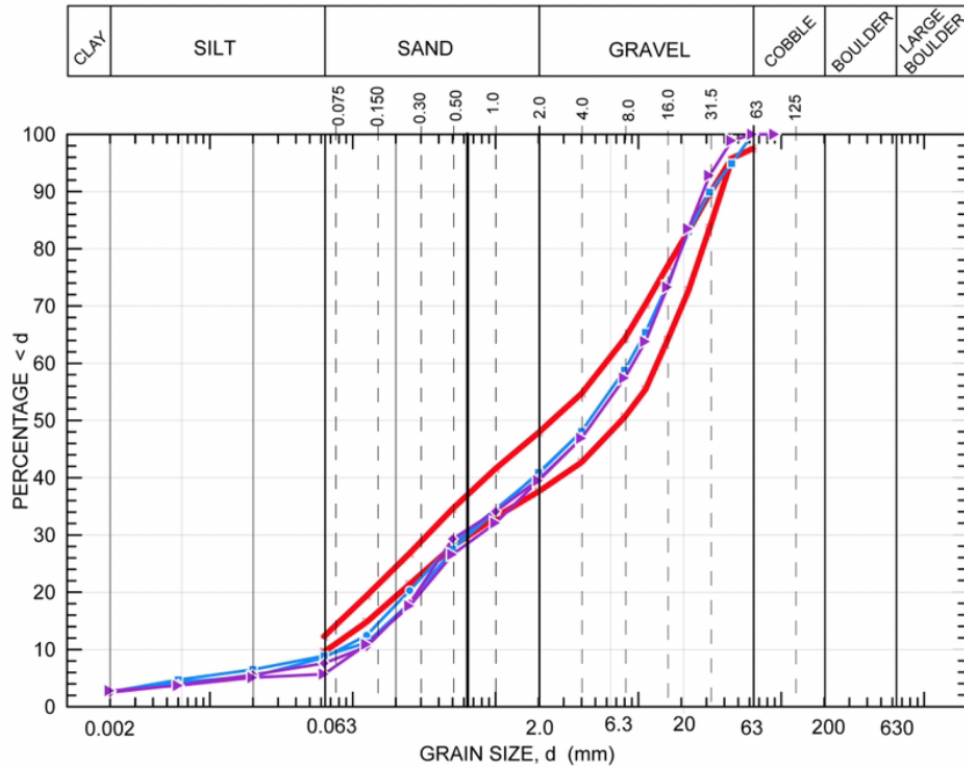
Figure 3.21 – *Grain size distribution from field excavation test 4. Blue and purple lines represent the samples taken at test 4, red lines show minimum and maximum expected TBM distributions from NGI (1986)*

3.3   Summary of deposit results

Table 3.4 shows a summary of the soil parameters found chapter 3.

Table 3.4 – *Summary of deposit data*

Parameter	Symbol		Average value
Plate load stiffness	E_1	MPa	26.5
Plate load stiffness	E_2/E_1		3.43
Water Content (Troxler)	w	%	6.40
Dry density (Troxler)	ρ_d	t/m^3	2.15
Dry density (Shaft tests)	ρ_d	t/m^3	2.28
Fines content (of d_{max})	-	%	10.69
Fines content (of material $< 22.4mm$)	-	%	14.1
Optimum moisture content	w_{opt}	%	8.23
Maximum dry density	$\rho_{d,max}$	t/m^3	2.15
Permeability	k	m/s	10^{-5} - 10^{-6}
Frost susceptibility	-		Yes, T$_2$
Water sensitive	-		Yes

4 Laboratory investigations

4.1 Sampling and transportation of TBM spoil

TBM spoil was collected from the spoil shed at Åsland 13.02.2018. Three sealed plastic barrels containing a total of 660 liters of spoil were transported to NTNU, Trondheim for laboratory testing. The spoil was collected with an excavator from various locations within the spoil shed. The outermost layers were avoided because the grains here are sorted by sliding down the sides of the piles.

4.2 Oedometer tests

Oedometer tests are conducted as part of the investigation of the deformation properties of the TBM spoil from the Follo line project. The oedometer test creates a one-dimensional deformation with walls restricting movement of the sample in any other direction than vertically. A load is applied pushing down on the material and the subsequent deformation is logged. Based on these logs, a resistance to deformation, or *oedometer modulus, M* is found and this is used to predict settlements during and after construction.

The materials strain is defined on the basis of the deformation (NTNU 2015):

$$\varepsilon = \Delta\delta/H_0 \tag{4.1}$$

where:
ε = strain
$\Delta\delta$ = change in height
H_0 = Initial height

The materials stiffness, or resistance to deformation is defined as the tangent line of the stress - strain curve:

$$M = d\sigma'/d\varepsilon \tag{4.2}$$

where:
M = the oedometer modulus
$d\sigma'$ = change in vertical effective stress
$d\varepsilon$ = change in strain

Equipment:
The oedometer cell, *K/Ø Anton* has an inner diameter of 49.9cm and inner height of 57.7cm. A vibrating compaction plate designed for use in the large scale oedometer was used for compaction of the material to create a sample in the oedometer cell. The vibrating plate has a diameter of 497mm and weighs 13.8kg. The maximum applied load with the current equipment is 7bar ($\approx$ 700kPa) applied through air pressure.

Figure 4.1 shows the oedometer cell and the vibrating plate used for compaction. A pressure gauge is mounted on the lid and the air pressure (load) is manually applied by rotating an adjustable pressure switch. The deformation measurement is transmitted to a computer which logs the data using LabView software.

Figure 4.1 – *K/Ø Anton - Equipment used for oedometer testing of TBM material. Picture to the right shows the vibrating compaction plate*

There are 6 open holes in the bottom of the cell to allow for drainage of water. There are no pore pressure monitors. A small crane is installed in the ceiling for handling the lid of the oedometer. The lid is secured with 10 bolts and a custom made gasket prevents air leakage. The standard *NS-EN ISO 17892-5:2017 Geotechnical investigation and testing-Laboratory testing of soil part 5: Incremental loading oedometer test* sets the following criteria for the oedometer cell:

- Diameter (D): Not less than 35mm

- Height (H): Not less than 12mm

- Ratio (D/H): not less than 2.5

It further states that the mean diameter of the largest particle within the specimen should not exceed 1/5 of the sample height (Standard norge 2017).

Methodology:
A fiber cloth is placed in the bottom of the oedometer cell in order to prevent material from falling out of the drainage holes. A layer of grease is applied to the walls of the apparatus followed by a cover of plastic sheet. This is done to minimize the friction of the stamp against the walls of the cell. The material is added using a bucket which is weighed before pouring the spoil into the cell. The compaction is done in layers of approximately 30kg for each layer.

The material is built into the oedometer cell as it was placed in the transport bins. The size and amount of the material made it difficult to mix the whole sample, and there was no sufficient equipment for mixing the spoil. The layers are affected by this as it is possible to see the differences in grain sizes and in water content especially. The advantage of this, on the other

hand, is that different limits of the material-mixes are tested. The build-in and compaction of each test is provided in Appendix B of this report. The samples were tested up to a load of 500kPa, due to the capacity of the air pressure pump. This corresponds with the maximum thickness of the landfill, and this pressure is therefor considered satisfying. The load was applied in increments which is provided in Appendix B for each of the four tests. Test 1 had increments of 30min, which was changed to 15min for the other tests as the primary consolidation of the material went quickly.

Grain size distribution and water content:
From each oedometer test a sample of 25 - 30kg was collected from different areas of the specimen and dried in a 110°C oven until completely dry. The weight before and after drying reveals the water content of the sample. It is assumed that little water dissipates from the tests during the building of the sample and during the loading. Figure 4.2 shows the sieves mounted on a vibrating machine used to shake the particles down through the sieves resulting in sorted fractions.

Figure 4.2 – *Dry sieving equipment*

From the available sieve sizes the following set was chosen [mm]: 40, 31.5, 22.4, 16, 11.2, 8, 4, 1, 0.5, 0.25, 0.125, 0.063. The material is not washed before sieving, as opposed to the tests conducted by KSR Maskin AS. Unfortunately, the equipment, which is normally used for pavement aggregates was not optimal for the amount of fines in the TBM spoil, and significant

leakage of small particles was clearly visible during sieving. This causes false distribution results for the finer fractions of the material.

4.2.1   Results of test 1:

The stress and strain versus time is presented in figure 4.3. The build-in of test 1 consisted of 4 compacted layers. The test reached a maximum strain of 8.3% with a maximum load of 500kPa. In this first test the load steps were maintained for about 30min after climbing to a load of 100kPa. Figure 4.4 shows the stress - strain relationship and the achieved oedometer modulus. It is believed that the high modulus at the beginning of the test is caused by the plastic sheet before it gets properly pushed down. The deformation of the plastic sheet along the edges of the cell is clearly visible in the pictures of the tests, Appendix B. The maximum achieved modulus is 11MPa at p=500kPa. The water content and final density of the sample is presented in table 4.1. The grain size distributions are presented in figure 4.11.

Table 4.1 – *Density and water content of Oedometer test 1*

		Before testing	After testing
Sample height	cm	49.5	45.5
Volume	l	96.8	89.0
Density	t/m^3	1.85	2.0
Dry density	t/m^3	1.69	1.83
Water content	%		10.2
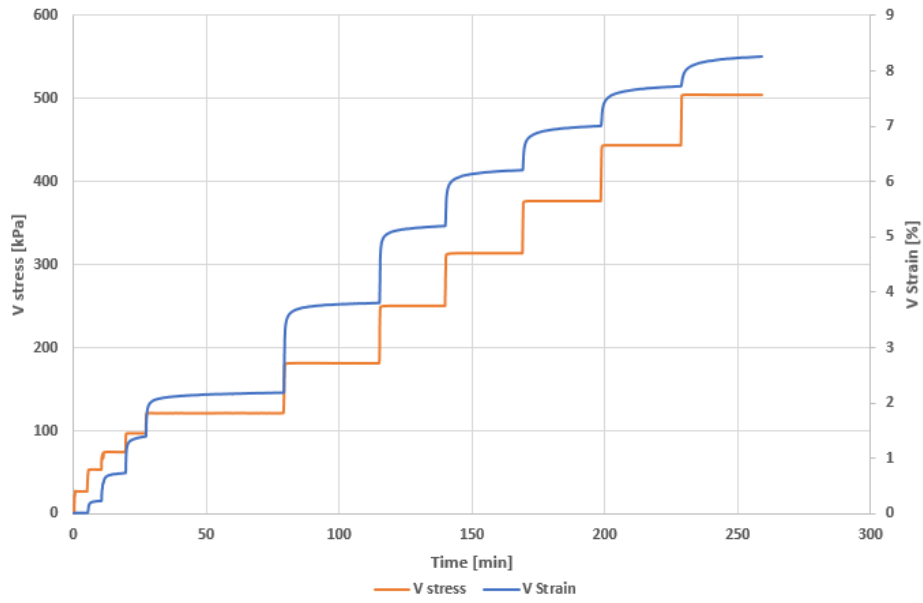
Figure 4.3 – *Stress and strain versus time for test 1. Strain(blue) on right hand axis and Stress(orange) on left axis*

Figure 4.4 – *Stress - strain - modulus: test 1*

4.2.2   Results of test 2:

Test 2 contained a high amount of water. The sample was built in the course of one day with some difficulty because of the muddy quality of the saturated material. The sample was built in 7 layers. After compaction of layer 3 and 4 free water gathered on the surface. The water was allowed to drain for an hour before the next layer was added to the cell. To prevent a water cushion effect the sample was allowed to drain for 2 days with the lid sealed. The expelled water was measured for back calculation of the original water content. As pressure reached 130kPa, water began bubbling up from the loading stamp. In order to make sure the measured stiffness is representative for the soil and not a water cushion, each load step was added once water had stopped expelling for some time. The expelled water was gathered with paper towels and weighed.

The stress and strain versus time is presented in figure 4.5. The test reached a maximum strain of 3.5% at a maximum load of 500kPa. In this test the load steps were held for about 20min. Figure 4.6 shows the stress - strain relationship and the resulting oedometer modulus. The maximum modulus is 23MPa at p=500kPa. The water content and final density of the sample is presented in table 4.2. The grain size distributions are presented in figure 4.11.

Table 4.2 – *Density and water content of Oedometer test 2*

		Before testing	**After testing**
Sample height	cm	44.5	43.5
Volume	l	87.0	85.1
Wet density	t/m^3	2.48	2.54
Dry density	t/m^3	2.20	2.27
Water content	%		min. 13

Large amounts of water in this test and the leakage of at least 4.7kg of water makes for uncertain dry density and water contents. There is no doubt however that the sample is densely packed well over dry density = 2.2 t/m^3
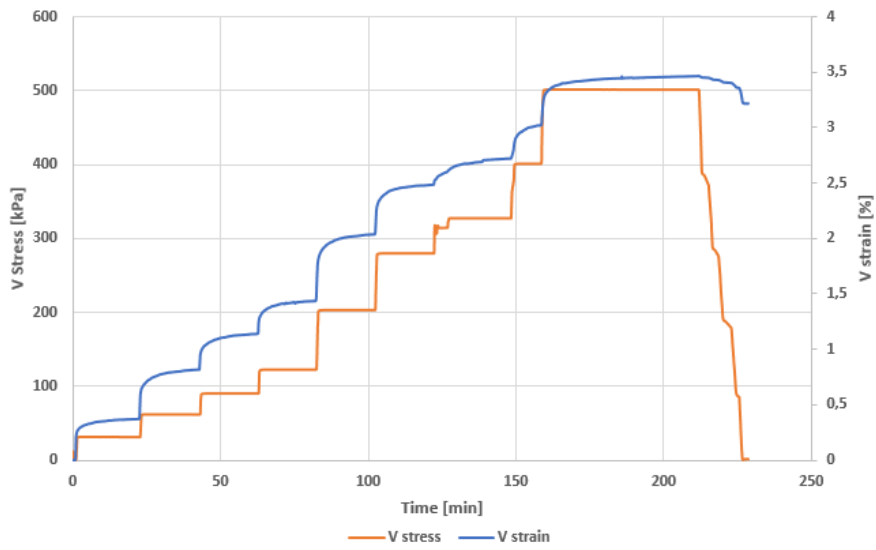
Figure 4.5 – *Stress and strain versus time for test 2. Strain(blue) on right hand axis and Stress(orange) on left axis*

Figure 4.6 – *Stress - strain - modulus: test 2*

4.2.3   Results of test 3:

In the third test it became evident at 90kPa that the load stamp had caught on the edge of the gasket and subsequently pulled it downwards until it broke. In order to not waste the sample and because of the time it took to get a new custom made gasket for the oedometer it was decided to start the test again, attempting to seal the cell with industrial grease and duct tape. This worked well until the seal broke at 410kPa. The last consolidated step was at a load of 360kPa.

The sample was built with 5 layers. The stress and strain versus time is presented in figure 4.7. The test reached a maximum strain of 10% with a maximum load of 360kPa. The load steps were maintained for about 15min. Figure 4.8 shows the stress - strain relationship and the resulting oedometer modulus. The modulus curve reflects the fact that the sample has been exposed to a preconsolidation stress of 90kPa from the first attempt with higher resistance to deformation within this stress range. The maximum achieved modulus is 6MPa at p=60kPa, within the preconsolidated stress range, and 5MPa at p=360kPa. The water content and final density of the sample is presented in table 4.3. The grain size distributions are presented in figure 4.11.

Table 4.3 – *Density and water content of Oedometer test 3*

|		Before testing	After testing
Sample height	cm	44.0	39.7
Volume	l	86.0	77.6
Wet density	t/m^3	1.82	2.02
Dry density	t/m^3	1.71	1.90
Water content	%		6.2
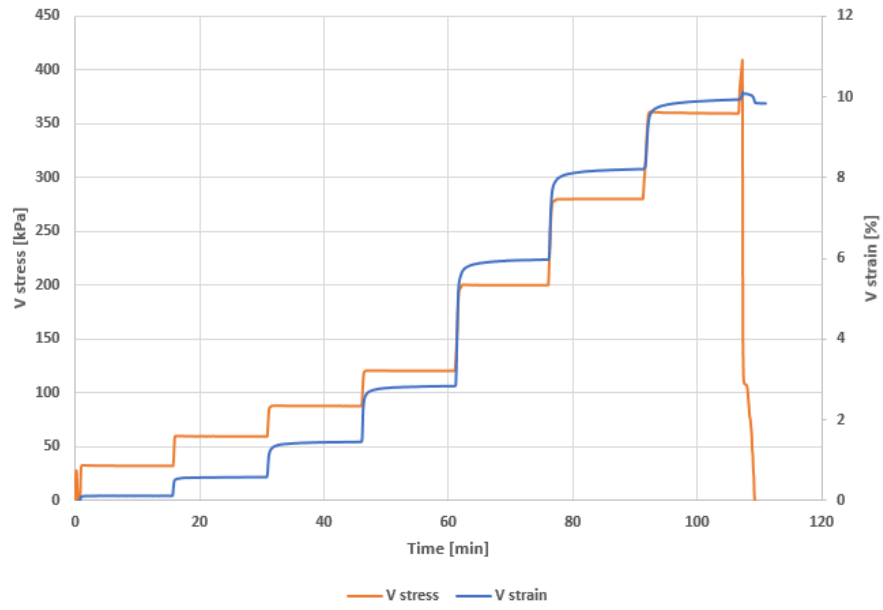
Figure 4.7 – *Stress and strain versus time for test 3. Strain(blue) on right hand axis and Stress(orange) on left axis*
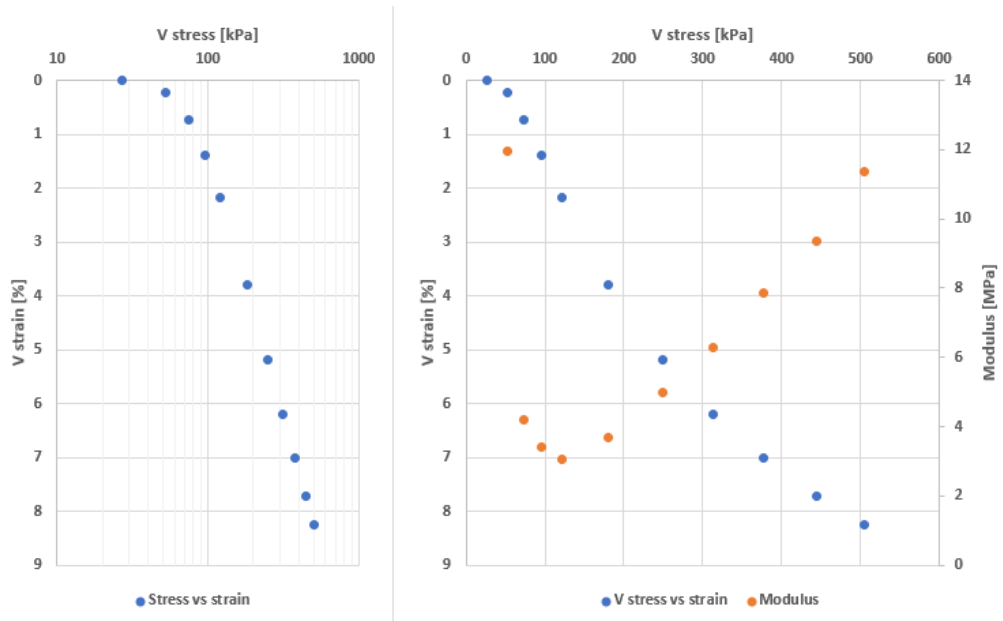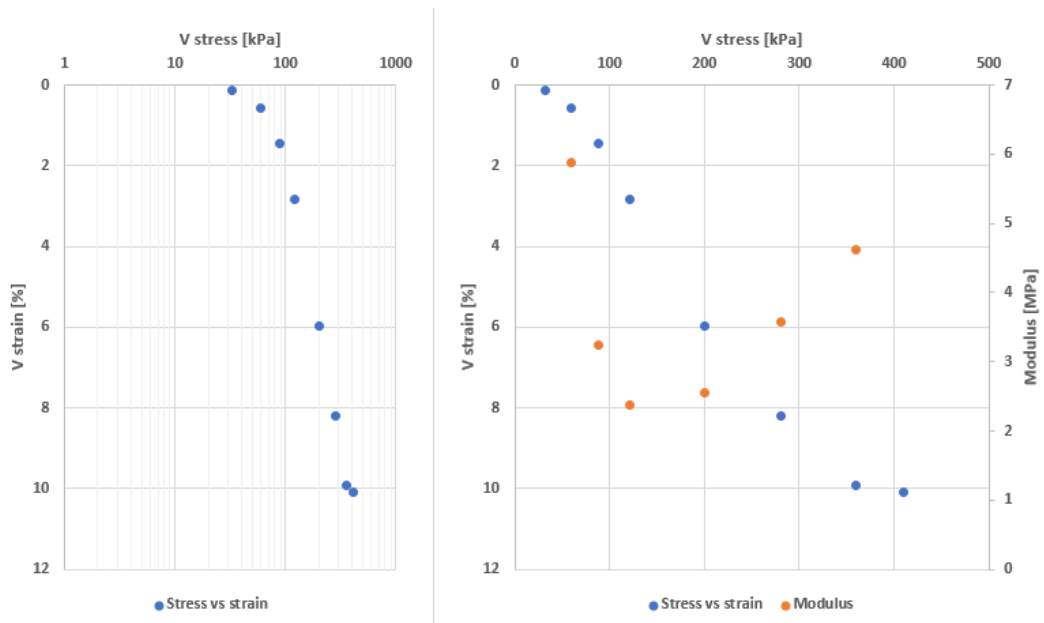

Figure 4.8 – *Stress - strain - modulus: test 3*

4.2.4   Results of test 4:

Test 4 consisted of 6 layers. The stress and strain versus time is presented in figure 4.9. The test reached a maximum strain of 4.9% with a maximum load of 500kPa. In this test the load steps were maintained for about 15min. Figure 4.10 shows the stress - strain relationship and the resulting oedometer modulus. The maximum achieved modulus is 14MPa at p=120kPa, it is believed that this may be caused by one or more large particles which resisted compaction until being crushed into place when load exceeded 120kPa and the deformation modulus decreased. Disregarding the high modulus in this point, the actual maximum achieved modulus is 11MPa at p=500kPa. The water content and final density of the sample is presented in table 4.4. The grain size distributions are presented in figure 4.11.

Table 4.4 – *Density and water content of Oedometer test 4*

|		Before testing	After testing
Sample height	cm	42.5	40.3
Volume	l	83.1	78.8
Wet density	t/m^3	2.10	2.20
Dry density	t/m^3	1.94	2.04
Water content	%		7.6
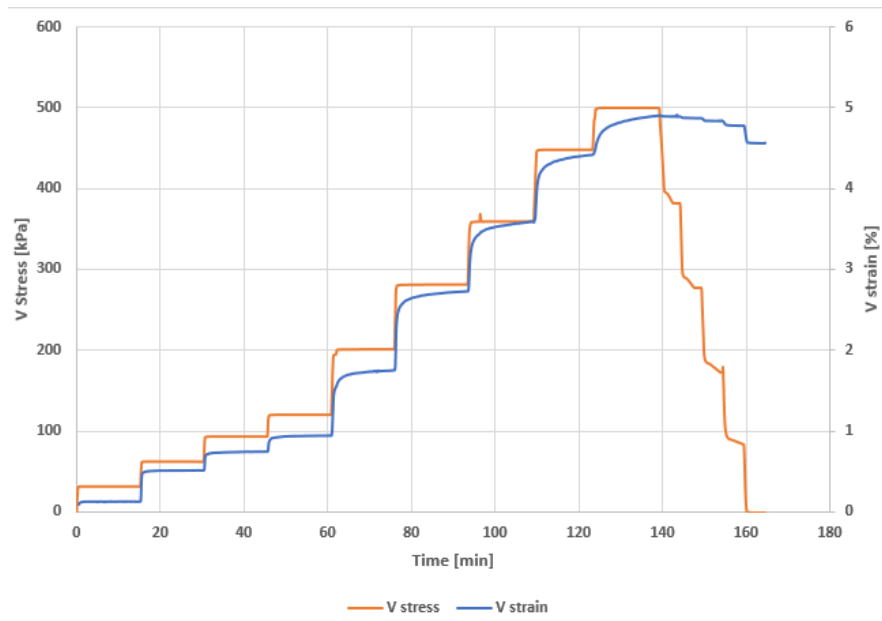
Figure 4.9 – *Stress and strain versus time for test 4. Strain(blue) on right hand axis and Stress(orange) on left axis*

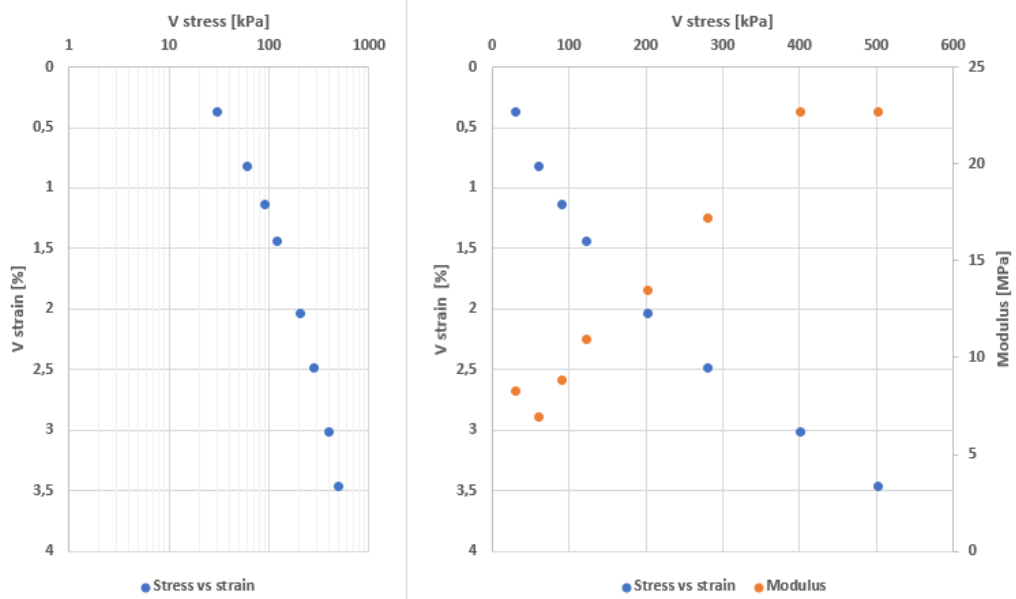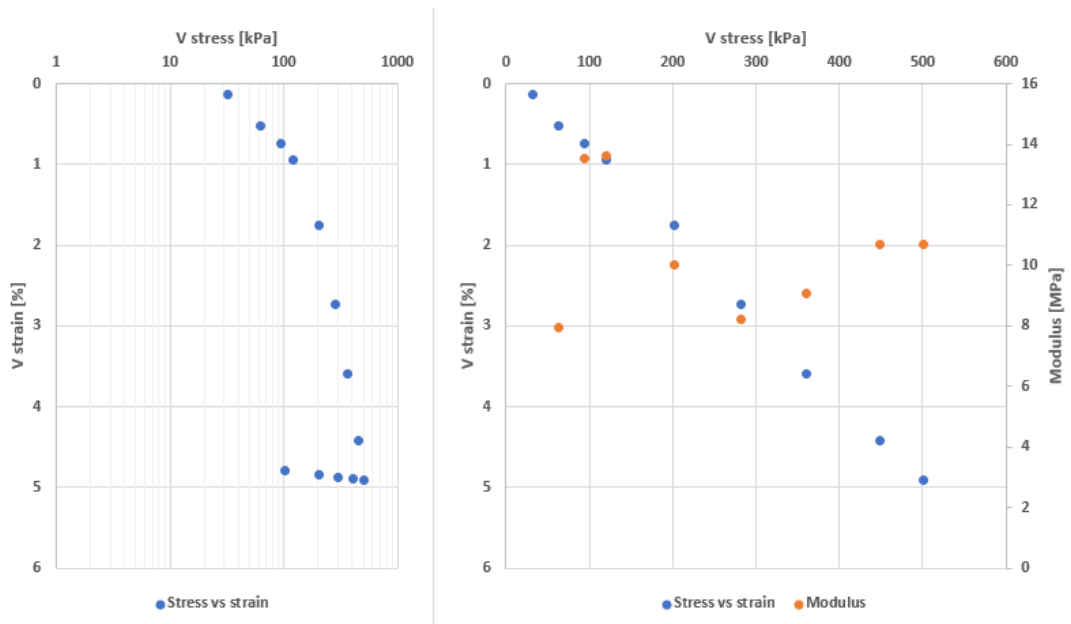**Figure 4.10** – *Stress - strain - modulus: test 4*

4.3   Summary and results from Oedometer testing:

4.3.1   Grain size distributions

Figure 4.11 shows the grain size distributions of oedometer tests 1 - 4 in comparison with the tests conducted at Åsland site.
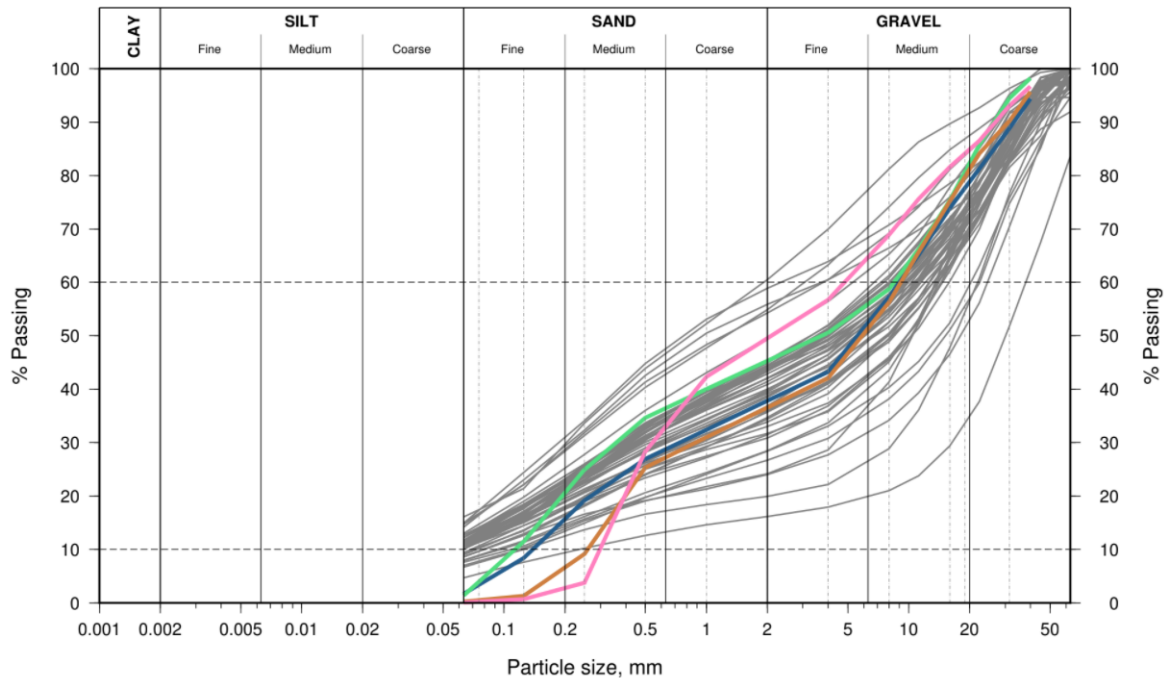
Figure 4.11 – *Grain size distributions from oedometer tests. The grey lines are the tests from the deposit. Oedometer tests 1-4 are drawn in blue, green, orange and pink, respectively.*

The grain size distributions from test 1 - 4 are corresponding well with the tests conducted by KSR Maskin AS for the coarser parts of the distribution. Because of the leakage of fine particles during sieving the distributions cannot be used in determining particle distribution beneath $\approx$ 0.5mm. There is however, no reason to believe that the material collected and used in the oedometer tests is not within the same range as the other tests conducted on the deposit at Åsland. The material is well graded.

4.3.2   Modulus and strain

Figure 4.12 shows the results of the oedometer tests in terms of stress - strain and dry density versus modulus. The suspected falsely high modulus in test 4 are removed from this graph as they are believed to be caused by crushing of stone rather than the overall stiffness of the material. The results are scattered, but with a clear tendency of less strain with higher achieved dry density (better compaction).
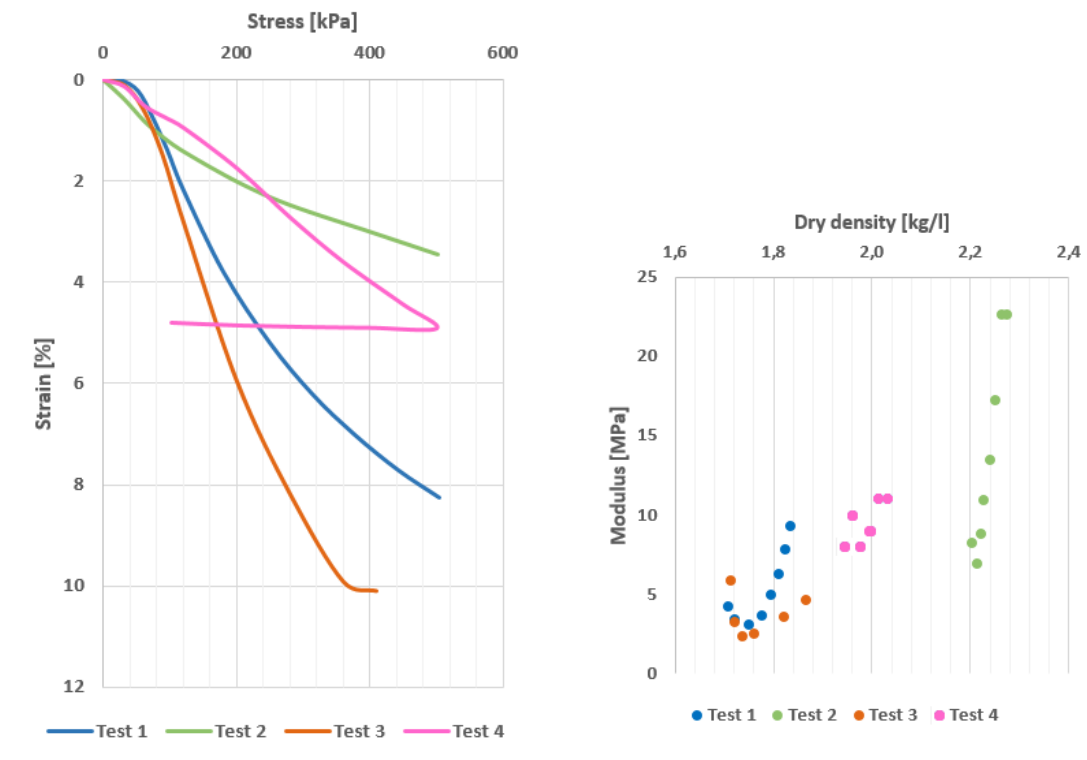
Figure 4.12 – *Results of oedometer tests. Stress-strain and density - modulus*

Figure 4.13 shows the oedometer modulus of the TBM spoil with increasing stress. Table 4.5 summarize the dry density at the beginning of and at the end of each test and the water contents of the samples. Standard Proctor tests revealed that the optimum water content for compaction of this material is 8.23%. The maximum oedometer stiffness, M for the material at the measured field density of roughly 2.15-2.2 t/m^3 is between 7 - 11MPa. Because of the naturally occurring differences in the material (grain size and orientation, water content, geology) it would however give utterly knowledge of the material to conduct more oedometer tests aiming to obtain a dry density $\geq$ 2t/m^3 before loading.
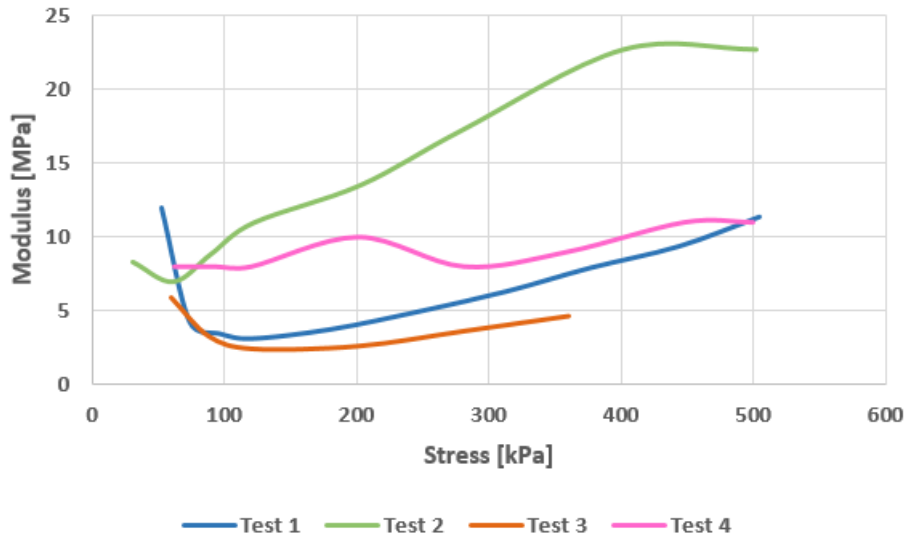
Figure 4.13 – *Stress - Modulus curves for all oedometer tests*

A summary of the oedometer test results is given in table 4.5.

Table 4.5 – *Summary of oedometer test results*

Test	ρ_d t/m^3	w %	M MPa	ε %	Increments min	Comments
1	1.69 - 1.83	10.2	11	8.3	30	Thicker layers
2	2.2 - 2.27	13	23	3.5	20	Leakage of water
3	1.71 - 1.90	6.2	6	10	15	Terminated at 360kPa
4	1.94 - 2.04	7.6	11	4.9	15	
Average		9.25	12.8	66.8		

5 Discussion and evaluation of material properties

5.1 Deformation properties

The oedometer test is one dimensional and the plate load test is three dimensional. $\mathbf{M} = \mathbf{E}_{oed}$ is the oedometer stiffness. This is used to describe the resistance to deformation of a soil element constrained to the sides but free to move in the vertical direction when exposed to a vertical stress σ_1'. The Young's modulus, $\mathbf{E}$ describes the resistance to deformation with applied vertical stress, σ_1' but for a soil element which is restrained only at the bottom and free to deform to the sides. Due to the different boundary conditions of the oedometer and plate load test the results are not directly comparable.

Under the assumption of constant soil behavior with increased stress an estimation of settlements may be found using the equation: (NTNU 2015)

$$\delta = \varepsilon_{repr} H = \frac{\Delta \sigma'}{E} H \tag{5.1}$$

Where:
δ = Deformation/settlement
ε_{repr} = Representative strain
H = Height
E = Young's modulus or appropriate modulus for the boundary conditions
$\Delta \sigma'$ = change in effective stress

This is often used in evaluation of over consolidated soil, where the relevant stress level is lower than the stress history of the soil. For considering the effect of applied stress higher than previous levels the materials behavior with increased stress must be taken into account.

5.1.1 Deformation based on oedometer tests

The development of resistance to deformation of a soil is used to characterize the behavior of the material. Figure 5.1 shows the oedometer modulus with increasing stress for the four oedometer tests conducted in this project.
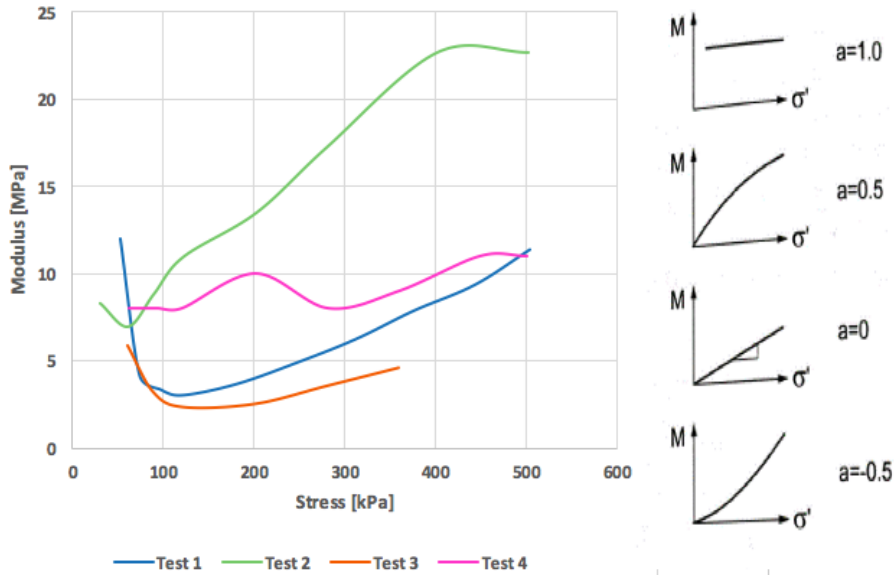
Figure 5.1 – *Modulus vs stress from the oedometer tests*

The results show indications of a material with both plastic and brittle properties. Test 2 and 4 indicate that the material can behave as a sensitive material where the soil particles collapse into a more stable state causing a rapid increase in stiffness. In materials such as TBM spoil from hard rock, this sensitivity is most likely caused by brittleness in the rock particles which are crushed into a more stable arrangement by the load. The materials can also behave like a plastic material with a linear increase in modulus until the modulus becomes constant in the last two loading steps, here a = 1 and the behavior has become elastic. This is typical for intact hard rock or well compacted soils. These results fit well with the dry density, where test 1 and 3 have lower compaction than test 2 and 4, as seen in figure 4.12.

A calculation of settlements based on an example from (Janbu 1970, p.180) is performed. For well compacted material it is assumed little change in behavior with increased stress: a = 1, M $= m\sigma'_a =$ constant and

$$\Delta p/M = \varepsilon \tag{5.2}$$

Where Δp is the added load of a construction. For this estimate an added load of 50kPa, roughly equal to the load of an 8 story building is used. Average p_0 (Initial stress state) for a 30m drained fill is 15m·22kN/m^3=330kPa. →M values from the oedometer tests are taken at p_0 =330kPa from figure 5.1. The expected settlements are shown in table 5.1.

Table 5.1 – *Estimate of settlements for compacted fill. Method from (Janbu 1970, p.180)*

Test	Modulus at p_0 MPa	Strain %	Deformation m
1	7	0.71	0.21
2	20	0.25	0.08
3	4.5	1.10	0.33
4	8	0.63	0.19

It is worth noting that the expected deformations even at poor compaction are not very high, only 33cm.

Figure 5.2 shows the %-deformation (strain) of the oedometer tests conducted on TBM spoil from Åsland together with Kjærnsli's oedometer investigations on different materials of 1968.
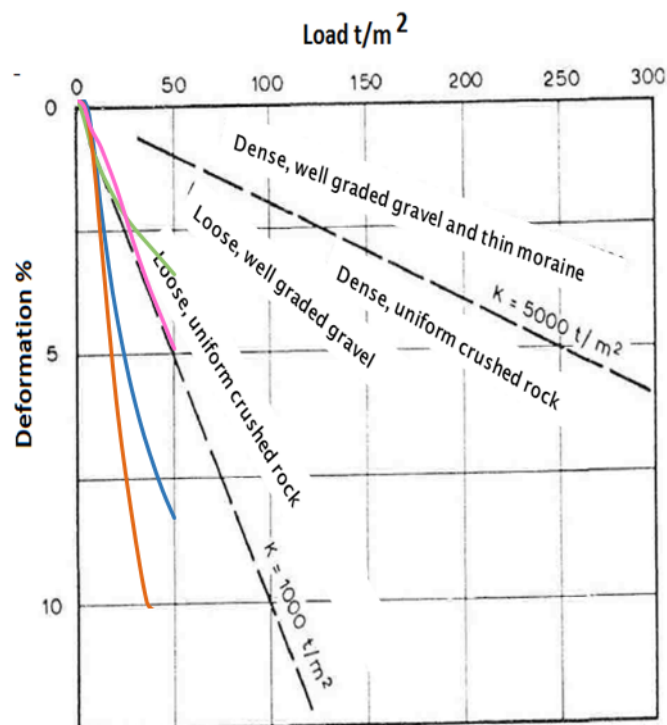
Figure 5.2 – *Results of oedometer on TBM spoil from Åsland compared with oedometer tests on other materials from (Kjærnsli, B. 1968, p.2)*

The results show that the TBM spoil sample with most resistance to deformation and highest dry density corresponds to the loose, uniform crushed rock from Kjærnsli. Kjærnsli & Sande (1963) researched the affect of water content on compatibility of coarse grained materials where they explain that when rock material is fully saturated or above optimum water content the shear strength is decreased and the deformation is increased. It is therefore possible that the high strains and low moduli of the oedometer tests performed in this project is caused by the water content of the samples or in parts of the samples being $> w_{opt}$.

Another explanation is form-effects. The oedometer used by Kjærnsli, B. (1968) had diameter D = 600mm, and H/D approximately 0.5. The Anton-oedometer has H = 577mm and D = 499mm, with H/D = 1.16. There is a possibility that the load from the lid not only goes to compact the rock, but also has a component of friction against the oedometer-walls, even if the walls were lined with grease and plastic membrane. Compared to the oedometer modulus on crushed rock referred to by Gustafsson (2014) in figure 2.8, the results from the oedometer-test on TBM-materials are significant lower.

Figure 5.3 is the stress and strain of oedometer test 1 with time. The loading increments of test 1 are longer as part of investigation on how quickly the primary consolidation finished.
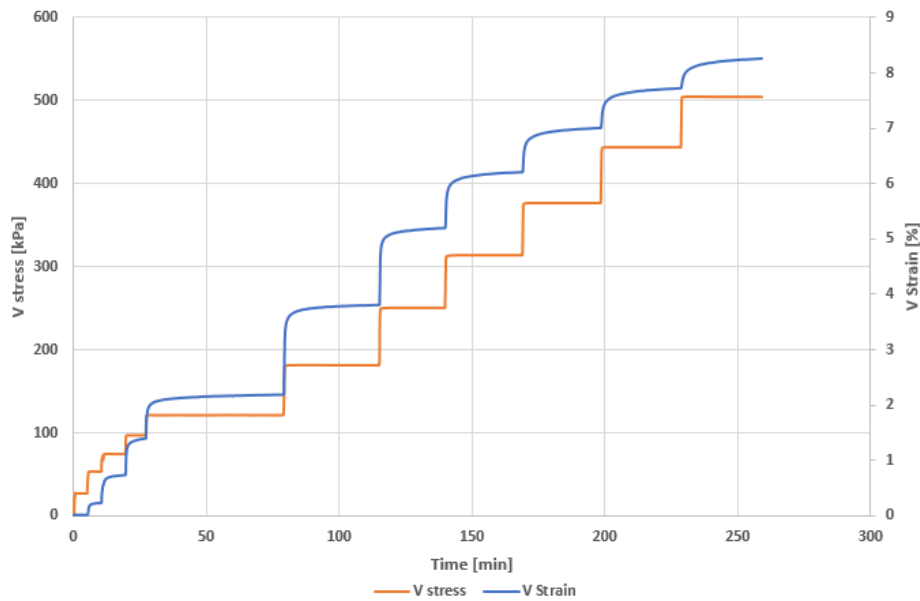
Figure 5.3 – *Stress and strain versus time for test 1. Strain(blue) on right hand axis and Stress(orange) on left axis*

For each increase in load the strain in the material immediately increase as the soil settles. This is the initial compression of the settlements. The strain stabilizes fairly quickly after each increment, as can be seen by the blue line. Settlements after the initial compression is small, indicating that the material is not prone to large creep settlements within this load range. For the final load steps a small increase in strain is visible (the blue line is not completely flat). This may indicate that the secondary consolidation might be more significant for higher loads than investigated in this report.

5.2   Compaction

The compaction is tested in several ways in the laboratory and field. The plate load tests stands out as the investigation with poorest results.
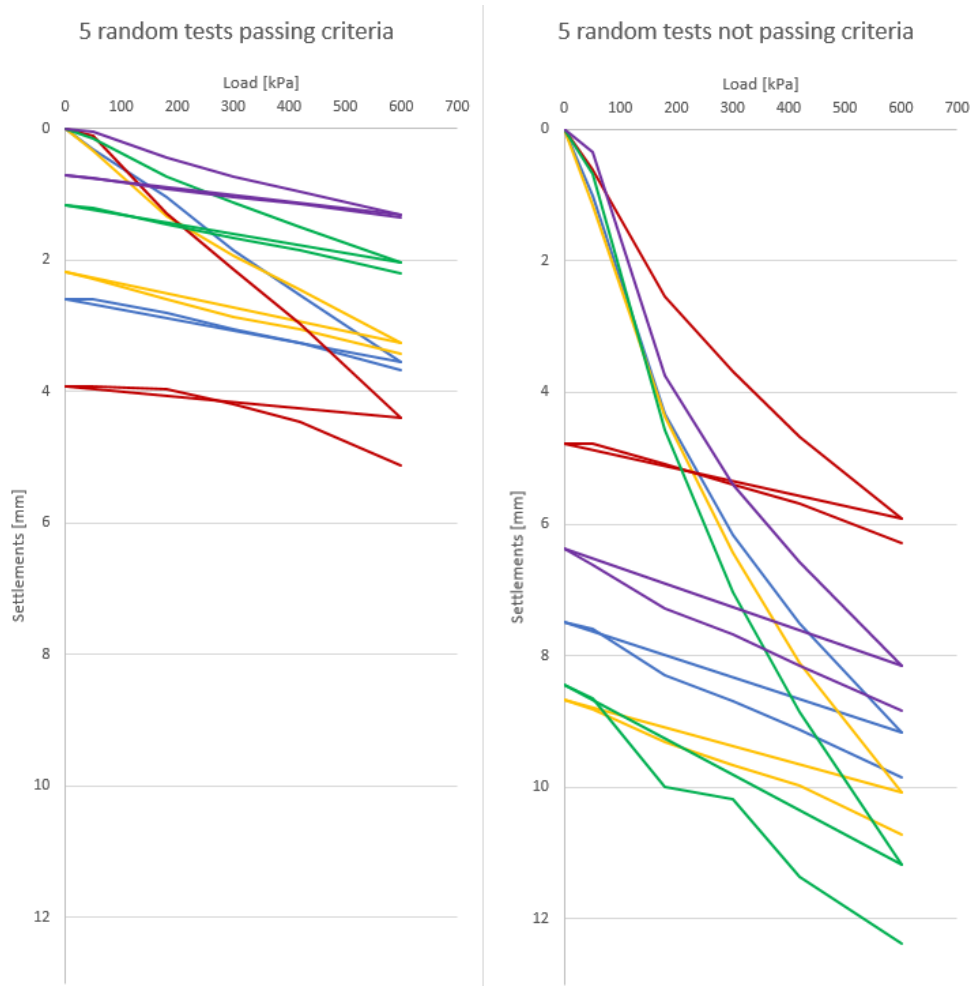
Figure 5.4 – *Comparison of plate load tests passing and not passing criteria. 5 tests from each group were picket at random and graphed to clearly show the differences in settlements*

Figure 5.4 shows 5 random PLT that are within the criteria set by NGI and 5 random PLT that did not pass the criteria (NGI 2015). The tests not passing the criteria measured a settlement beneath the loading plate of up to 2.4 times higher than the largest settlement of the passing tests. 58/80 have too high deformations to pass the criteria set for the project. As such, the plate load test results point to poor compaction of the layers.

Troxler density readings reveal that the average achieved dry density is the same as the average optimum dry density from standard Proctor testing and within 95% of the optimum dry density corrected for compaction control in field. The achieved dry density of the deposit is shown to

be at or above proctor optimum by the field excavation tests, which revealed a dry density with an average of $2.28t/m^3$. Figure 5.5 show the measured dry density in the deposit layers after compaction.
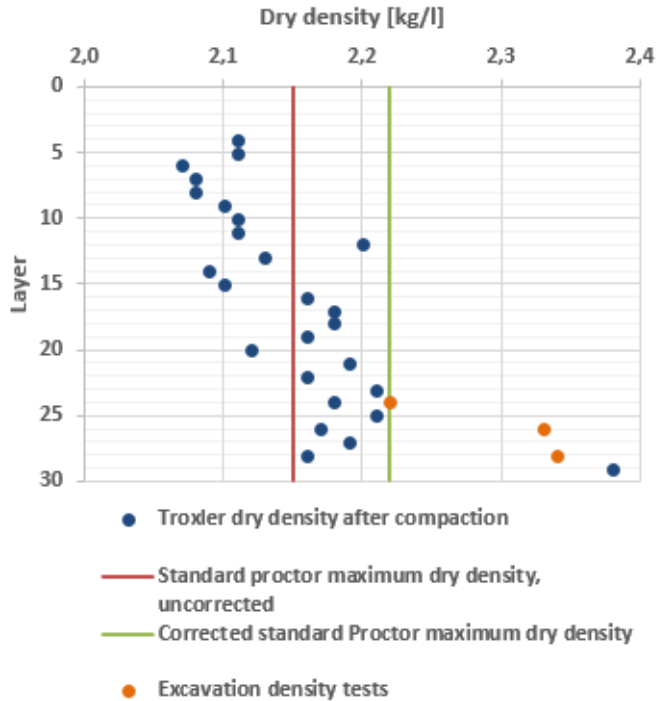
Figure 5.5 – *Average measured dry density after compaction for each layer. The green line marks the maximum dry density corrected for compaction control and the red line is the uncorrected maximum dry density. The orange dots shows the dry density of the material from the shaft test*

Shaft tests 1 and 4 were conducted in different sections of the deposit in the same layer. The tests overlap with dry density results of 2.22 and $2.23t/m^3$. The shaft tests indicates that the fill has received a sufficient compaction.

By comparing the stress - strain curves of the plate load tests in figure 5.4 with the typical stress - strain curves from figure 5.6 it is assumed that the soil behavior reflects that of a partially cohesive soil. This cohesion effect is also mentioned in NGI (1986) where it is described as a "false" cohesion created by the lief-shape of the TBM grains and that it is therefore expected to be anisotropic.
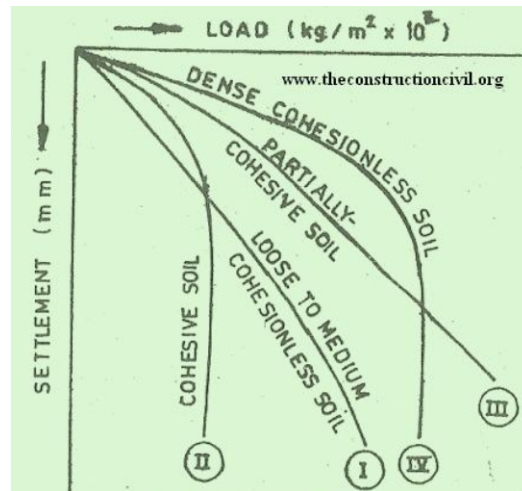
Figure 5.6 – *PLT characteristic load - settlement curves of different materials (Construction civil 2018)*

Because the plate load tests are performed right after compaction of the layer and excess water has not had time to dissipate, with a permeability measured in the field tests in the magnitude of 10^{-5} - 10^{-6} m/s. This permeability corresponds to a fine sand or coarse silt, as shown in figure 5.7 (Grunnvann i Norge 2016).
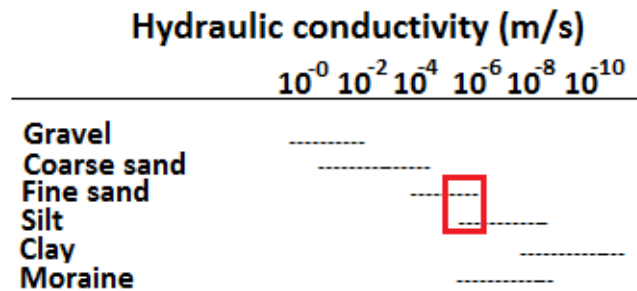
Figure 5.7 – *Hydraulic conductivity of different materials - Translated from Grunnvann i Norge (2016)*

The material is shown to drain well, however it could take a day or two for the water to dissipate from the newly compacted layer, depending on the climate conditions. Hence, it is possible that the material is still consolidating when the plate load tests are performed. Because density and water content is not measured at the same locations as the plate load tests, it is not possible to see the exact density at the time and place of the load test.

After being allowed to learn and perform a plate load test at the deposit site it was discovered that the tests are conducted without the use of sand or plaster to level the surface beneath the loading plate. It is difficult to assess the effect of not using plaster to even the load plate on the surface. However, Flatvad (2012) conducted plate load tests on three different materials with and without use of plaster in order to investigate the effect on the measured soil stiffness. Fladvad compared three sets of tests conducted on cobble, four conducted on gravel 0/32 and three on recycled asphalt material. Her investigations revealed that the use of plaster greatly influence the settlements of the first loading cycle, making E_1 stiffer, while the second loading cycle remained unaffected. This is because the plaster is performing some of the leveling work otherwise being pushed in place during the first loading cycle.

According to Fladvad's investigation it is therefore plausible that the lack of plaster causes "falsely" low E_1 values and thereby increasing the value of E_2/E_1. Because the criteria set by NGI and the standards are given under the assumption that plaster or sand has been used, the results are not directly comparable to the criteria. It is reasonable to assume that this may be the cause of the inconsistency between the poor plate load results and the good achieved compaction which is within 95% of standard Proctor. The dry density in the oedometer tests corresponds to- or is lower than what is found from the Proctor-tests, Troxler tests and shaft tests. The estimated potential settlements based on the results from the oedometer tests are small. This indicates that the fill is sufficiently compacted, even if the plate load tests are not fulfilling the expected criteria.

6 Summary and conclusion

The investigation of the TBM spoil from Åsland deposit site in Oslo, Norway covered in this report consists of the following investigations:

- standard Proctor compaction tests

- *in situ* Troxler moisture/density readings

- washing and dry sieving

- plate load tests

- wet sieving and falling drop

- field excavation tests

- field permeability tests

- large scale oedometer tests

The standard Proctor, washing and dry sieving, Troxler and plate load tests are conducted by KSR Maskin AS for each layer of the deposit and the results are systematized and presented in this report. In addition, large scale oedometer tests have been conducted at the NTNU geotechnical laboratory in Trondheim, Norway by the author of this report. Four field excavation tests were conducted in April, the first of which contained a layer of frozen ground. The excavations investigated the achieved dry density of larger volumes and the permeability of the soil. During the last excavation test, soil samples were collected for sieving and investigation of fines content to investigate the frost susceptibility of the material. Table 6.1 shows a summary of the material properties of the TBM spoil:

Table 6.1 – *Summary of material properties*

Parameter	Symbol		Average value
Plate load stiffness	E_1	MPa	26.5
Plate load stiffness	E_2/E_1		3.43
Water Content (Troxler)	w	%	6.40
Dry density (Troxler)	ρ_d	t/m^3	2.15
Dry density (Shaft tests)	ρ_d	t/m^3	2.28
Fines content (of d_{max})	-	%	10.69
Fines content (of material $< 22.4mm$)	-	%	14.1
Optimum moisture content	w_{opt}	%	8.23
Maximum dry density	$\rho_{d,max}$	t/m^3	2.15
Permeability	k	m/s	10^{-5} - 10^{-6}
Frost susceptibility	-		Yes, T_2
Water sensitive	-		Yes
Oedometer modulus	M	MPa	5 - 20

The TBM spoil is found to be a well graded, water sensitive material with a light frost susceptibility. The Troxler density gauge and the dry density from the excavation tests reveal that the achieved compaction is within 95% of the standard Proctor maximum for field control of 2.22t/m^3. While only 22% of plate load tests pass the requirements set for the specific project it

is suspected that this might be caused by lack of plaster for leveling the surface before conducting the test.

The permeability of the soil is in the magnitude of 10^{-5} - 10^{-6} m/s, roughly equivalent to that of a fine sand or a coarse silt. This corresponds well with the fines content revealed by the dry sieving $\approx 10\%$.

The oedometer tests were conducted on material with 6 - 13% water content. The water content affected the achieved compaction and strains of each test. The tests resulted in strains of 3.5 to 10% with a maximum load of 500kPa. The oedometer modulus is between 5 - 20MPa and the achieved dry density at the end of the tests were 1.83 - 2.27t/m^3. For a possible load of 50kPa on terrain level, the results indicate a maximum settlement of ≈ 0.33m for a 30m fill.

7   Recommendations for further work

It could be beneficial to conduct some plate load tests with the use of plaster to level the surface beneath the loading plate in order to establish a correlation of the old results with new tests using plaster. This may be used for correction of the results made in this report in order to further investigate the compaction work, E_2/E_1 and possible settlements of footings.

The plate load test results are highly scattered. Performing Troxler moisture and density readings at the time and location of plate load tests may reveal in greater detail how the degree of compaction and water content affects the results of these tests for the material.

Because of the resources and time a large scale oedometer test on TBM spoil demands, it could be beneficial to conduct a study on whether smaller scale oedometer tests on sieved material samples may contribute to the evaluation of deformation properties. This could potentially contribute to other investigations of such materials.

At higher loads, 400 - 500kPa, the strains of oedometer test 1 showed some increase with time between loading. This indicates that the material may be more prone to secondary consolidation for higher loads. The effect of higher loads and long time between increments to study the creep effect is suggested.

References

Anyang, Atarigiya, Ofori-Addo & Allotey (2018), *Plate load test: Getting it right from 49th Ghana Institution of Engineers (GhIE) Annual Conference, March 2018*.

Bane NOR (2018), *Prosjekt Follobanen: Pressebilder*. Available at: http://www.banenor.no/Prosjekter/prosjekter/follobanen/om-follobaneprosjektet/pressebilder/ - Accessed: 01.06.2018.

Bellopede, R., Brusco, F., Oreste, P. & Pepino, M. (2011), 'Main aspects of tunnel muck recycling', *American Journal of Environmental Sciences* **7**(4), 338–347.

Berdal, T. (2017), Use of excavated rock material from tbm tunnelling for concrete proportioning, Master's thesis, NTNU.

Bertram, G. E. (1987), *Field tests for compacted rockfill in Casagrande Memorial Vol.1: Embankment dam engineering*, John Wiley and sons.

Bruland, A. (1998), 'Hard rock tunnel boring vol 3 of 10. advance rate and cutter wear', *NTNU project report 1B-98* .

Construction civil (2018), *Plate load test: determining the bearing- capacity of soils*. Available at: https://www.theconstructioncivil.org/ - Accessed: 28.03.2018.

Deutscnes Institut fur Norrnung (2012), *Soil-Testing procedures and testing equipment-Plate load test, English translation of DIN 18134:2012-04*, Berlin.

Emdal, A. (2014), *Introduksjon til Geoteknikk*, NTNU Faggruppe for Geoteknikk.

Flatvad, M. (2012), Kontinuerlig komprimeringskontroll, Master's thesis, NTNU.

Gertsch, L., Fjeld, A., Nilsen, B. & Gertsch, R. (2000), 'Use of TBM muck as construction material', *Tunnel Construction Materials* **15**(4), 379–402.

Grunnvann i Norge (2016), *Grunnvannsstrømning og permeabilitet*, NGU. Available at: http://www.grunnvanninorge.no/grunnvann$_h$va$_e$r.php $- Accessed : 28.05.2018$.

Gustafsson, V. (2014), *Creep deformation of rockfill*, KTH Department of Civil and Architectural Engineering Division of Soil and Rock Mechanics.

Janbu, N. (1970), *Grunnlag i Geoteknikk*, Tapir akademisk forlag.

Jernbaneverket (2014), 'The Follo Line, Tunnel Section: Summary Geoloical Data Report', *The Follo Line Project* .

Ketelaars, M. & Saathof, L. (2000), 'From spoil to soil: Reuse of soil form TBM's in the Netherlands', *Geotechnical Aspects of Underground Construction in Soft Ground* pp. 239–243.

Kim, Fratta & Wen (2014), 'Field measurements for the effectiveness of compaction of coarse-grained soils', *KSCE Journal of Civil Engineering* **2**(18), 497–504.

Kjærnsli, B. (1968), 'Fundamentering på grus- og steinfyllinger', *Norwegian Geotechnical Institute* **Publication 073**.

Kjærnsli, B. & Sande, A. (1963), *Compressibility of some Coarse-Grained Materials*, NGI.

Kjærnsli, B., Valstad, T. & Höeg, K. (2003), *Hydropower Development 10: Rockfill Dams*, Norwegian Geotechnical Institute.

Leps, T. M. (1970), *Review of shearing strength of rockfill in Journal of soil mechanics and foundation Vol.96*, ASCE.

Moum, J. (1965), 'Falling drop used for grain-size analysis of fine-grained materials', *Sedimentology* **5**(4), 343–347.

Multiquip (2011), *Soil compaction handbook Rev.A*, MULTIQUIP INC. Available at: http://www.multiquip.com/multiquip/pdfs/SoilCompactionHandbooklowres0212 DataId59525Version1.pdf - Accessed: 31.01.2018.

NGI (1986), *Oppdragsrapport: Prosjekt fullprofilmasser materialegenskaper 85607-1*, Norges Geotekniske Institutt.

NGI (2015), 'Follobanen tunnel TBM: Application of TBM spoil as quality fill for Gjersrud/Stensrud township', *NGI Report* .

Norwegian Soil and Rock Engineering Association (1998), *Norwegian TBM tunnelling: 30 years of experience with TBMs in Norwegian tunnelling*, Norwegian tunnelling society, NFF.

NTNU (2015), *MSc course TBA4110. Geotechnics: Field and Laboratory Investigations*, NTNU Geotechnical division.

Oggeri, C., Fenoglio, T. M. & Vinai, R. (2014), 'Tunnel spoil classification and applicability of lime addition in weak formations of muck reuse', *Tunnelling and Underground Space Technology* (44), 97–107.

Oggeri, C., Fenoglio, T. M. & vinai, R. (2017), 'Tunnelling muck classification: definition and application', *Proceedings of the World Tunnel Congress 2017, Surface challenges - Underground solutions. Bergen, Norway* .

Olbrecht & Studer (1998), 'Use of tbm chips as concrete aggregate', *Materials and Structures* **31**, 184–187.

Olson, R. E. (1989), *Secondary consolidation*, Chaoyang University of Technology.

Pantelidis, L. (2005), *Determination of soil strength and charcteristics performing the plate bearing test in 3rd International Conference „Modern Technologies in Highway Engineering" Poznań, 8–9 September, 2005.*

Ritter, S., Einstein, H. H. & Galler, R. (2013), 'Planning the handling of tunnel excavation material - a process of decision making and uncertainty', *Tunnelling and Underground Space Technology* (33), 193–201.

Standard Norge (2004), *NS 3458:2004. Compaction Requirements and execution.*

Standard Norge (2009), *NS-EN 13242:2002+A1:2007+NA:2009. Aggregates for unbound and hydraulically bound materials for use in civil engineering work and road construction.*

Standard norge (2017), *NS-EN ISO 17892-5:2017 Geotechnical investigation and testing – Laboratory testing of soil - Part 5: Incremental loading oedometer test*, Standard norge.

Statens vegvesen (2014), *Håndbok N200: Vegbygging*, Vegdirektoratet.

Statens vegvesen (2015), *Håndbok 761: Prosesskode 1. Standard beskrivelsestekster for vegkontrakter*, Vegdirektoratet.

Statens vegvesen (2016), *Håndbok R210: Laboratorieundersøkelser*, Vegdirektoratet.

Statens vegvesen (2018), *Håndbok R211: Feltundersøkelser*, Vegdirektoratet.

Tan, T. S., Phoon, K. K., Hight, D. W. & Leroueil, S. (2003), *Characterisation and Engineering Properties of Natural Soils, Volume 2*, A.A. Balkema publishers.

Teodoru, I. B. & Toma, I. O. (2009), *Numerical analysis of plate loading test in BULETINUL INSTITUTULUI POLITEHNIC DIN IAŞI*, Universitatea Tehnică ,,Gheorghe Asachi'' din Iaşi Tomul LV (LIX).

Terzaghi, K., Peck, R. B. & Mesri, G. (1996), *Soil mechanics in engineering practice Third edition*, John Wiley & sons.

Tokgöz, N. (2013), 'Use of TBM excavated materials as rock filling material in an abandoned quarry pit designed for water storage', *Engineering Geology* **153**, 152–162.

Troxlerlabs (2018), *Troubleshooting FAQs*, Troxlerlabs. Available at: http://www.troxlerlabs.com/Services/Troubleshooting-FAQs - Accessed: 27.04.2018.

APPENDIX A: Field excavation tests

Results of Troxler test before excavation:

Dry density: [kg/l]	Wet density: [kg/l]	Moisture: [kg]	Moisture: [%]
2,18	2,36	179,7	8,2
2,173	2,381	178,3	8,2
2,136	2,314	178,3	8,3
2,142	2,323	181,1	8,5
2,149	2,324	175,5	8,2
2,167	2,344	176,9	8,2
		Average:	**8,3**
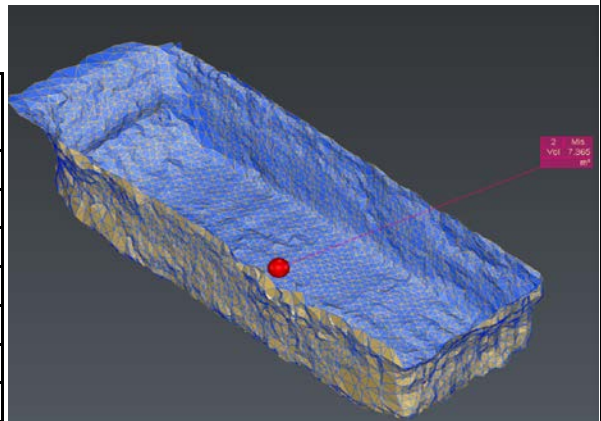
* Troxler measurements in frozen layer

Excavation density test:

Weight:		Volume:	
Truck:	14350 kg	Frame:	834,5 liters
Truck + material:	31800 kg	Frame + hole:	8031 liters
Material:	17450 kg	Hole:	6501 liters
Material, dry:	16008 kg		
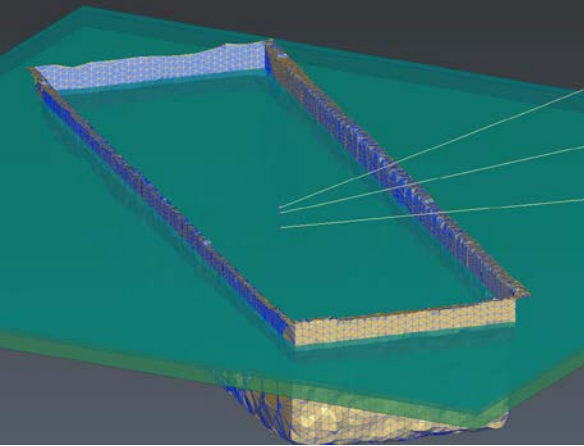
Test shaft:		Troxler: (Frozen ground)	
Dry density:	**2,22 kg/l**	Dry density:	2,16 kg/l

Permeability:

Volume: [l]	Time: [min]	Height: [mm]	Permeability, k [l/min]
80	15	-10	5,33
1382	882	-179	1,58

Cold temperatures during the night created a layer of ice on the water and the sun melted nearby snow causing water to flow during the day

Date:	11.04.2018	Position:	A03 - Layer 28	Test 2

Results of Troxler test before excavation:

Dry density: [kg/l]	Wet density: [kg/l]	Moisture: [kg]	Moisture: [%]
2,088	2,343	255,5	12,2
2,095	2,331	235,8	11,3
2,235	2,443	207,8	9,3
2,235	2,432	196,5	8,8
1,959	2,163	203,5	10,4
2,057	2,256	197,3	9,7
		Average:	**10,3**

Excavation density test:

Weight:		Volume:	
Truck:	14600 kg	Frame:	1878 liters
Truck + material:	29050 kg	Frame + hole:	7426 liters
Material:	14450 kg	hole:	6346 liters
Material, dry:	12964 kg		

Test shaft:		Troxler:	
Dry density:	**2,34 kg/l**	Dry density:	2,11 kg/l

Permeability:

Volume: [l]	Time: [min]	Height: [mm]	Permeability, k [l/min]
1686	15	-230	112,4
4144	47	-610	88,2
6346	197	Empty	-

A-2

Date:	13.04.2018	Position:	A06 - Layer 26	Test 3

Results of Troxler test before excavation:

Dry density: [kg/l]	Wet density: [kg/l]	Moisture: [kg]	Moisture: [%]
2,21	2,37	162,80	7,40
2,22	2,37	158,60	7,20
2,11	2,27	155,80	7,40
2,20	2,37	175,50	8,00
2,20	2,36	165,70	7,50
2,20	2,36	160,00	7,30
		Average:	**7,5**

Excavation density test:

Weight:		Volume:	
Truck:	17450 kg	Frame:	2015 liters
Truck + material:	34250 kg	Frame + hole:	8684 liters
Material:	16800 kg	hole:	6669 liters
Material, dry:	15546 kg		

Test shaft:		Troxler:	
Dry density:	**2,33 kg/l**	Dry density:	2,19 kg/l

Permeability:

Volume: [l]	Time: [min]	Height: [mm]	Permeability, k [l/min]
278	2	-40	139
416	4	-60	104
4176	58	-630	72

A-3

Date:	25.04.2018	Position:	A11 - Layer 24		Test 4

Results of Troxler test before excavation:

Dry density: [kg/l]	Wet density: [kg/l]	Moisture: [kg]	Moisture: [%]
2,22	2,37	107,30	4,80
2,21	2,32	111,50	5,10
2,31	2,44	126,90	5,50
2,32	2,45	125,50	5,40
2,30	2,43	124,10	5,40
2,26	2,38	126,90	5,60
		Average:	**5,3**

Results of Troxler test at the bottom of the pit:

Dry density: [kg/l]	Wet density: [kg/l]	Moisture: [kg]	Moisture: [%]
2,10	2,21	112,90	5,40
2,11	2,22	108,70	5,20
2,07	2,17	103,10	5,00
2,07	2,17	97,60	4,70
2,07	2,19	121,30	5,90
2,05	2,17	117,10	5,70
		Average:	**5,3**

Excavation density test:

Weight:		Volume:	
Truck:	17500 kg	Frame:	1755 liters
Truck + material:	32050 kg	Frame + hole:	7938 liters
Material:	14550 kg	hole:	6183 liters
Material, dry:	13779 kg		

Test shaft:		Troxler:	
Dry density:	**2,23 kg/l**	Dry density: 1	2,27 kg/l
		Dry density: 2	2,08 kg/l

Permeability:

Volume: [l]	Time: [min]	Height: [mm]	Permeability, k [l/min]
311	30	-40	10,4
1088	183	-140	5,9

Grain size distributions were conducted on samples from the bottom of this pit, the result show:

Moisture content:	5,5 %
% < 0.063mm of mass less than 22.4mm:	12,9 %
Fines content:	10,7 %

Grain size distributions from field excavation test 4

Sample 1

Mass wet sample	22832
Mass dry sample	21678
Mass dry after washin	19633

Screen	Dry sieve sample 1					Sample 1A			Sample 1B		
	Material g	Retain g	Material %	Retain %	Pass %	Pass (HYD) %	Pass total %	Retain total %	Pass (HYD) %	Pass total %	Retain total %
90	0	0	0	0	100		100	0,0		100	0,0
63	0	0	0	0	100		100	0,0		100	0,0
45	1102	1102	5,1	5,1	94,9		94,9	5,1		94,9	5,1
31,5	1085	2187	5	10,1	89,9		89,9	10,1		89,9	10,1
22,4	1506	3693	6,9	17	83		83	17,0		83	17,0
16	1994	5687	9,2	26,2	73,8		73,8	26,2		73,8	26,2
11,2	1807	7494	8,3	34,6	65,4		65,4	34,6		65,4	34,6
8	1442	8935	6,6	41,2	58,8		58,8	41,2		58,8	41,2
4	2318	11253	10,7	51,9	48,1		48,1	51,9		48,1	51,9
2	1483	12736	6,8	58,7	41,3	98,8	40,7	59,3	99	40,9	59,1
1	1261	13996	5,8	64,6	35,4	83,5	34,5	65,5	83	34,2	65,8
0,5	1254	15251	5,8	70,4	29,6	69,1	28,5	71,5	67	27,5	72,5
0,25	1467	16717	6,8	77,1	22,9	49,1	20,3	79,7	44	18,1	81,9
0,125	1394	18111	6,4	83,5	16,5	30,3	12,5	87,5	28	11,5	88,5
0,063	1197	19308	5,5	89,1	10,9	20,8	8,6	91,4	22	8,9	91,1
0,02						13,0	5,3	94,7	16	6,5	93,5
0,006						10,4	4,3	95,7	11	4,7	95,3
0,002						6,3	2,6	97,4	6	2,6	97,4

Dry sieveing in black, hydrometer in blue

A–5

Sample 2

Mass wet sample	22853	
Mass dry sample	21697	
Mass dry after washin	19686	

Screen	Dry sieve sample 2					Sample A			Sample B		
	Material	Retain	Material	Retain	Pass	Pass (HYD)	Pass tota	Retain total	Pass (HYD)	Pass total	Retain total
g	g	g	%	%	%	%	%	%	%	%	%
90	0	0	0	0	100		100	0,0		100	0,0
63	0	0	0	0	100		100	0,0		100	0,0
45	233	233	1,1	1,1	98,9		98,9	1,1		98,9	1,1
31,5	1336	1569	6,2	7,2	92,8		92,8	7,2		92,8	7,2
22,4	2017	3586	9,3	16,5	83,5		83,5	16,5		83,5	16,5
16	2213	5799	10,2	26,7	73,3		73,3	26,7		73,3	26,7
11,2	2046	7845	9,4	36,2	63,8		63,8	36,2		63,8	36,2
8	1398	9243	6,4	42,6	57,4		57,4	42,6		57,4	42,6
4	2280	11522	10,5	53,1	46,9		46,9	53,1		46,9	53,1
2	1458	12980	6,7	59,8	40,2	98,7	39,7	60,3	98,4	39,5	60,5
1	1198	14178	5,5	65,3	34,7	85,0	34,1	65,9	80,0	32,1	67,9
0,5	1236	15415	5,7	71	29	72,8	29,3	70,7	66,3	26,6	73,4
0,25	1413	16828	6,6	77,6	22,4	44,7	18,0	82,0	43,7	17,6	82,4
0,125	1350	18178	6,2	83,8	16,2	26,1	10,5	89,5	27,2	10,9	89,1
0,063	1205	19383	5,6	89,3	10,7	18,9	7,6	92,4	14,3	5,7	94,3
0,02						14,1	5,6	94,4	12,8	5,1	94,9
0,006						9,4	3,8	96,2	9,2	3,7	96,3
0,002						6,1	2,5	97,5	7,0	2,8	97,2

Dry sieveing in black, hydrometer in blue

A–6

APPENDIX B: Oedometer tests

Test 1:

Table B.1 – *Building of test 1*

Layer	Weight of material [kg]	Compaction [min]
1	43.675	1
2	45.722	1
3	44.955	1
4	45.171	1
Total	**179.523**	

Table B.2 – *Density and water content of Oedometer test 1*

Water content: 10.2 %

		Before testing	After testing
Sample height	cm	49.5	45.5
Volume	l	96.8	89.0
Wet density	t/m^3	1.85	2.0
Dry density	t/m^3	1.69	1.83

Table B.3 – *Increments and modulus of Oedometer test 1*

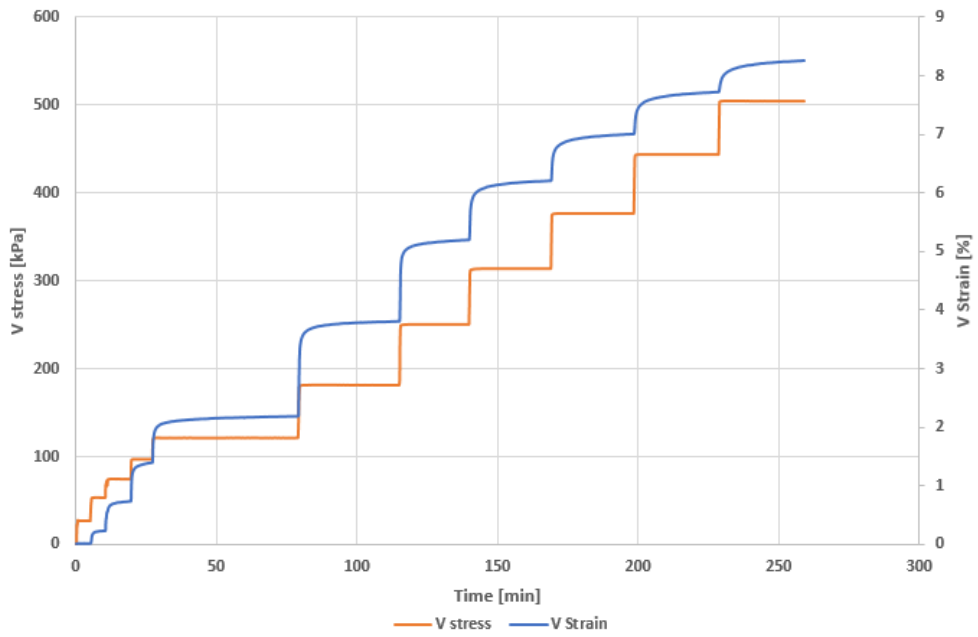| Increment	Time [min]	Time interval [min]	V stress [kPa]	V strain [%]	M [MPa]
-	0	-	0	0	-
1	5	5	26.8	0.006	446
2	10	5	52.7	0.222	12
3	19	9	73.9	0.727	4
4	27	8	96.4	1.388	3
5	79	52	120.7	2.180	3
6	115	36	180.9	3.804	4
7	140	25	250.0	5.194	5
8	169	29	313.6	6.205	6
9	198	30	376.4	7.004	8
10	229	30	443.7	7.723	9
11	259	31	504.6	8.260	11

Figure B.1 – *Stress and strain versus time for test 1. Strain (blue) on right hand axis and Stress (orange) on left axis*
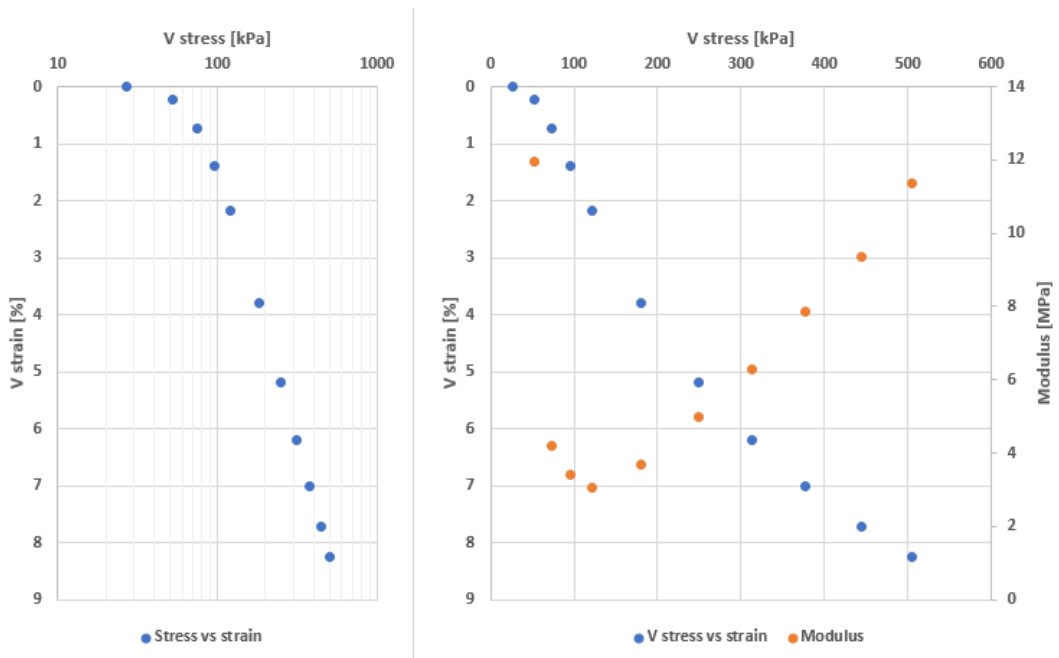

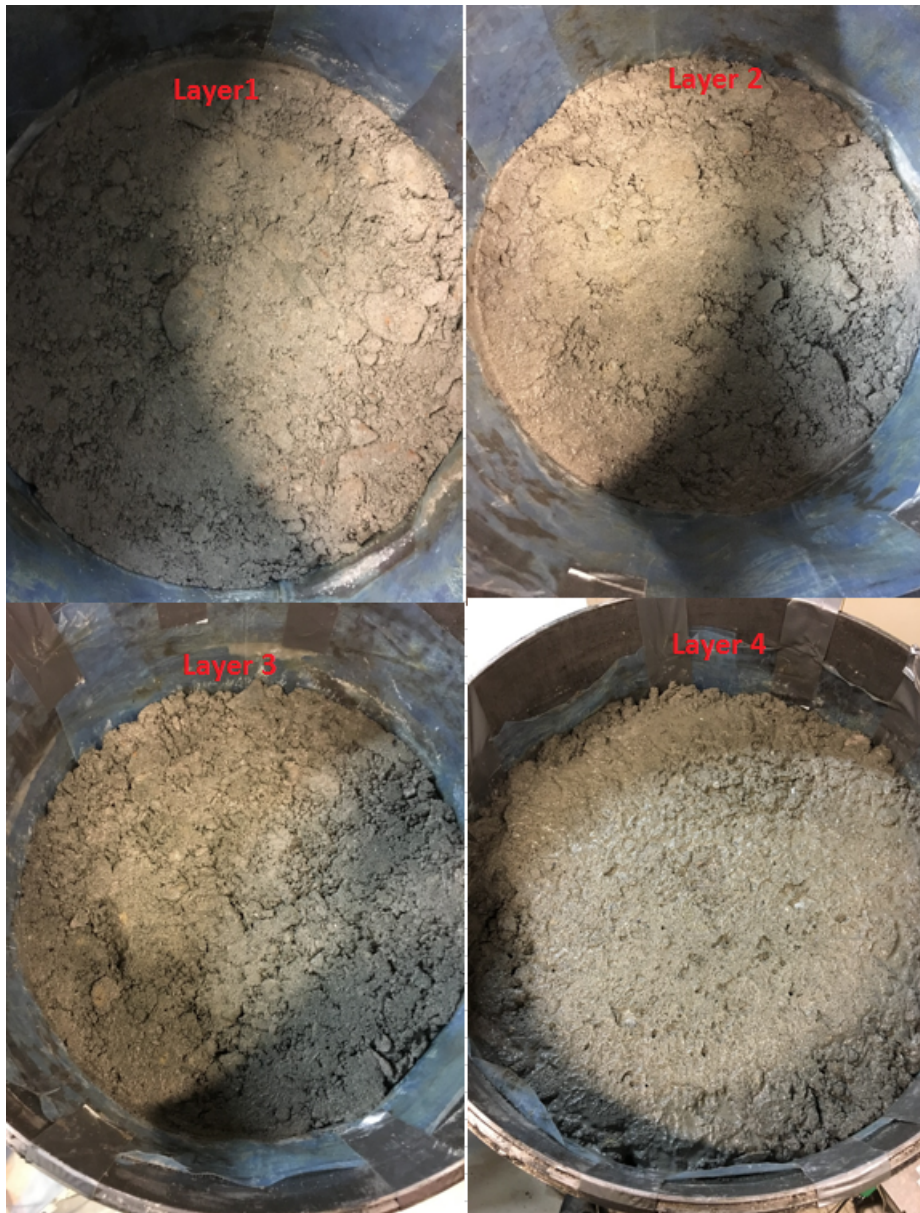**Figure B.2** – *Stress - Strain - Modulus: Test 1*

Figure B.3 – *Pictures of layers after compression. The increase in water conten is clearly visible from layer 1 - 4*

Test 2:

Table **B.4** – *Building of test 2*

Layer	Weight of material [kg]	Compaction [min]
1	26.744	0.5
2	35.206	0.5
3	32.335	0.5
4	36.592	0.5
5	33.161	0.5
6	31.370	0.5
7	20.438	0.5
Total	**215.846**	

Table **B.5** – *Density and water content of Oedometer test 2*

Water content: Minimum 13 %

		Before testing	After testing
Sample height	cm	44.5	43.5
Volume	l	87.0	85.1
Wet density	t/m^3	2.48	2.54
Dry density	t/m^3	2.20	2.27

Large amounts of water in this test and the leakage of at least 4.7kg of water makes the dry density and water contents unsure. There is no doubt however that the sample is densely packed well over 2t/m^3

Table **B.6** – *Increments and modulus of Oedometer test 2*

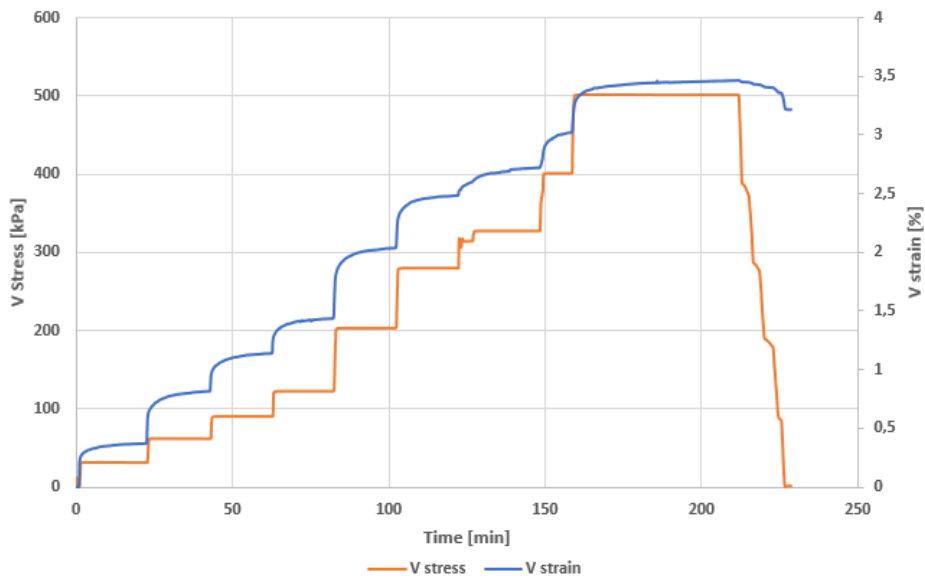| Increment	Time [min]	Time interval [min]	V stress [kPa]	V strain [%]	M [MPa]
-	0	-	0	0	-
1	23	23	30.8	0.372	8
2	43	20	61.5	0.815	7
3	63	20	90.0	1.139	9
4	83	20	122.4	1.436	11
5	103	20	203.1	2.035	13
6	122	20	280.1	2.481	17
7	159	36	401.7	3.018	23
8	229	53	502.1	3.460	23

Figure B.4 – *Stress and strain versus time for test 2. Strain (blue) on right hand axis and Stress (orange) on left axis*
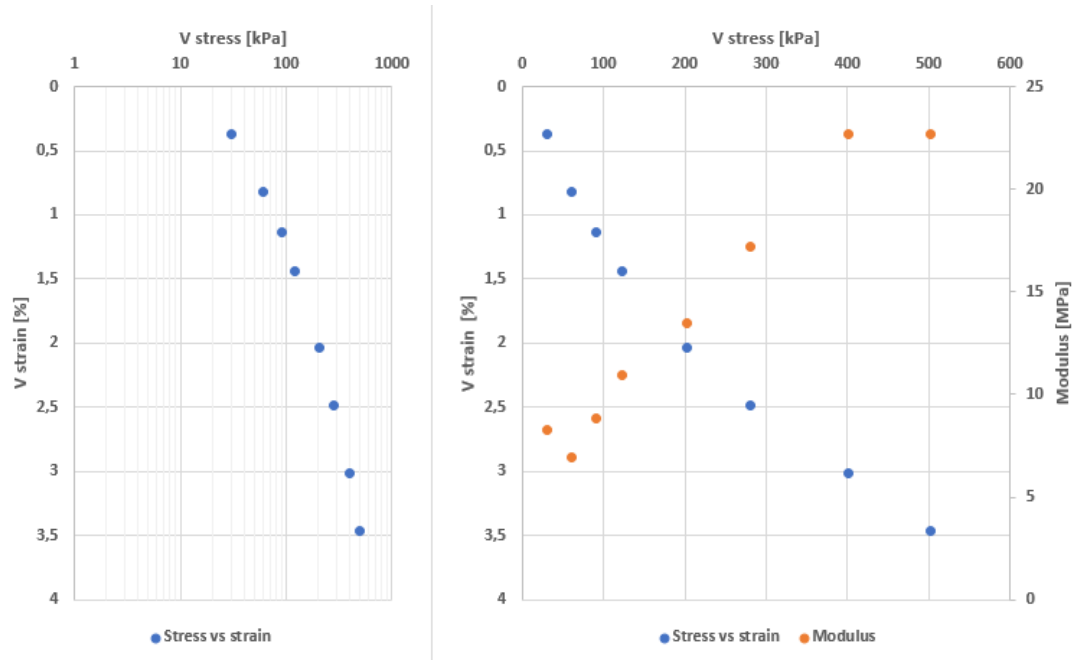

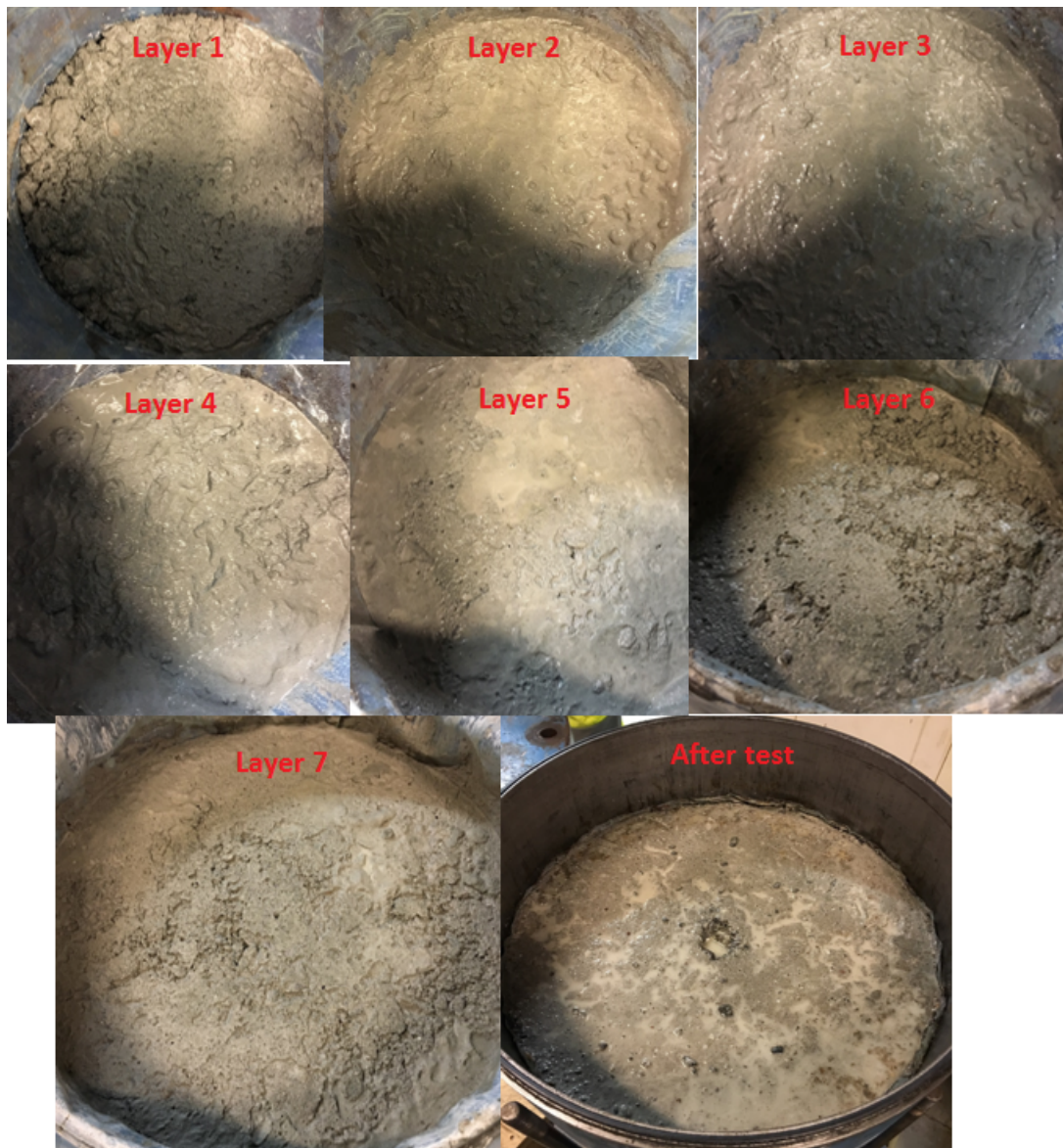**Figure B.5** – *Stress - Strain - Modulus: Test 2*

Figure B.6 – *Layers after compression - test 2. High amounts of water created a muddy substance*

Test 3:

Table B.7 – *Building of test 3*

Layer	Weight of material [kg]	Compaction [min]
1	31.087	0.5
2	32.588	0.5
3	32.582	0.5
4	30.003	0.5
5	30.162	0.5
Total	**156.422**	

Table B.8 – *Density and water content of Oedometer test 3*

Water content: 6.2 %

		Before testing	After testing
Sample height	cm	44.0	39.7
Volume	l	86.0	77.6
Wet density	t/m^3	1.82	2.02
Dry density	t/m^3	1.71	1.90

Table B.9 – *Increments and modulus of Oedometer test 3*

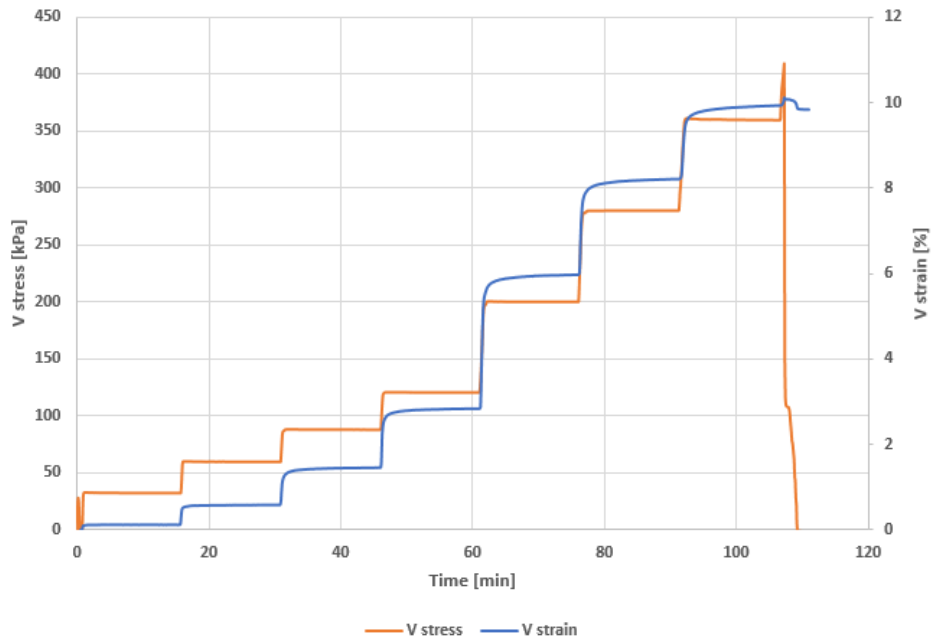| Increment	Time [min]	Time interval [min]	V stress [kPa]	V strain [%]	M [MPa]
-	0	-	0	0	-
1	16	16	32.7	0.119	
2	31	15	60.1	0.584	6
3	46	15	88.3	1.456	3
4	61	15	121.0	2.834	2
5	76	15	200.6	5.962	3
6	91	15	280.7	8.199	4
7	106	15	360.0	9.918	5
8	107	1	409.2	10.098	
9	111	4	-0.9		

Figure B.7 – *Stress and strain versus time for test 3. Strain (blue) on right hand axis and Stress (orange) on left axis*
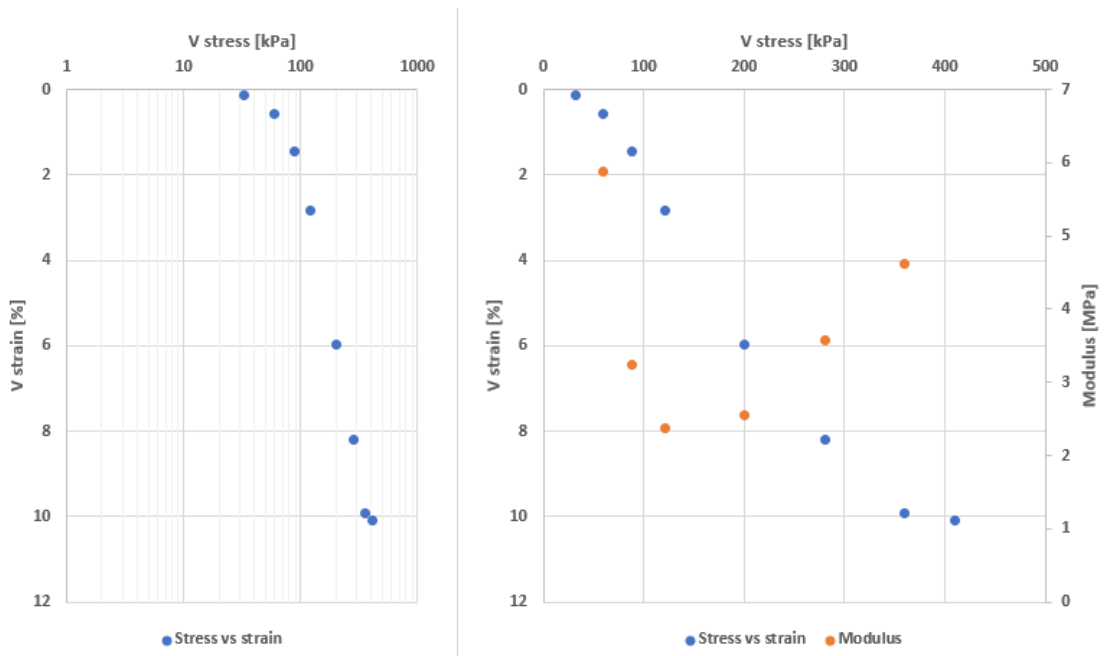

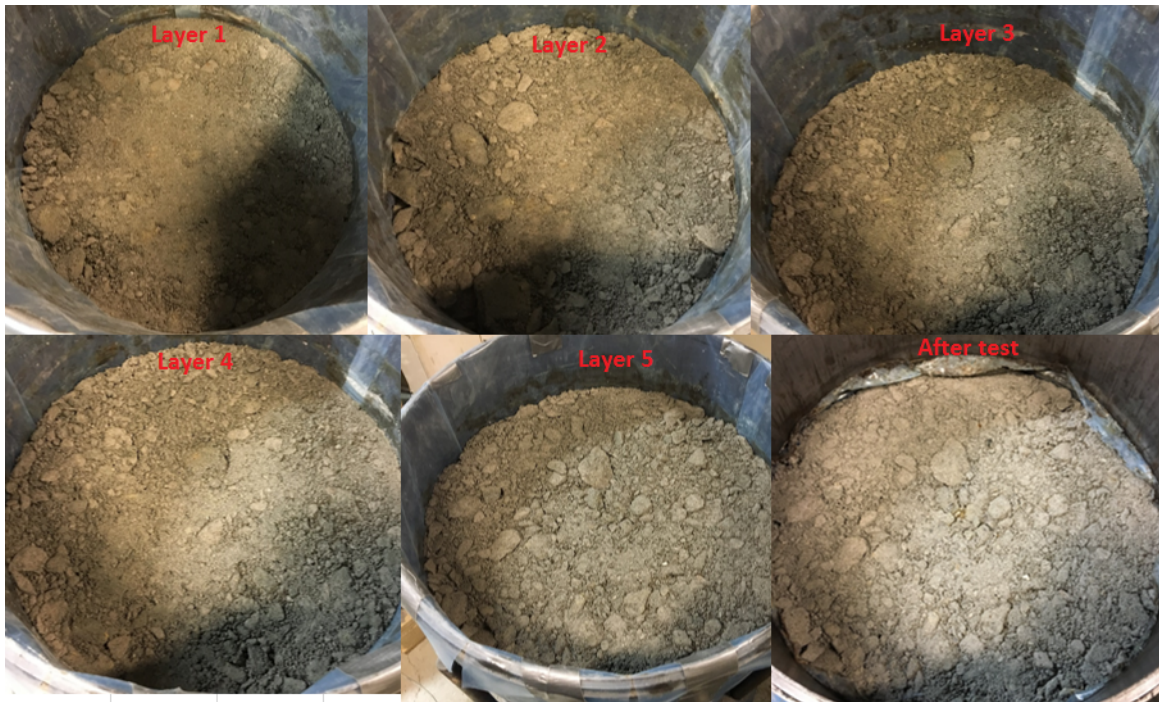**Figure B.8** – *Stress - Strain - Modulus: Test 3*

Figure B.9 – *Layers after compression - test 3*

Test 4:

Table B.10 – *Building of test 4*

Layer	Weight of material [kg]	Compaction [min]
1	30.065	0.5
2	31.647	0.5
3	31.643	0.5
4	31.490	0.5
5	32.158	0.5
6	16.661	0.5
Total	**173.663**	

Table B.11 – *Density and water content of Oedometer test 4*

Water content: 7.6 %

		Before testing	After testing
Sample height	cm	42.5	40.3
Volume	l	83.1	78.8
Wet density	t/m^3	2.10	2.20
Dry density	t/m^3	1.94	2.04

Table B.12 – *Increments and modulus of Oedometer test 4*

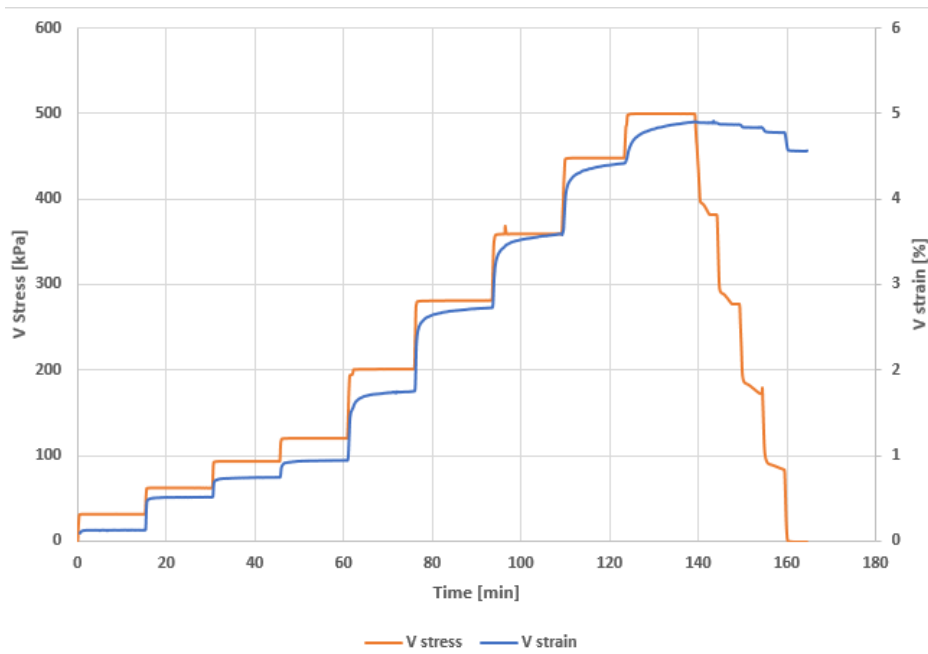| Increment	Time [min]	Time interval [min]	V stress [kPa]	V strain [%]	M [MPa]
-	0	-	0	0	-
1	15	15	31.8	0.134	
2	30	15	62.4	0.519	8
3	45	15	93.5	0.749	14
4	61	15	120.6	0.948	14
5	76	15	201.6	1.756	10
6	94	17	281.9	2.733	8
7	109	16	359.9	3.591	9
8	123	14	448.6	4.420	11
9	139	16	500.4	4.904	11

Figure B.10 – *Stress and strain versus time for test 4. Strain (blue) on right hand axis and Stress (orange) on left axis*
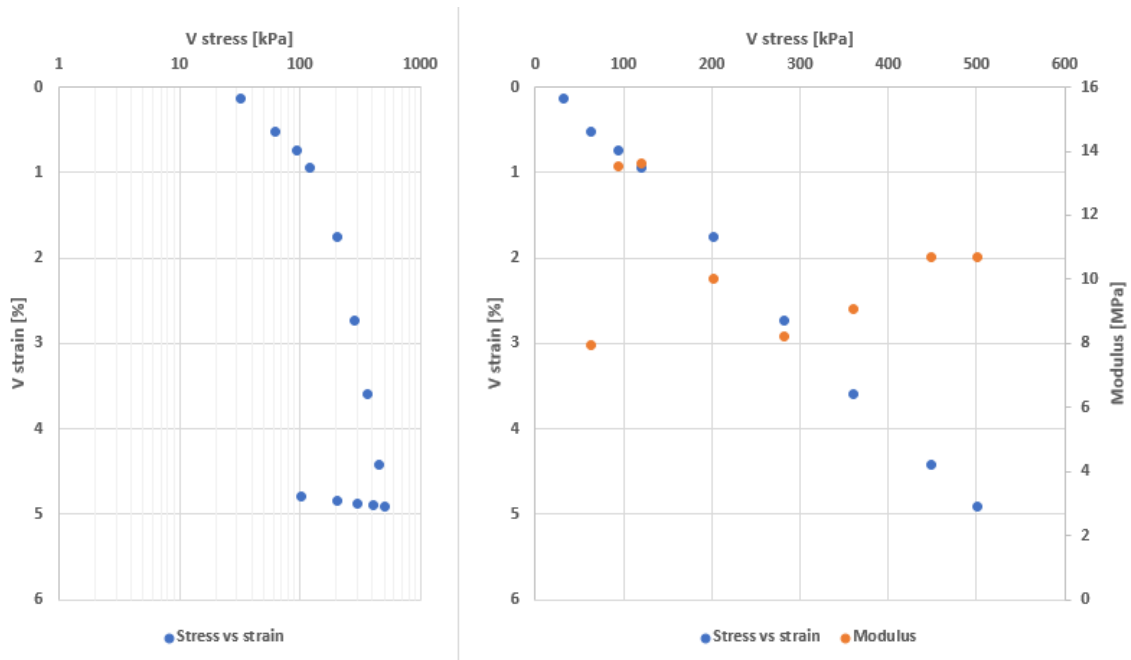

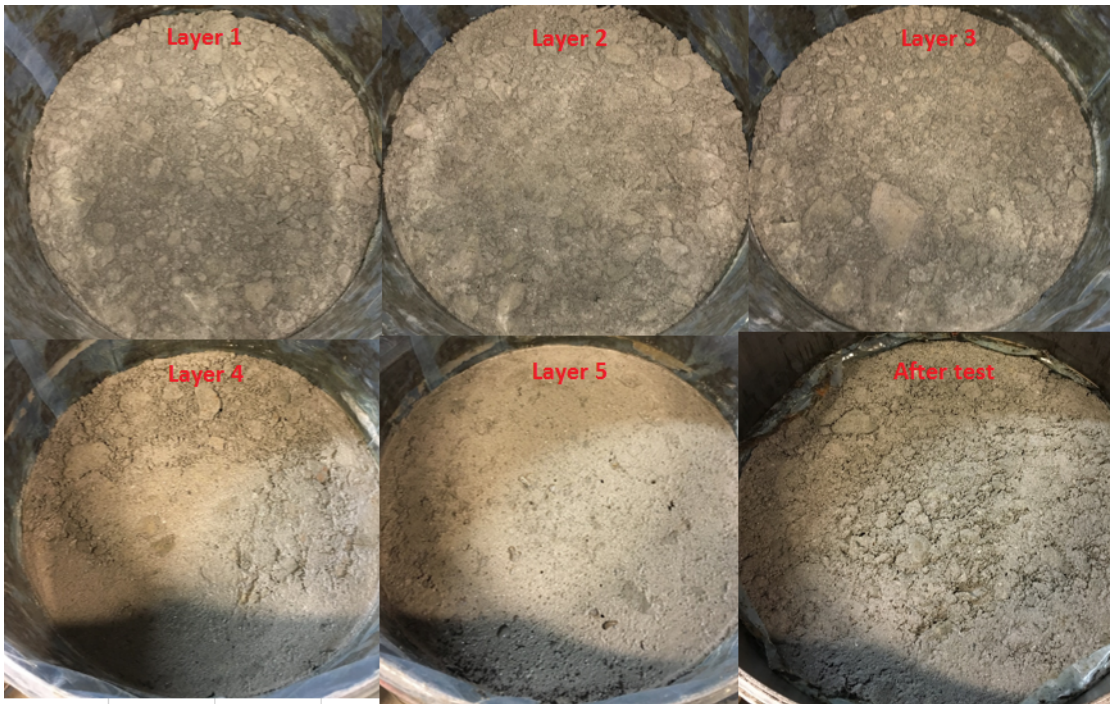**Figure B.11** – *Stress - Strain - Modulus: Test 4*

Figure B.12 – *Layers after compression - test 4: Picture of layer 6 before test is missing*